Landau and spin splitting in tilted magnetic fields for a two-dimensional electron gas in AlGaAs/GaAs heterostructures

Koning, J.J.

Award date:
1988

Landau and spin splitting in tilted magnetic fields for a two-dimensional electron gas in AlGaAs/GaAs hetero-structures.

J.J.Koning Augustus 1988.

Dit is een verslag van het afstudeerwerk van J.J.Koning.

Afstudeerhoogleraar: Prof. Dr. J.H. Wolter.

Vakgroep Vaste Stof Fysica, onderwerpgroep Halfgeleiderfysica.

Technische Universiteit Eindhoven, Postbus 513, NL-5600 MB Eindhoven.

Het afstudeerwerk is verricht in de groep van

Prof. Dr. K. von Klitzing.

Max-Planck-Institut für Festkörperforschung.

Heisenbergstrasse 1, D-7000 Stuttgart 80, B.R.D.

Begeleider: Dr. R.J. Haug.

Landau and spin splitting in tilted magnetic fields for a two-dimensional electron gas in AlGaAs/GaAs hetero-structures.

J.J.Koning August 1988.

This is a report on the diplom-work of J.J.Koning, student of
Prof. Dr. J.H. Wolter, Solid State Physics/Semiconductor Physics
Eindhoven University of Technology, P.O.Box 513, NL-5600 MB Eindhoven
The Netherlands.

The work is carried out in the group of professor Dr. K. von Klitzing
Max-Planck-Institut für Festkörperforschung
Heisenbergstrasse 1, D-7000 Stuttgart 80, F.R.G.

Coach: Dr. R.J. Haug.

My stay in Stuttgart came to an existence after an initiative of professor Dr. Joachim Wolter. I thank him for this opening to a wonderful experience. I am very grateful for the pleasant and fruitful time I had in the group 'VK' at the Max-Planck-Institut für Festkörperforschung in Stuttgart, and I would like to thank professor Klaus von Klitzing for the very kind opportunity to work in his group during eight months.

I say thanks to Hans Sigg for the nice cooperation, doing the cyclotron resonance experiments. And I thank everybody in the group for the help and advice, the jokes and fun, the tea and coffee.

But most of all I would like to thank my supervisor, Rolf Haug, for everything that I learned from him, and who I know as a very kind and friendly person and as a talented physicist.

Abstract

Thermally activated conductivity is used as a tool to investigate the cyclotron energy and the spin splitting of Landau levels in a two-dimensional electron gas (2-DEG) in a high mobility AlGaAs/GaAs heterostructure (n_s= 1.45 $10^{11}cm^{-2}$; μ = 6.1 $10^{5}cm^{2}/Vs$) under quantum Hall conditions.

The activation energy between two spin levels (filling factor υ=1) increases by 23%, and between two Landau levels (υ=2) it decreases by 20%, if parallel magnetic fields up to 12 Tesla are applied.

For an odd filling factor (υ=1) the enhanced g-factor is found to be larger than for the case that the filling factor has an even value (υ=2). The decrease of the activation energy between two Landau levels is mainly due to a decrease of the cyclotron energy, as is confirmed with second order perturbation theory and cyclotron resonance experiments. This implies that the coincidence method of Fang and Stiles cannot be used to determine the spin splitting in tilted magnetic fields.

Contents

Chapter 1: Introduction

1.1: Introduction to this report

Since 1980 when K.v.Klitzing discovered the quantized Hall effect(*) (QHE) in a two-dimensional electron gas in silicon metal-oxid-semiconductor field effect transistors (Si-MOSFET) [1] a tremendous amount of research has been done on systems with a two dimensional electron gas (2-DEG). The Hall resistance of a 2-DEG in strong magnetic fields shows, independent of the sample, steps as a function of the magnetic field at very well defined values of the resistance. These values are only related to fundamental constants and are equal to the Planck constant h divided by the elementary charge e squared times an integer: $h/\nu e^2$ with $\nu = 1, 2, 3, \ldots$. On one hand the QHE is of fundamental interest because it offers the opportunity to study the quantum character of nature. On the other hand the QHE can be applied for a determination of $h/\nu e^2$ as a resistance standard. Since 1986 the QHE is used in metrology to represent the standard resistance with high accuracy. For the discovery of this effect the Nobel Prize was awarded to K.v.Klitzing in 1985.

The development of growth techniques like molecular beam epitaxy (MBE) and metal-organic chemical vapour phase deposition (MOCVD) cleared the way to very pure semiconductor crystals and hetero-structures that serve as model systems for optical and electrical investigations. The samples used here consist of an aluminium gallium arsenide ($Al_xGa_{1-x}As$) crystal grown on a gallium arsenide (GaAs) crystal, with an electron gas that is confined near the interface of the two materials. Because of the confinement in one plane

(*)Also known as the von Klitzing effect, see f.i. [2].

perpendicular to the growth direction, one speaks of a 2-DEG. The samples (W1527b and W1561b) are grown with MBE by G.Weimann at the Forschungsinstitut der Deutschen Bundespost, FTZ.

Topic of our interest is the conductivity in the direction of the voltage applied to the 2-DEG under quantum Hall conditions. This conductivity (σ_{xx}) shows oscillations as a function of the magnetic field known as the Shubnikov-de Haas (SdH) effect. The quantum Hall effect and the Shubnikov-de Haas effect are both due to the electron density of states of a 2-DEG in a strong magnetic field and are thus closely related effects.

In this work we report on the temperature dependence of the SdH minima in a range of 0.5 to 20 Kelvin. The thermally activated conductivity is studied and used as a tool to collect information about the density of states around the Fermi-energy, especially the splitting of the Landau levels as will be explained later, and the spin splitting of the Landau levels, the so-called Zeeman effect. The spectrum of the Landau levels is thought to be mostly due to the component of the magnetic field that is pointing perpendicular to the plane of the 2-DEG. Contrary to this, the spin splitting of the Landau levels is thought to be dependent on both the perpendicular and the parallel, i.c. the total magnetic field. Therefore, the measurements are done in quantizing perpendicular fields with parallel components up to 13.6 Tesla to investigate the behaviour of both splittings. The theory about these two splittings and the model that is used to understand the SdH effect are described in chapter 2. Chapter 3 presents the samples, the equipment and the determination of the temperature and the conductivity σ_{xx}. Chapter 4 deals with the SdH effect as it is measured in different tilted magnetic fields and at

different temperatures. The resulting activation energies with the Fermi-energy between two spin levels are described in chapter 5. In chapter 6 the results with the Fermi-energy between two Landau levels are given and discussed together with second order perturbation theory and cyclotron resonance experiments. Chapter 7 presents measurements of the temperature dependence for the case that the absolute value of the spin minima is comparable to the absolute value of the Landau minima. In chapter 8 we give the general conclusions. A summary is given in chapter 9. Finally, two appendices are added. Appendix A, in which a second order perturbation calculation is summarized, and appendix B, in which extra results of the temperature dependent measurements are discussed that are related to the theory of localization.

We note that a part of the results was already presented at the Frühjahrstagung Karlsruhe 1988 des Arbeitskreises Festkörperphysik der DPG is a poster, entitled:

"Landau- und Spinaufspaltung in gekippten Magnetfeldern für das zweidimensionale Elektronengas einer AlGaAs/GaAs-Heterostruktur"
J.J.Koning, R.J.Haug, K.v.Klitzing, G.Weimann.
Verhandlungen der Deutschen Physikalische Gesellschaft,
Physik-Verlag GmbH, Weinheim, 1988 (Fachsitzung Halbleiterphysik,
HL-11.69, p.61).

1.2: The Max-Planck-Institut für Festkörperforschung

On the initiative of Prof. Dr. Joachim Wolter this work has been carried out at the Max-Planck-Institut für Festkörperforschung (MPI FKF) in Stuttgart in the group of Prof. Dr. Klaus von Klitzing under the supervision of Dr. Rolf J. Haug.

Basic research at the Max-Planck-Institut für Festkörperforschung is dealing with the investigation of the structural, electronic and vibrational properties of solid materials. The institute is divided in ten scientific departments in Stuttgart which are supported by nine scientific service groups. The eleventh department, the Hochfeld Magnetlabor, is situated in Grenoble.

Professor von Klitzing's department is mainly concerned with electronic properties of semiconductors, especially the influence of quantum phenomena on the electronic transport in one and two dimensional electronic systems, quantumwells and superlattices. Thermoelectric and transport measurements in magnetic fields up to 15 Tesla and temperatures down to 50 mK are used to analyse the electronic transport in low dimensional systems. Far infrared techniques are used to identify quantum levels in low-dimensional systems. Time-resolved photo-conductivity measurements is one of the methods to characterize the electronic properties of optically excited carriers. In close cooperation with the MBE and technology group the influence of the design parameters of the samples on the experimental results are analysed. The development of a microscopic picture of the quantum Hall effect and investigations of the physical and chemical properties of conductive polymers are two of the topics of the research program.

This work is covered under 'Elektronische und spinabhängige Eigenschaften', project I-13 'Untersuchungen zum quantisierten Hallwiderstand' as mentioned in the annual report of MPI-FKF Stuttgart 1987.

Chapter 2: Theory

2.1: 2-DEG

Two typical crystal structures are commonly used to investigate the properties of a 2-DEG. The silicon metal-oxide-semiconductor field effect transistor in which the quantum Hall effect was discovered [1], and the AlGaAs/GaAs-heterostructure, like the ones used here. The technology for the Si-MOSFET is highly developed in semiconductor industry and has led to many applications for its electrical properties. Galliumarsenide is technologically not explored on the same scale as silicon but it offers as a direct semiconductor in contrast with silicon more opportunities for optical purposes like the solid state laser, and because of the higher mobility in the AlGaAs/GaAs 2-DEG it is also of interest for the development of the high electron mobility transistor (HEMT). A high mobility is achievable in heterojunctions by the very well controlled growth of an AlGaAs crystal on a GaAs crystal. The lattice constants of the two materials are almost equal, so that the total structure can be grown as one crystal with very few misfits. The electron affinities of the two materials are different. This causes a discontinuity in the conduction band U_o (fig.2.1).

When the two crystals are in thermodynamical equilibrium, i.e. the Fermi-energy (E_F) being the same everywhere, an asymmetric potential well of more or less triangular shape as a function of the z coordinate exists. This well is provided with electrons coming from additional donors, often silicon, in the AlGaAs bulk material. Usually, to prevent the dopants from lowering the mobility of the electrons in the well by scattering, an undoped region in AlGaAs is

held free of silicon. This is named 'spacer'. The Fermi-energy in AlGaAs is at the donor level and in GaAs at the acceptor level. These acceptors are usually present in MBE samples at low ($\simeq 10^{14} cm^{-3}$) concentrations compared to the concentration of donors ($\simeq 10^{17} cm^{-3}$). The potential in GaAs has a shape that is determined by the charge at the interface. As indicated in fig.2.2 one subband lies under the

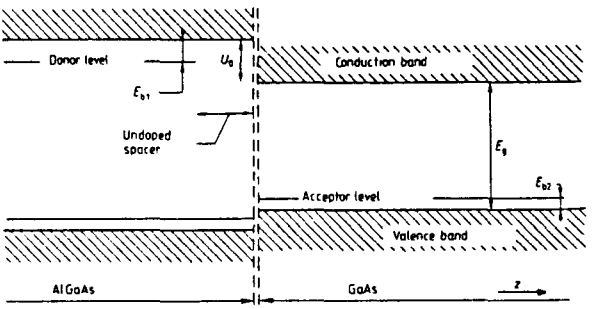

Fig.2.1. Two crystals shown separate: AlGaAs and GaAs. The growth took place in the -z direction.

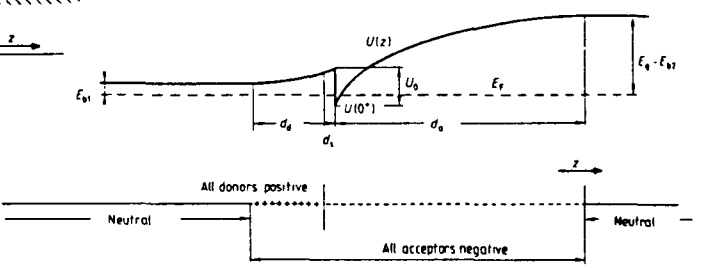

Fig.2.2 The heterojunction in equilibrium. One subband is occupied. Only the conduction band minimum is shown. Reasonable parameters: E_{b1}= 50 meV, E_{b2}= 25 meV, E_g = 1.4 eV, U_o= 300 meV.

Fermi-energy. The electrons in this subband come from the donors. The presence of the electrons influences the potential as is described by the Poisson equation. In order to calculate the shape of this electrostatic potential, the subband energy of the electrons, and the electron density that again influences the potential, one has to solve the Schrödinger equation in a self-consistent manner. The envellope of

the as a function of z fast oscillating electron density has an extension of 100 to 200 Å in the z-direction [3,4,55] (fig.2.3).

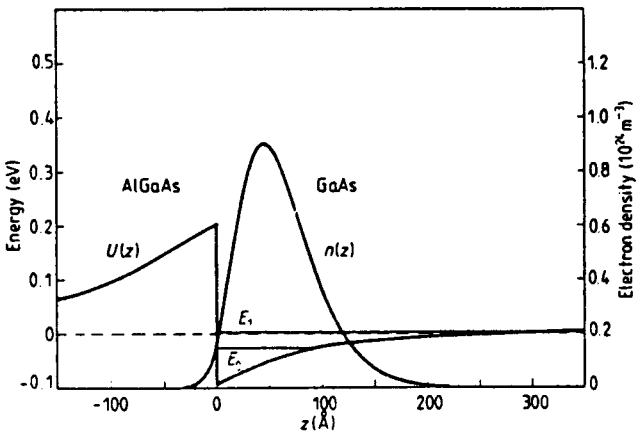

Fig.2.3. A typical envellope function for an AlGaAs/GaAs 2-DEG [4].

The penetration of the envellope function in both bulk materials will cause effective mass effects of the order of magnitude of 2% [5,6] and a spin splitting at the interface being about 10% smaller than in bulk GaAs as is measured by means of electron spin resonance (ESR) [7]. The electrons in this subband are confined in the z-direction. The high purity of the crystal and the freedom to move in the xy-plane is resulting in a two dimensional gas of almost free electrons with a high mobility. The interactions that limit this mobility can be [8]

- optical phonons (T › 100 K),
- acoustical phonons,
- random location of aluminium atoms at gallium lattice positions, known as alloy scattering,
- interface roughness, which is not very important in AlGaAs/GaAs heterojunctions with low electron density n_s, according to Ando and Murayama [9],

- Coulomb interaction with charged impurities, like the silicon donors in bulk AlGaAs.

The undoped spacer layer between the doped region and the 2-DEG reduces the Coulomb scattering. The invention of the spacer has made these heterostructures to the model system for 2-DEG investigations with the highest mobilities. Finally, we assume the electron density in the heterojunction to be constant as long as the Fermi-energy is connected to the outside world.

2.2: 2-DEG in a strong magnetic field

To describe the energy and the wave function of each electron in the 2-DEG in a static homogeneous magnetic field we have to solve the Schrödinger equation. Replacing the momentum

$$\underline{p} \rightarrow \underline{p} + e\underline{A} \tag{2.1}$$

with electron charge -e, we get for the Hamiltonian

$$H = \frac{1}{2m^*}(\underline{p} + e\underline{A})^2 + V[n(z)] \tag{2.2}$$

in which the electrostatic potential is written as a density-functional to express the dependence on the electron density. This electron density is assumed to be uniform along the interface, so it is only a function of z. m^* is the effective mass (= 0.067 times electron restmass m_o) which is assumed to be isotropic and equal in both AlGaAs and GaAs. This effective mass is independent of energy in the case of a parabolic energy band in k-space. We refer to [3,10,11] for anisotropy and non-parabolicity effects and we conclude that they are neglegible in our case. We define the magnetic field with a zero component in the x direction, which is an arbitrary choice:

$$\underline{B} = (0, B_y, B_z) \ . \tag{2.3}$$

B_y is the parallel magnetic field component and B_z is the perpendicular component, both in Tesla. Here we choose the gauge

$$\underline{A} = (zB_y, xB_z, 0) \tag{2.4}$$

fulfilling

$$\underline{B} = \underline{\nabla} \times \underline{A} \ , \tag{2.5}$$

assuming that the magnetization in the material is neglegible small [19]. The Hamiltonian is now

$$H = \frac{1}{2m^*} [(p_x + eB_y z)^2 + (p_y + eB_z x)^2 + p_z^2] + V[n(z)] \ . \tag{2.6}$$

Actually, we are talking about quasiparticles being Fermions with charge -e and mass m^*. The spin dependent part will be discussed later. Because H is independent of y we can use $[p_y, H] = 0$ which means that p_y is a constant of motion and can be replaced by $\hbar k_y$. If we transform

$$x \rightarrow x' - \hbar k_y/(m^* \omega_{cz}) \tag{2.7}$$

with the definition $\omega_{cz} = eB_z/m^*$ and use $p_x \rightarrow p_x$, , the Hamiltonian becomes, writing x' as x again,

$$H = \frac{1}{2m^*} [(p_x + eB_y z)^2 + m^{*2}\omega_{cz}^2 x^2 + p_z^2] + V[n(z)] \ . \tag{2.8}$$

In the Hamiltonian we recognize the following parts

$$H_o = \frac{p_z^2}{2m^*} + V[n(z)] \tag{2.9a}$$

$$H_1 = \frac{1}{2m^*} (p_x^2 + m^{*2}\omega_{cz}^2 x^2) \tag{2.9b}$$

$$H_2 = \frac{eB_y}{m^*} z p_x \tag{2.9c}$$

$$H_3 = \frac{e^2 B_y^2}{2m^*} z^2 \tag{2.9d}$$

with

$$H = H_o + H_1 + H_2 + H_3 \ . \tag{2.10}$$

In the case of a perpendicular total magnetic field the last two terms are vanishing and H_o is the z dependent part of the Hamiltonian. The

wave function can then be separated

$$\psi(x,y,z) = \exp(ik_y y)\ \varphi(x)\ \varphi(z)\ . \qquad (2.11)$$

H_o gives rise to the confinement in the z direction. The eigenvalues are the subband energies E_i ($i = 0,1,2,\ldots$) and the envellope of the eigenfunctions is like in figure 2.3. H_1 stands for a parabolic potential well that represents the simple one-dimensional harmonic oscillator. H_1 acts only on $\varphi(x)$. The eigenvalues form equidistant energy levels, the so-called Landau levels

$$\epsilon_N = (N + 1/2)\ \hbar\omega_{cz} \qquad (2.12)$$

with quantum number N (N=0,1,2...). The eigenfunctions are the harmonic oscillator eigenfunctions, f.i. described in [12]. In a perpendicular field the energy of the electrons in subband i and Landau level N is

$$E_{i,N} = E_i + (N + 1/2)\ \hbar\omega_{cz}\ . \qquad (2.13)$$

The spectrum of the density of states is discrete.

The "movements" in the z-direction and in the plane parallel to the interface are coupled by H_2 when the parallel magnetic field is non-zero. Ando treated this problem mathematically and derived expressions for numerical calculations from which can be concluded that this mixing term in the Hamiltonian perturbs the Landau levels N by interaction with Landau levels with different N and different i [13].

In appendix A second order perturbation theory is presented to estimate the influence of the first subband on the first three Landau levels in the ground subband. This will be discussed further on in relation to the measurements in chapter 6.

H_3 is the magnetic contribution to the potential energy. In the limit of very strong parallel fields the magnetic potential dominates

over the electrostatic potential V and the total potential becomes almost parabolic with equidistant subband energies. The shift of the electrostatic subbands due to this part of the Hamiltonian is an upward shift relative to E_F for the subbands which are higher than the Fermi-energy, and is often referred to as the diamagnetic shift [13]. The complete Hamiltonian can be solved analytically if the electrostatic potential is parabolic [14,15]. For other potential wells H cannot be separated in a simple way for other potential wells due to the mixing term H_2. We shall now focus on the case without parallel field and return to the spectrum of Landau levels, especially the degeneracy.

The symmetry of the problem allows electrons at different (x,y) coordinates in the plane of the 2-DEG to have the same energy. It does not matter for the energy of an electron in a certain Landau level what its position in the (x,y) plane is. Therefore, many electrons are in one Landau level being degenerate. The degeneracy per Landau level can be calculated in the two-dimensional case by summing the allowed states in (k_x,k_y) space per area. The quantity

$$k^2 = k_x^2 + k_y^2 \tag{2.14}$$

has a definite value, determined by $(N+1/2)\hbar\omega_{cz}$. For every subband i with a value k_{zi} there is a surface of $4\pi^2/A$ available in k-space, in which A is the area of the interface. The density of 2-D states is in k-space $2\pi k dk/(4\pi^2/A).1/A = kdk/2\pi = m^*/(2\pi\hbar^2)dE$ using the effective mass formalism. The density of states for a 2-DEG is thus

$$D(E) = m^*/2\pi\hbar^2 . \tag{2.15}$$

This is independent of energy. We have to integrate over one level to get the number of states in one Landau level. Suppose the levels to have equal width, then we have to integrate from 0 to $\hbar\omega_{cz}$, where the

next level is thought to be starting:

$$\int_0^{\hbar\omega_{cz}} m^*/(2\pi\hbar^2)\, dE = eB_z/h \ . \qquad (2.16)$$

Now we have to take into account that every state can have an electron with spin up and an electron with spin down. Thus we have to multiply by 2 and it follows that the degeneracy per Landau level is

$$2eB_z/h \ . \qquad (2.17)$$

It is important to notice that the degeneracy of the Landau levels is proportional to the perpendicular magnetic field. A constant total number of electrons n_s in the 2-DEG implies that the number of Landau levels that can be filled at zero temperature is decreasing with increasing perpendicular magnetic field. The number of filled Landau levels is represented by the filling factor

$$\upsilon_L = n_s/(2eB_z/h) \ . \qquad (2.18)$$

For integer values of the filling factor it follows that

$$E_F = E_i + (\upsilon_L - 1/2)\ \hbar\omega_{cz} \ . \qquad (2.19)$$

A method to change υ_L with a constant magnetic field is to change n_s by means of a gate or a light emitting diode (LED). In both cases the self-consistent electrostatic potential will change. The energy of the 2-D electrons in a tilted magnetic field is still independent of the (x,y) coordinates [14]. The degeneracy of the Landau levels is thus to be assumed not to change as long as the perpendicular field is constant. In spite of the fact that (2.13) is not the eigenvalue equation of the Hamiltonian with parallel fields we still use the name Landau level to refer to the original levels, because they are still recognizable as such, but possibly with a different cyclotron energy.

2.3: Spin splitting

To complete the picture of the density of states in AlGaAs/GaAs heterojunctions in strong magnetic fields we have to add the Zeeman splitting of each Landau level. In a perpendicular field one gets for the eigenvalues

$$E_{i,N,s} = E_i + (N+1/2)\,\hbar\omega_{cz} + sg\mu_B B_{tot} \quad . \tag{2.20}$$

Each Landau level splits into two spin polarized levels with eB/h states per spin level (see (2.17)). μ_B is the Bohr magneton, s is the spin quantum number ($\pm 1/2$), and g is the Landé g-factor which should be equal to the free electron g-factor, but is changed by material dependent spin-orbit coupling. Here, s = -1/2 corresponds to the spin up situation. This g-factor should be determined experimentally by means of adiabatic rf-absorption (ESR) which is a very fast process and is thought not to be influenced by many-particle Coulomb interaction [17]. Contrary to this, the conductivity measurements can be seen as isothermal; we start with a system in thermal equilibrium, change something, let equilibrium be re-established and then compare the two equilibrium states. It is not very surprising that the spin splittings determined by different methods appear to be different. In figure 2.4 are given g-factors of ESR induced photocurrent measurements [7]. The ESR-induced photocurrent effect takes place when the energy of the microwave radiation is equal to the one-electron spin splitting ΔE_s. The upper part of fig.2.4 is measured in tilted fields. The frequency for each series of measurements is indicated in GHz. Different symbols are used for the Landau level in which the spin flip takes place. The g-factor is determined by $g := \Delta E_s/(\mu_B B_{tot})$. B_{tot} is the magnetic field at whih the photocurrent effect is seen.

The lower part in fig.2.4 shows ESR with varying frequencies in perpendicular magnetic fields for N = 0, 1 and 2.

Kukushkin [18] measured the density of states by means of photoluminescence (fig.2.5a). A_o is the zero subband peak which is very small, and A_1 is caused by the first subband. The wave function of the electrons in the first subband is more extended and shows larger overlap with the wave function of the free holes in the valence band. Thus A_1 is larger than A_o. For a detailed analysis we refer to [18]. The densities in the two subbands are indicated (n_{so},n_{s1}) as well as the total electron density in the 2-DEG (n_s). In magnetic fields of 2 and 4 Tesla two resp. one Landau levels are occupied in the first subband. The spin splitting is determined from the details of the spectrum [18]. From this method only changes Δg_e of the g-factor can be determined (fig.2.5b). Up to now, Kukushkin did not investigate this extensively in tilted magnetic fields.

Janak [17] proposed a model trying to explain the conductivity measurements of Fang and Stiles [19] on Si-MOSFETs who observed an enhancement of the spin splitting. Fang, Stiles and Janak [17,19] presented this as an enhanced g-factor g^*, having the source for its enhancement in the exchange interaction of quasiparticles. Now, our description is based on a picture of quasiparticles at the Fermi surface with charge -e, mass m^*, an enhanced g-factor g^* and spin 1/2. First, we give the formula as derived by Janak and later we take a closer look at the exchange interaction. Janak represented the exchange interaction as $\sum(k,E_k)$. This is calculated with a Coulomb potential which is screened by the electron dielectric function $\epsilon(q,\omega)$.

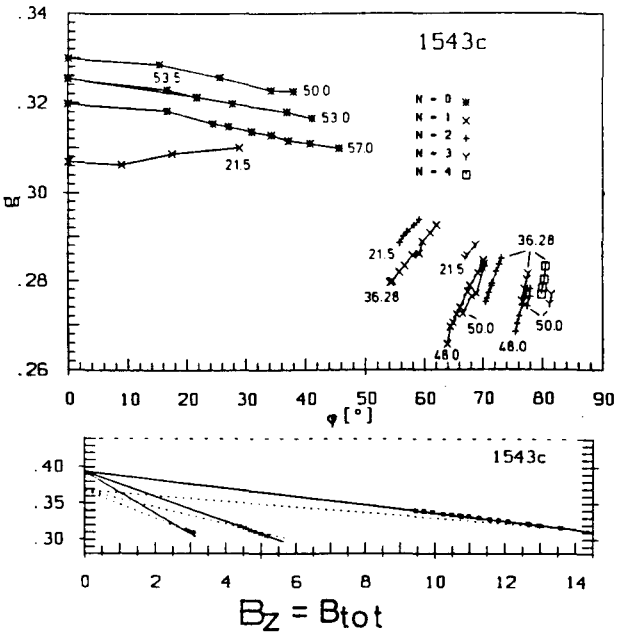

Fig.2.4. ESR by Dobers. The frequency at which the resonance takes place, is indicated in GHz. $n_s = 3{,}3.10^{11}cm^{-2}$, $\mu = 3{,}6.10^{5}cm^{2}/Vs$.

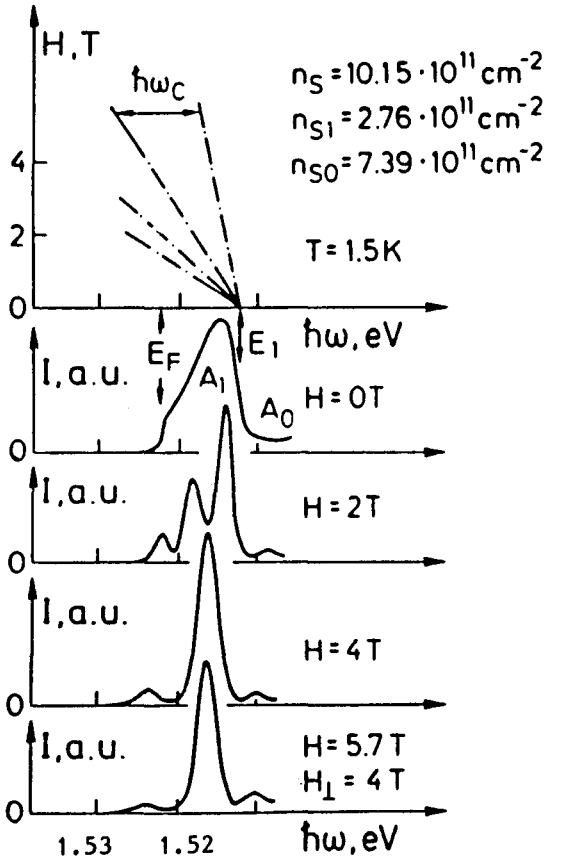

Fig.2.5a. Recombination spectrum of 2-DEG electrons with free holes in a heterostructure [18].

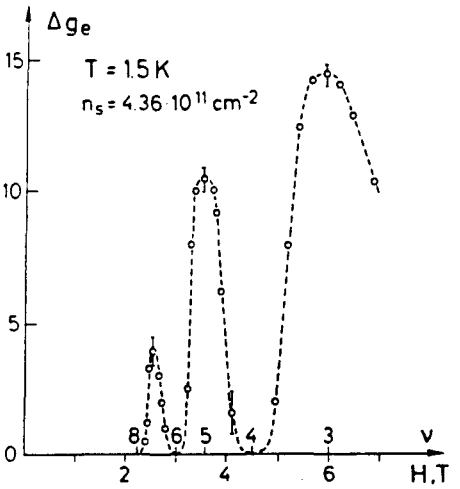

Fig.2.5b. The change Δg_e of the g-factor as a function of filling factor ν [18].

It follows that per spin orientation

$$E_{k,up} = \epsilon_k + 1/2 g_o \mu_B B + \Sigma_{up}(k, E_{k,up}) = E_k + 1/2 g_k^* \mu_B B$$

$$E_{k,down} = \epsilon_k - 1/2 g_o \mu_B B + \Sigma_{down}(k, E_{k,down}) = E_k - 1/2 g_k^* \mu_B B$$

so

$$g_k^* \mu_B B = E_{k,up} - E_{k,down} = g_o \mu_B B + \Sigma_{up}(k, E_{k,up}) - \Sigma_{down}(k, E_{k,down}). \quad (2.21)$$

Later, Ando and Uemura [20] improved the calculation to get quantitative agreement with the interpreted g-factors of Fang and Stiles. Their first order perturbation formula for the spin splitting is in strong magnetic fields and neglecting the overlap between different Landau levels:

$$g^* \mu_B B_{tot} = g_o \mu_B B_{tot} + E_{ex} \quad (2.22a)$$

with

$$E_{ex} = \sum_{q,N} \frac{V(q)}{\epsilon(q,0)} J_{NN}(q) \cdot (n_{N\,up} - n_{N\,down}) \cdot \quad (2.22b)$$

$\epsilon(q,0)$ are the Fourier components of the static dielectric function, $V(q)$ are the Fourier components of the Coulomb interaction V_{Coul} and $J_{NN}(q)$ are products of Laguerre polynomials and exponential functions. It should be noted here that Fang and Stiles compared the splitting of Landau levels to the spin splitting to find a value for the g-factor. They assumed the cyclotron energy in Si-MOSFETs to be constant in tilted fields with angles up to 60^o. Kukushkin explained the observation of an oscillating g-factor (fig.2.5b) assuming a Coulomb exchange dependent on the occupation difference of the two spin levels.

The theory of Ando and Janak starts from a Zeeman term in the Hamiltonian which already includes the exchange energy. It is usual to describe this part of the Hamiltonian as H(exchange) + H(Zeeman). The

existence of a constant exchange energy E_{ex} refers to a zero field spin splitting. The theory that the exchange energy depends on the spin splitting via the difference in occupation can be made plausible in the following way. The exchange energy is based on the Pauli principle for Fermions. The wave functions of these particles are antisymmetric and are composed of products of spin and orbital wave functions $\varphi(\underline{r})\varphi(\text{spin})$. The strongest interaction between electrons is the Coulomb interaction. For a first order calculation of the Coulomb interaction of electrons with overlapping wave functions, $\langle\zeta_N|V_{Coul}|\zeta_N\rangle$, has to be calculated with ζ_N being antisymmetrical total wave functions. This means that one will get a difference in energy, namely for the Coulomb interaction between electrons with even spin wave function combinations and for the ones with odd combinations. This gives rise to $\langle V_{Coul}\rangle \pm 1/2E_{ex}$. In fact, the exchange energy is the energy difference by exchanging two Fermions with opposite parities of their overlapping orbital wave functions. The Coulomb interaction of two arbitrary electrons with real space coordinates $\underline{r}_i$ and $\underline{r}_j$ and spins in the p direction is included in a pre-factor $J_{i,j}$. We write the exchange energy as $-2J^{PP}_{i,j}\, S^P_i\, S^P_j$, similar like the Heisenberg model for isotropic systems [21,59]. S^P is the p-component of the spin operator. In a 2-DEG the exchange can take place with any electron with opposite spin in the same Landau level N;

$$E_{ex} = -2\sum_j{}' J^{PP}_{i,j}\, \sigma^P_i\, \sigma^P_j \ .$$

$\sum_j{}'$ has the meaning of a summation over all electrons at place $\underline{r}_j$ in Landau level N except for $\underline{r}_i = \underline{r}_j$. these electrons need to have an overlap of the wave function with the electron at $\underline{r}_i$. From this it is plausible that the exchange energy is related to the difference of the

occupation. From the point of view of the experimentalist who is measuring g^* it is a nice feature of this notation that the exchange interaction is included in the phenomenological parameter g^*, because it is impossible at the moment to distinguish between all different contributions to the spin splitting. We note here that the exchange energy is a function of the state of the system via the magnetization. This is different from systems in which the spin particles are fixed at atoms and only have exchange interaction with spins at adjacent atoms, often resulting in a zero field spin splitting. To summarize we mention that the exchange interaction is a spin - spin interaction, while the Zeeman term is a magnetic field - spin interaction. Now we leave this discussion and look at the Zeeman term for the spin splitting.

We extend the description of H_4 := H(Zeeman) for both parallel and perpendicular magnetic fields and consider the case in which the electron spins are sensitive to the total magnetic field in an anisotropic manner. Our system has two different directions, the one perpendicular to the plane of the 2-DEC, where we have B_z, and the one in the plane of the 2-DEC, where we have B_y. The spin part of the Hamiltonian is for fermions

$$H_4 = 1/2\ \mu_B\ g\ \underline{B}.\underline{\sigma} \tag{2.23}$$

with $\underline{S} = 1/2\hbar\underline{\sigma}$, in which $\underline{\sigma}$ consists of the Pauli spin matrices:

$$\sigma_x = \begin{vmatrix} 0 & 1 \\ 1 & 0 \end{vmatrix},\quad \sigma_y = \begin{vmatrix} 0 & -i \\ i & 0 \end{vmatrix} \text{ and } \sigma_z = \begin{vmatrix} 1 & 0 \\ 0 & -1 \end{vmatrix} \tag{2.24}$$

and $\underline{B} = (0,B_y,B_z)$ like before. Actually, g is a matrix where g_{pq} is coupling B_p with σ_q, what is a standard notation in the area of magnetism of solid state physics [59,60,61,62]. Using the same basis of real space coordinates for both $\underline{B}$ and $\underline{S}$, the g-matrix is diagonal, because a magnetic dipole only has interation with the magnetic field

in its own direction. We take for the contribution of the z direction a value g_z and for the in-plane direction a value g_y. To solve the eigenvalue equation

$$H_4\,\varphi(\text{spin}) = 1/2\,\mu_B\,(g_y B_y \sigma_y + g_z B_z \sigma_z)\,\varphi(\text{spin}) = E\,\varphi(\text{spin}) \qquad (2.25)$$

we use

$$\det\,[E\,\underline{1} - H_4] = 0 \qquad (2.26)$$

and find

$$E^2 - (1/2\,\mu_B g_z B_z)^2 - (1/2\,\mu_B g_y B_y)^2 = 0 \qquad (2.27)$$

thus

$$E = \pm\,\sqrt{\{\Delta_z^{\,2} + (1/2\,\mu_B B_y g_y)^2\}}\ . \qquad (2.28)$$

It is clear that in the case of $B_y = 0$

$$E = s\mu_B g_z B_z = s\Delta_z \quad \text{with} \quad s = \pm\,1/2 \qquad (2.29)$$

as expected. If the exchange interaction does not play a role, one can determine g_z by measuring Δ_z under the condition $B_y = 0$. Then, via the spin splitting $\Delta E_s = 2E$ as measured for constant B_z and varying B_y, we immediately get g_y:

$$g_y^{\,2} = \frac{4}{\mu_B^{\,2} B_y^{\,2}}\,\{(1/2\,\Delta E_s)^2 - \Delta_z^{\,2}\}\ . \qquad (2.30)$$

This is independent of the sign of B_y as it should be for reasons of symmetry. Using $B_z = B_{tot}\cos\varphi$, $B_y = B_{tot}\sin\varphi$ and (2.27) we conclude for a 2-DEG that

$$g^2 = \cos^2\varphi\ g_z^{\,2} + \sin^2\varphi\ g_y^{\,2} \qquad (2.31)$$

with

$$g := \frac{\Delta E_s}{\mu_B B_{tot}}\ . \qquad (2.32)$$

When the exchange interaction is important, then g is equal to g^* as in (2.21).

2.4: Transport in 2-DEG

In a system of electrons with charge -e, the velocity $\underline{v}$ of the electrons in the classical picture will be limited by the characteristic scattering time τ. An electron with effective mass m^* will get an incremental velocity $\Delta\underline{v}$ between two collisions in a homogeneous electrostatic field $\underline{E}$ [21]

$$\Delta\underline{v} = -e\underline{E}\tau/m^* \quad . \tag{2.33}$$

The mobility μ of an electron is defined by the relation

$$\underline{v} = \mu\underline{E} \quad . \tag{2.34}$$

In the Drude-model it follows that

$$\mu = \frac{-e\tau}{m^*} \qquad /[m^2/Vs] \quad . \tag{2.35}$$

The effective mass in AlGaAs/GaAs is taken to be $0.067m_o$ (m_o is the restmass of an electron). Due to this relatively small effective mass higher electron mobilities can be achieved in AlGaAs/GaAs heterojunctions than in Si-MOSFETs. In the two dimensional case the conductivity tensor is defined by

$$\underline{J} = \underline{\sigma}\ \underline{E} \qquad /[A/m] \tag{2.36}$$

with

$$\underline{\sigma} = \begin{vmatrix} \sigma_{xx} & \sigma_{xy} \\ -\sigma_{xy} & \sigma_{xx} \end{vmatrix} \qquad /[\Omega^{-1}] \quad . \tag{2.37}$$

The resistivity tensor $\underline{\rho}$ is the inverse of the conductivity tensor $\underline{\sigma}$. It follows that

$$\rho_{xx} = \frac{\sigma_{xx}}{\sigma_{xx}^2 + \sigma_{xy}^2} \qquad \text{and} \qquad \rho_{xy} = \frac{-\sigma_{xy}}{\sigma_{xx}^2 + \sigma_{xy}^2} \quad . \tag{2.38}$$

Because of $\sigma_{xx} = J_x/E_x$ and Ohm's law

$$\underline{J} = -ne\underline{v} = ne^2\tau\underline{E}/m^* \quad , \tag{2.39}$$

the tensor component σ_{xx} without magnetic field is related to the

mobility by

$$\sigma_{xx} = n_s \, e \, \mu \qquad (2.40)$$

with n_s being the electron density of the 2-DEG in m^{-2}. In our experiments we use (2.40) to find the value of μ via n_s and σ_{xx} (measured without magnetic field).

When we use the word conductivity without further indication we always mean σ_{xx} in this report.

2.5: The quantum Hall effect

In 1980 K. von Klitzing discovered that in a very strong magnetic field in Si-MOSFETs the Hall voltage shows steps as a function of the gate voltage in a Si-MOSFET. The values of the Hall resistance

$$R_H = V_y \, / \, I_x \qquad (2.41)$$

appear to be h/ie^2 with $i = 1,2,3...$ (fig.2.6), independent of the sample in which the 2-DEG is confined. Classical principles already lead to the correct Hall voltage at integer filling factors. When we assume that

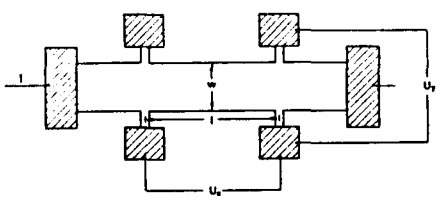

Fig.2.6a. The current is flowing through 1 and 4. V_x can be measured over 2 and 3 (4-terminal) and V_y over 2 and 5 (Hall voltage). B points in the z-direction.

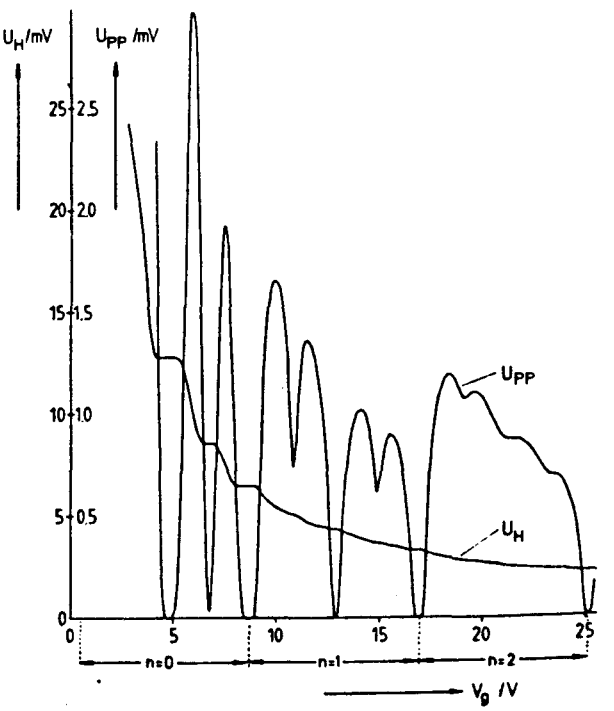

Fig.2.6b. The step-like curve is V_{25} (QHE), the oscillations are V_{23} (SdH), [1].

no current flows in the y-direction, then it follows from the Lorentz force

$$eE_y = - v_x B_z \tag{2.42}$$

and for the current density

$$j_x = - n_s e v_x = n_s e E_y/B_z . \tag{2.43}$$

The Hall resistance will be

$$R_H = \frac{V_y}{I_x} = \frac{E_y L_y}{j_x L_y} = \frac{E_y}{j_x} = \rho_{xy} = \frac{B_z}{e n_s} . \tag{2.44}$$

As long as all electrons n_s contribute to the Hall voltage, the Hall resistance will be linear in B_z. In a strong magnetic field where i spin levels are fully occupied the eB_z/h electrons in each level contribute to the Hall voltage. For integer values of the filling factor one gets a straight dependence on the number of filled levels:

$$R_H = \frac{B_z}{e} / \left(\frac{i\, e\, B_z}{h}\right) = \frac{h}{i\, e^2} \quad (i = 1,2,3,\dots) . \tag{2.45}$$

Actually, this is an oversimplified model.

Laughlin suggested a non-classical theory that results in the measured plateau resistances, and that offers an opportunity to understand localization in strong magnetic fields [22].

Von Klitzing [1,53] assumed that in the plateau region (fig.2.6b) localization of electrons prevents them from contributing to the current, when an integer number of Landau levels is filled, and D(E) at E_F is finite but small. Under this condition of an infinitely flat Hall plateau, all the electrons are moving exclusively perpendicular to the electric field. It is assumed that no diffusion originating from scattering in the direction of the electric field is possible. This explains the very low Shubnikov-de Haas minima when a plateau in σ_{xy} appears (fig.2.6b). When the Fermi-energy lies between two Landau

levels the conductivity can be thermally activated. To explain the width of the Hall plateaus it is assumed that a broad range in the density of states exists, in which the electrons of the 2-DEG are localized. As will be pointed out in section 2.7 the existence of localized states prevents the Fermi-energy to jump from one level to the other when the magnetic field increases.

2.6: Level broadening

The Landau levels (2.20) appear at discrete values, but they are broadened due to scattering. In general, one can distinguish between short-range scattering, that gives rise to large changes of the

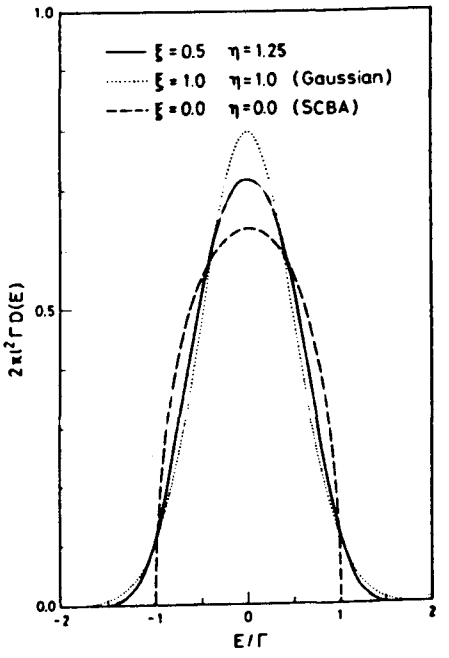

Fig.2.7. Three calculated shapes of Landau levels [22]. SCBA stands for self-consistent Born approximation [20] and includes short-range collisions.

wave vector, and long-range scattering, that does not change the momentum of the electrons very much. A typical length scale in strong magnetic fields is the magnetic length or cyclotron radius l_c. By putting this length l_c in a harmonic oscillator potential $1/2m^*\omega_c^2 l_c^2$, that is equal to the kinetic energy of the first Landau level $1/2\hbar\omega_c$, one gets

$$l_c^2 = h/eB \ . \qquad (2.46)$$

The influence of scatterers on the broadening of the Landau levels without taking into acount the spin splitting, is calculated for Si-MOSFETs by Ando et al [23,24] (fig.2.7) and later for AlGaAs/GaAs heterojunctions by Ando and Murayama [9]. It is suggested that the level width Γ is proportional to $1/\sqrt{\tau}$ where τ is the short-range scattering time without magnetic fields. Their formula for AlGaAs/GaAs is [9]

$$\Gamma_N^2 = 4 \sum_{\mu} \int dz\, N_i^{(\mu)}(z) \int \frac{dq}{(2\pi)^2} \left\{\frac{v^{(\mu)}(q,z)}{\epsilon(q)}\right\}^2 J_{NN}(q)^2 \qquad (2.47)$$

where $N_i^{(\mu)}(z)$ describes the distribution of the μth kind of impurities in the z direction perpendicular to the interface, $v^{(\mu)}(q,z)$ is the two-dimensional Fourier transform of its potential. Because the screening depends on the density of states at the Fermi-energy the shape of the Landau levels is predicted to be oscillating as a function of filling factor. Kukushkin [18] determined the

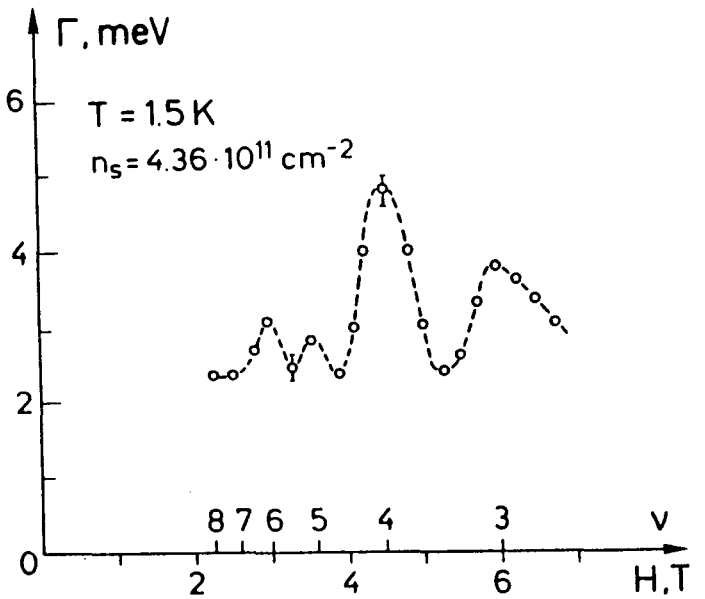

Fig.2.8. The level width as is measured by Kukushkin [18].μ is about $6.10^5 cm^2/Vs$.

width of the spin splitted Landau levels as a function of filling factor (fig.2.8). This indicates that the Landau levels overlap each other when the filling factor is an integer. The level width seems to be oscillating. The minimum of the level width in fig.2.8 is probably limited by the width of the energy distribution function of the holes that recombine with the electrons [18].

Numerical calculations of Ando and Aoki [25] on the influence of short-range scatterers show delocalization of the wave function of electrons in states near the centre of a Landau level (fig.2.9).

Experimental evidence for the influence of charged impurities on the broadening of the Landau levels is given by the measurements of Haug et al [26].

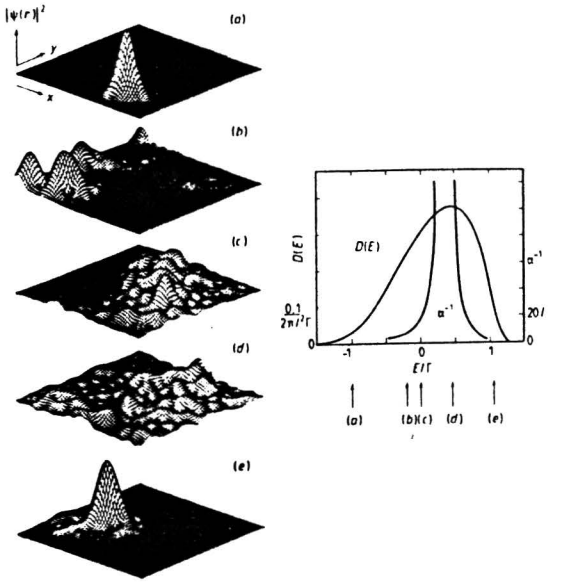

Fig.2.9 $c_i = 2\pi\, l_c^2 n_i$. n_i is the concentration of attractive short range scatterers. Left: the wave function squared. Right: the density of states D(E) and localization length α^{-1} (c_i=5) [25]. The letters indicate the corresponding figures on the left.

They carried out measurements on heterostructures with Be or Si dopants in the plane of the 2-DEG. Be is an acceptor and thus a repulsive scatterer. Si is a donor and thus an attractive scatterer. The Hall plateaus in the Be-doped sample shift to a higher magnetic field compared to the extrapolated line for the classical Hall effect (fig.2.10a). Also the minima in the SdH effect appear at non-integer filling factors. In the density of states an impurity band of localized states at the high energy side of each spin polarized level is believed to be created by scattering with the negative Be ions. This results in a higher density of localized states at the high energy side of the level. If a certain number of localized states appears at an energy that is higher than the energy of the extended states in the next level, then the conductivity has a minimum at a non-integer filling factor and the Hall plateau is shifted (fig.2.10a). In the Si-doped sample the opposite as in the Be-doped sample happens.

The level broadening and the small ranges of D(E) in which current

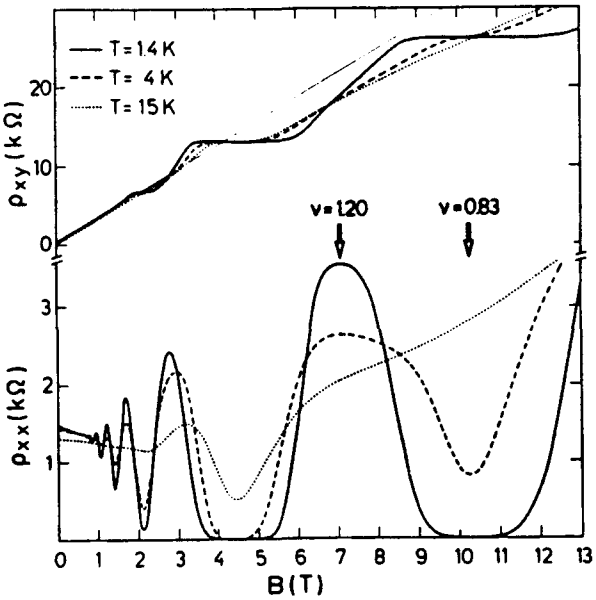

Fig.2.10a. Be δ-doping in the heterojuncion.

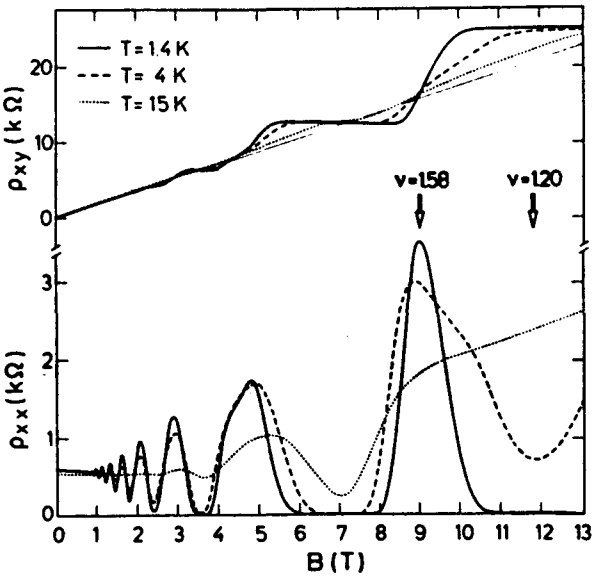

Fig.2.10b. Si δ-doping in the heterojunction.

carrying states exist, are adopted for the interpretation of our experiments. Narrow Landau levels which only contain extended states without any localized states [27] can also be used to explain the temperature dependent experiments. But this does not seem to explain the width of the Hall plateaus and the measurements of Kukushkin [18] and Haug [26]. Our model for the density of states (figure 2.11)

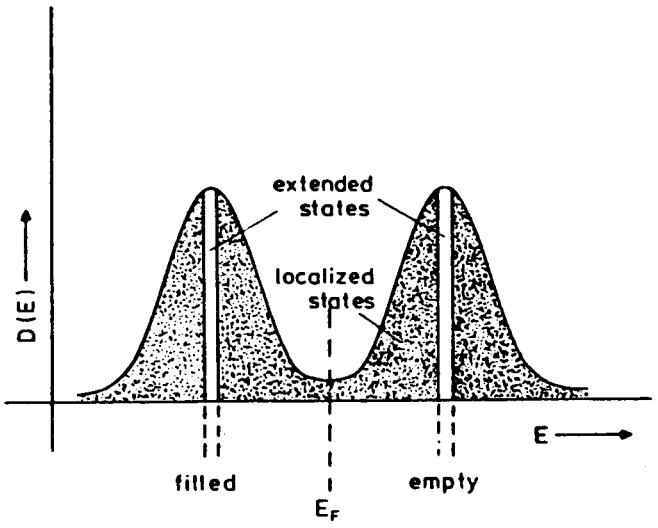

Fig.2.11. Model for the density of states.

contains symmetrically broadened levels with localized states which are defined as states in which electrons can not contribute to σ_{xx}. The states that can carry current are thought to be lying between two mobility edges at the centre of each level. The mobility edges are thought to be sharp.

Now we focus on the thermal activation of the conductivity to see how to gather information about the energy spectrum.

2.7: Activation energy

The minimum value of the conductivity corresponds to the situation in which the Fermi-energy lies between two ranges with extended states. The conductivity is assumed to be proportional to the occupation of the extended states with electrons in the next higher level or with holes in the next lower level relative to the Fermi-energy (fig.2.12). Pepper et al. [28] named this mode of conduction "excitation to the mobility edge". Consider kT to be smaller than E_a, and the level broadening to be neglegibly small. Assuming that E_F and the level broadening are both independent of the temperature we can write the Fermi-Dirac statistics in good approximation as a Boltzmann exponent

$$\sigma_{xx} = \sigma_o \exp(-E_a/kT) \qquad (2.48)$$

with equal contributions of the electrons and the holes. A plot of $\ln\sigma_{xx}$ versus $1/T$ (fig.2.13) directly gives the activation energy. Thus from the temperature dependence of σ_{xx} an estimation of the mobility gap between two levels should be obtained. The pre-factor in (2.48) can be determined by extrapolating the straight line to $1/T = 0$ (appendix B). Kawaji and Wakabayashi [29] already tried in 1977 to determine activation energies in Si-MOSFETs, followed by Englert and von Klitzing [30] and Nicholas et al [31]. They used a gate to manipulate the electron density. Paalanen, Tsui and Gossard [66] did a preliminary study on the temperature dependence of σ_{xx} in an AlGaAs/GaAs heterojunction. Tausendfreund and von Klitzing [32] reported on activation energies in both materials. These values are in reasonable agreement with the values deduced from the cyclotron energy at high magnetic fields ($B > 10$ T) but they are smaller than the

values expected in low magnetic fields. In 1984 von Klitzing et al [33] reported in 1984 on activation energies in both Si-MOSFETs and AlGaAs/GaAs heterojunctions

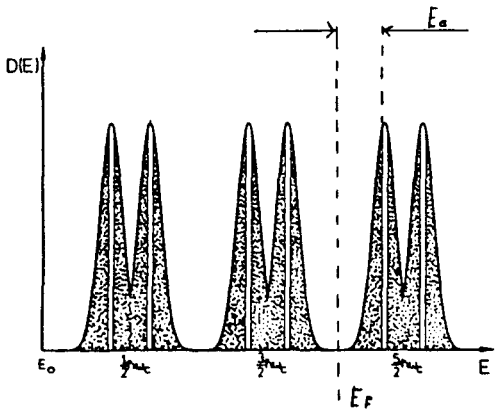

Fig.2.12. Thermally activated conductivity from the electrons respectively holes in the extended states.

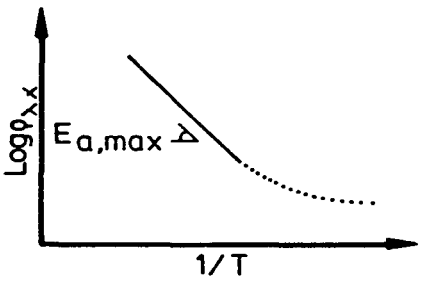

Fig.2.13. Determination of the activation energy. The hopping tail showing up at lower temperatures.

between spin and Landau levels. They measured the SdH effect in Si-MOSFETs using a gate. The AlGaAs/GaAs data in different fields, however, were obtained in structures with different electron densities. They found activation energies between Landau levels which clearly exceed the expected values.

Kleinmichel [33,34] carried out measurements on Si-MOSFETs with gates and determined activation energies in several Landau minima and in the two spin minima with Landau quantum numbers N = 0 and 1, for magnetic fields between 6 and 14 Tesla. In the perpendicular case the

activation energy for the first Landau minimum (between N = 0 and N = 1) is found to be almost equal to $1/2\hbar\omega_c$. For higher filling factors this is measured in magnetic fields of the same range, thus having the same the same number of electrons per Landau level. For larger filling factors the activation energy is found to be smaller relative to $1/2\hbar\omega_c$, than for smaller filling factors. He suggested this effect to be due to an increasing line width [34]. Between two spin levels the activation energy as a function of electron density in perpendicular fields higher than 6 Tesla shows a linear increase with magnetic field and the extrapolation of this straight line approximately goes through zero for zero magnetic field. The constant g-factor g^* that is belonging to each straight line is found to be 3.8 for the spin splitting of the second Landau level (N=1), and lies between 8 and 9 for the spin splitting of the first Landau level (N=0). Earlier, Englert et al [49] reported on a large g-factor (g^*=5) in an AlGaAs/GaAs heterojunction in perpendicular magnetic fields. They fitted SdH oscillations for different temperatures.

Kleinmichel also measured the activated conductivity by adding a parallel magnetic field with maximum tilt angles of about 70^o in magnetic fields larger than 6 Tesla. For the first two Landau minima he found in both cases a linear decreasing activation energy. He expected this to be due to an increasing spin splitting caused by the increasing total field. This decreasing activation energy would have given constant g-factors g^* in the range of 2.4 to 3.8. Apparently, this was not found to be a satisfactory explanation. His measurements with the Fermi-energy between two spin levels in a tilted field with a constant perpendicular component show a linear increasing activation energy as a function of the total magnetic field. Extrapolation to

$B_{tot} = 0$ leads to a positive intersection with the energy axis. The slope of the linear curve suggests a constant g-factor of 2.4. Kleinmichel made the comment that the behaviour in tilted fields is not very clear and he restricted himself to the definition of g^* without an interpretation. Nicholas [51] mentioned that the g-factor g^* as determined by activation energies in a number of AlGaAs/GaAs heterojunctions in untilted samples is $\simeq 7.5$ for both filling factors $\nu = 1$ and $\nu = 3$ and for densities with magnetic fields of about 2 to 9 Tesla. He also reported on the enhancement of the Landau splitting in the same samples.

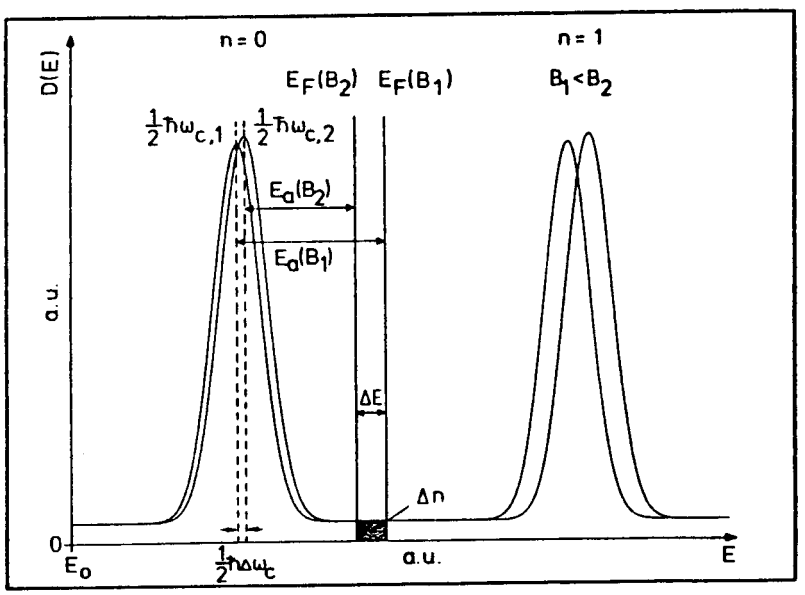

Fig.2.14 Determination of the thermodynamical density of states (DOS).

Stahl and Weiss [35] used activated resistivities in AlGaAs/GaAs to investigate how fast the Fermi-energy moves as a function of the perpendicular field to determine dn/dE_F, which is equal to the

thermodynamical density of states. In this report the thermodynamical density of states, which is defined as dn/dE_F, is named DOS. An increase in B_z results in a higher degeneracy of each level (fig.2.14). The level absorbs Δn electrons and E_F shifts to another E_a.

$$\Delta n = e\ \Delta B_z/h \tag{2.49}$$

and

$$DOS = \frac{e}{h}\frac{\Delta B_z}{\Delta E_a} \tag{2.50}$$

neglecting any change of $1/2\hbar\omega_{cz}$ or the mobility edges. Δn should be small compared to n_s. With E_F in the middle of the two levels one has to calculate the contributions from both levels thus [29]

$$\sigma_{xx} = \sigma_{o1}\ \exp(-E_{a1}/kT) + \sigma_{o2}\ \exp(-E_{a2}/kT)\ . \tag{2.51}$$

This DOS appeared to be considerable and constant in the region between two Landau levels [35]. Stahl [36] fitted the equivalent of (2.48) for ρ_{xx} with a pre-factor ρ_o being constant and also with ρ_o being proportional with 1/T and with T. He found that it is very difficult to determine the DOS in samples with mobilities higher than about 5.10^5 cm^2/Vs.

Gavrilov and Kukushkin [37] used gated Si-MOSFETs and showed that the same kind of flat DOS between Landau levels can be obtained in Si-MOSFETs as in AlGaAs/GaAs heterojunctions. They found evidence that this DOS is dependent on the parameter $\mu H = \omega\tau$ and suggested that not only weak short-range scattering is important when the Fermi-energy lies between two Landau levels. Gudmundsson and Gerhardts [38] found good agreement of these activation measurements and their theory for the DOS based on statistical inhomogeneities. Shaskin et al [39] compared different experimental methods for determining the DOS.

A second dissipative process which can be responsible for an exponential temperature dependence of the conductivity is variable range hopping, i.e. electron tunneling between states within an energy range of order kT around E_F on short distances in real space [40]. The temperature dependence for hopping is in general described by [41]

$$\sigma_{xx} = \frac{\alpha}{T^{\beta}} \exp(-T_o/T)^{\gamma} \qquad (2.52)$$

with a characteristic temperature T_o. For two dimensions Mott's model resulted in $\beta = 0$, $\gamma = 1/3$. Different experimentalists explained their measurements by Mott's model [28,42,43]. Later, in 1982 Ono [67] published a theory using the percolation theory of hopping conduction in disordered systems. He finds $\beta = 1$, $\gamma = 1/2$, and Ebert et al [41] found in AlGaAs/GaAs heterostructures better agreement with Ono's theory than with Mott's model. The typical temperature range for hopping is found to be 0.25 - 0.03 K and is indicated in fig.2.13.

From the previously mentioned thermally activated conductivities it is expected that the increasing spin splitting will affect the activation energies in AlGaAs/GaAs heterojunctions at even filling factors. But because the bulk g-factor in GaAs is five times smaller than in bulk silicon this effect is foreseen to be very small. The activation energies at an odd filling factor in an AlGaAs/GaAs heterojunction between two spin levels are already measured by Haug et al [44]. For their results we refer to chapter 5, where they are shown together with our measurements.

Chapter 3: Experimental methods

3.1: The set up

The experiments are essentially DC-voltage measurements as is explained in the next section, and are carried out in a top loading Oxford Instruments cryostat with a superconducting coil. Magnetic fields up to 14.3 T are generated for which a maximum current of 111.72 A is needed. The magnetic field has a vertical direction, which is defined as the z direction. The cryostat is shown in figure 3.1, and the sample holder for measurements in helium-4 ($T > 1.4$ K) in figure 3.2. For measurements at lower temperatures a specially prepared helium-3 insert is placed in the VTI (Variable Temperature Insert, fig.3.1). It consists of a similar sample holder like in fig.3.2, but enclosed in an extra partially thermal isolating shield and connected to a helium-3 reservoir. Around the sample inside this closed circuit can circulate helium-3. In the optical experiments the radiation that is transmitted by the sample, is let through by a window. Underneath this window the radiation is detected by a resistor (bolometer). This construction is provided to achieve thermal insulation of the bolometer.

The temperature at the sample can be regulated by lowering the vapour pressure of the helium in the VTI, or by heating with the current device underneath the sample holder. This heater can also be used in gaseous helium ($T \geq 4$ K) to stabilize the temperature in combination with the magnetic field insensitive capacitor.

The temperature in the helium-3 system is determined by using the pressure at the top of a capillar, that is reaching to the sample. This pressure measurement is calibrated by means of a germanium

four-terminal temperature sensor without magnetic field. The germanium resistor is sensitive to the magnetic field, thus it is necessary to use the pressure for a reproducible temperature measurement. The calibration is done twice, namely under the conditions of a slow and a fast changing pressure. However, this did not lead to significant differences. The measurements in helium-4 are done with a calibrated four-terminal carbon resistor. This calibration was corrected for the slight sensitivity to the magnetic field.

The DC-type measurement for one fixed temperature is carried out by, first, choosing the pressure, which is the vapour pressure of the helium. When the pressure is stabilized, the temperature is determined with help of the temperature sensor, which is corrected for the magnetic field. The current through the coil is used to find the value of the magnetic field. The determination of the temperature is followed by sweeping the magnetic field high with the voltage source for the sample switched on, and sweeping it down with the voltage source switched off. During these sweeps σ_{xx} is recorded in order to determine σ_{xx} around a SdH minimum. Then, the pressure and the resistance are registrated again. This procedure is repeated for different temperatures, starting at about 10 K and going down to 1.5 K. One such a temperature run results in a value for the activation energy. Before and after each series of temperature dependent measurements for a fixed tilt angle the complete SdH curve is recorded. This serves as a check on the electron density in the 2-DEG. The temperature dependent measurements are carried out for different tilt angles. The sample has not been warmed up during one series of tilt angles. The measurements are done for different filling factors.

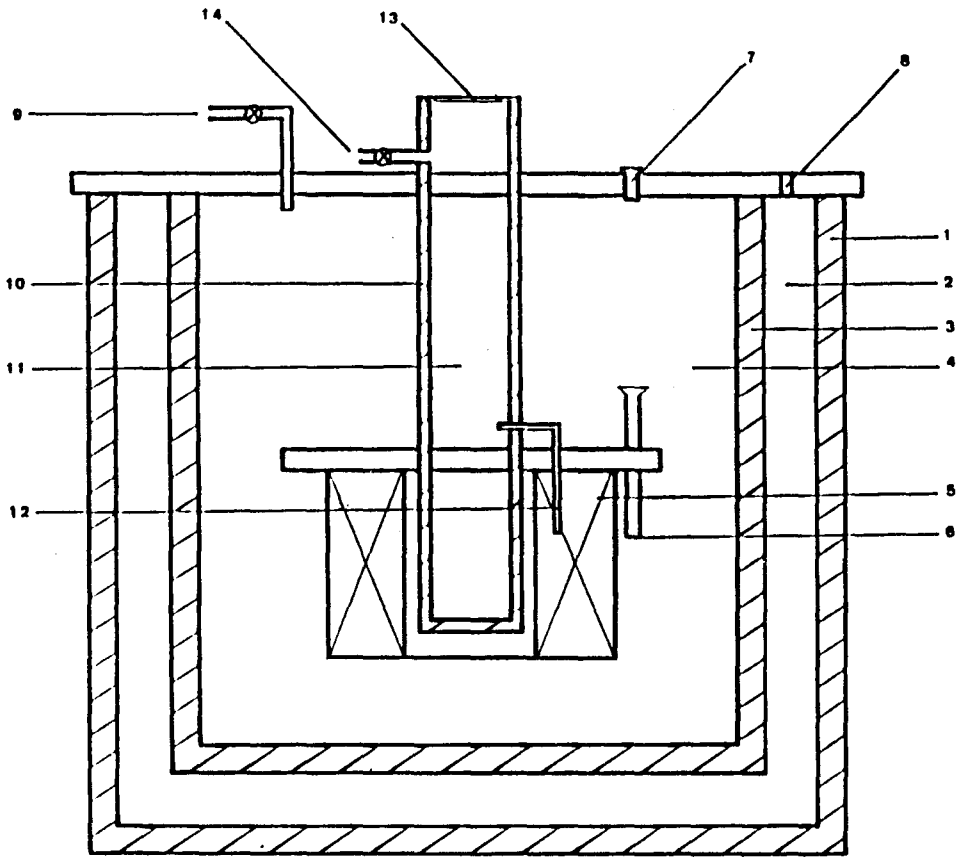

um one
id nitrogen vessel
um two
id helium-4 bath
-2.2 K)
rconducting coil
ing capillary
ance for a helium siphon
ing to fill the nitrogen
el
um pump for the bath
the coil
vacuum
chamber for helium-4
um-4 capillar into VTI
heater and external valve
ance for sample holder
um pump to the VTI

The Oxford Instruments cryostat. The opening in top (12) is as entrance for the sample holder or, if needed, for the insert.

1. sample holder
2. rotation gear for the sample
3. radiation shield
4. connections to sample contacts
5. rotation wheel on sample holder
6. sample
7. carbon-resistance temperature sensor
8. heater
9. capacitor

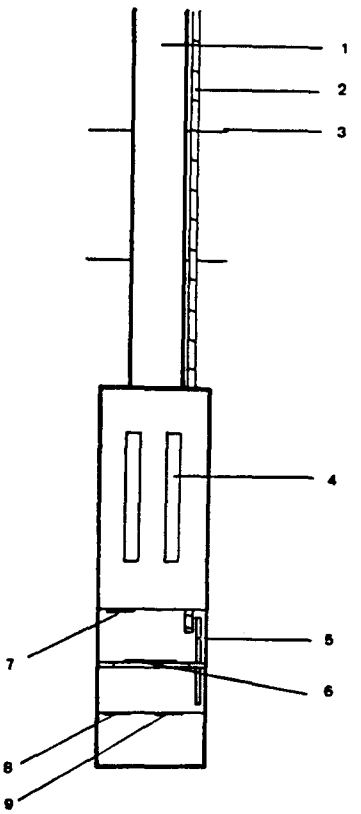

Fig.3.2 The helium-4 sample holder and the helium-3 insert as constructed around a similar sample holder for two samples.

The cyclotron resonance experiment is carried out as a far-infrared transmission measurement at a fixed temperature. The resistance of the bolometer is sensitive to the intensity of the transmitted radiation. The light of the laser has a fixed frequency. A peak in the absorption takes place when the cyclotron energy is equal to the energy of the radiation. The magnetic field is swept up and down to find the magnetic field where the cyclotron resonance takes place.

3.2: The samples

Both samples are single $Al_xGa_{1-x}As/GaAs$ heterojunctions with silicon dopants in $Al_xGa_{1-x}As$. The spacer is consisting of undoped $Al_xGa_{1-x}As$ near the interface with GaAs. The samples have Au/Ge circular contacts known as disc or Corbino geometry. The outer contact is simultaneous current contact for a Hall bar geometry (fig.3.3). For more information about the preparation of the contacts we refer to [54].

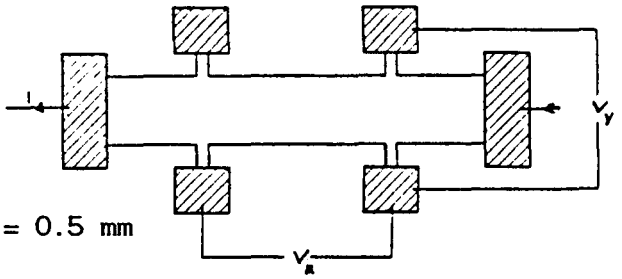

r_i = 0.5 mm

r_a = 0.7 mm

w = 0.40 mm

l = 1.0 mm

$\ln(r_a/r_i)/2\pi$ = 0.05355

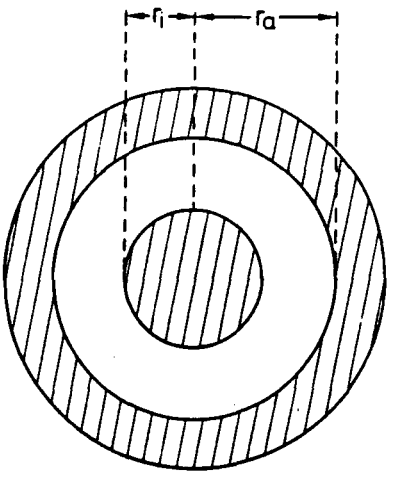

Fig.3.3 The Corbino and the Hall bar geometry. The contacted regions are shaded.

R_{shunt}: 1kΩ

V_s: 1 mV (fixed)

V_s: Keithley 230 programmable voltage source

V_m: EM dc nanovoltmeter Model 1a (battery-source) connected to a Philips PM 8133 xy-recorder

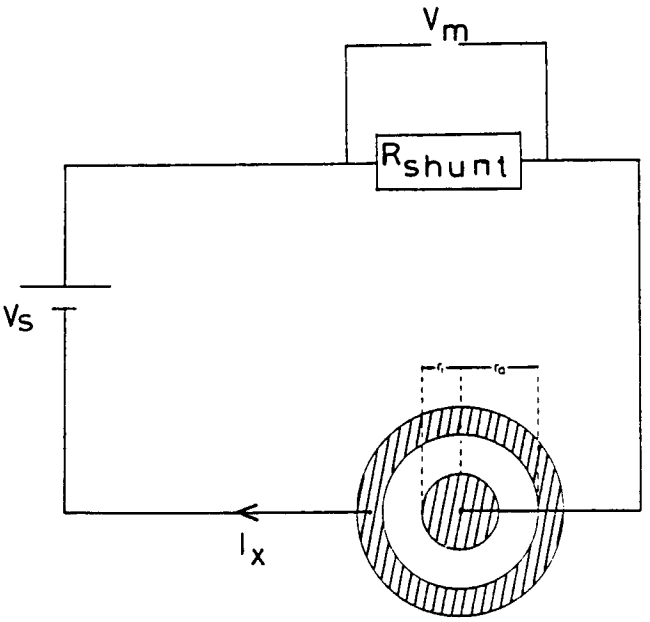

Fig.3.4 The measured value is V_m, the flowing current is $I=V_m/R_{shunt}$, the voltage over the sample is V_s-V_m.

Table 3.1

	μ (cm^2/Vs)	n_s (cm^{-2})	x %	doped range (nm)	spacer (nm)
W1527b	6.1 10^5	1.45 10^{11}	35	35	43.0
W1561b	9.3 10^5	2.59 10^{11}	39	43	27.0

The formulas for the Hall bar geometry are

$$\rho_{xx} = \frac{1}{w} V_x/I_x \ , \quad \rho_{xy} = V_y/I_x \qquad (3.1)$$

and for the Corbino geometry ($r_a-r_i \ll r_a+r_i$)

$$\sigma_{xx} = j_x/E_x = \ln(r_a/r_i)/2\pi \ \frac{I_x}{(V_s-V_m)} \ . \qquad (3.2)$$

When $V_m \ll V_s$ then

$$\sigma_{xx} \ /[\Omega^{-1}] \ = 54 \ I \ /[A] \ . \qquad (3.3)$$

The Hall geometry is used to determine μ at 4.2 K. The contact resistances of the Corbino structures can be estimated when μ is assumed to be the same for both structures on the same sample. With

$\sigma_{xx}(B=0)$ from the Hall structures it follows that the contact resistances are 32 Ω (W1527b) and 16 Ω (W1561b). The disadvantage of corbino contacts compared to a Hall bar geometry is that contact resistances can be important. However, it will turn out in chapter 4 that they are neglegible in our experiments. The advantage of the corbino geometry is that it is a direct measurement of σ_{xx}.

The voltage source generates an extra 'offset' voltage of 40 ± 2 μV which appears to be the main source for our offset signal. Actually, due to the offset, V_s is not 1 mV but 1.040 mV, thus the difference between the offset signal and the signal with the voltage source set-on is V_m. Finally, we note that all the series of measurements are done without changing the direction of the current and the magnetic field, in order to avoid asymmetry effects. Tests with reversed magnetic field and current do not indicate that this would lead to different results.

Chapter 4

Thermally activated conductivity in tilted magnetic fields

Under the assumption of a constant electron density in the 2-DEC the degeneration per level and the filling factor will be dependent on the quantizing component of the magnetic field, i.e. B_z, only. This means that for different tilt angles a minimum in the Shubnikov-de Haas oscillations always has to appear at the same value of the perpendicular field. Thus the value of the total magnetic field at which a certain minimum appears, has to increase with increasing tilt angle. In other words, for a certain minimun we add a parallel field to the perpendicular component by tilting the sample. Figure 4.1 shows the SdH effect with different tilt angles. The angle is determined by

$$B_z = \cos\varphi . B_{tot} \qquad (4.1)$$

in one or if possible more SdH minima, with B_z and n_s are determined in the untilted case. By reading the tilt angle from the sample holder it is checked that the minima always appear at the same value of the perpendicular field. The accuracy of (4.1) is limited by the error in the 1/B period of the SdH oscillations at zero angle and the deviation from zero degrees in this case. For large angles the accuracy is better than 0.05^{o}.

In fig.4.1 we see that with increasing parallel field the spin minimum at $\upsilon = 1$ decreases. The number of occupied extended states around the Fermi-energy decreases when the energy difference between the Fermi-energy and the extended states increases. Thus the decreasing spin minimum indicates an increase of the spin splitting. The Landau minima at $\upsilon = 2$ and $\upsilon = 4$ become shallower, thus they indicate a decreasing energy difference of the Fermi-energy and the

neighbouring mobility edges at even filling factors. This is further investigated by measuring the temperature dependence in the SdH minima.

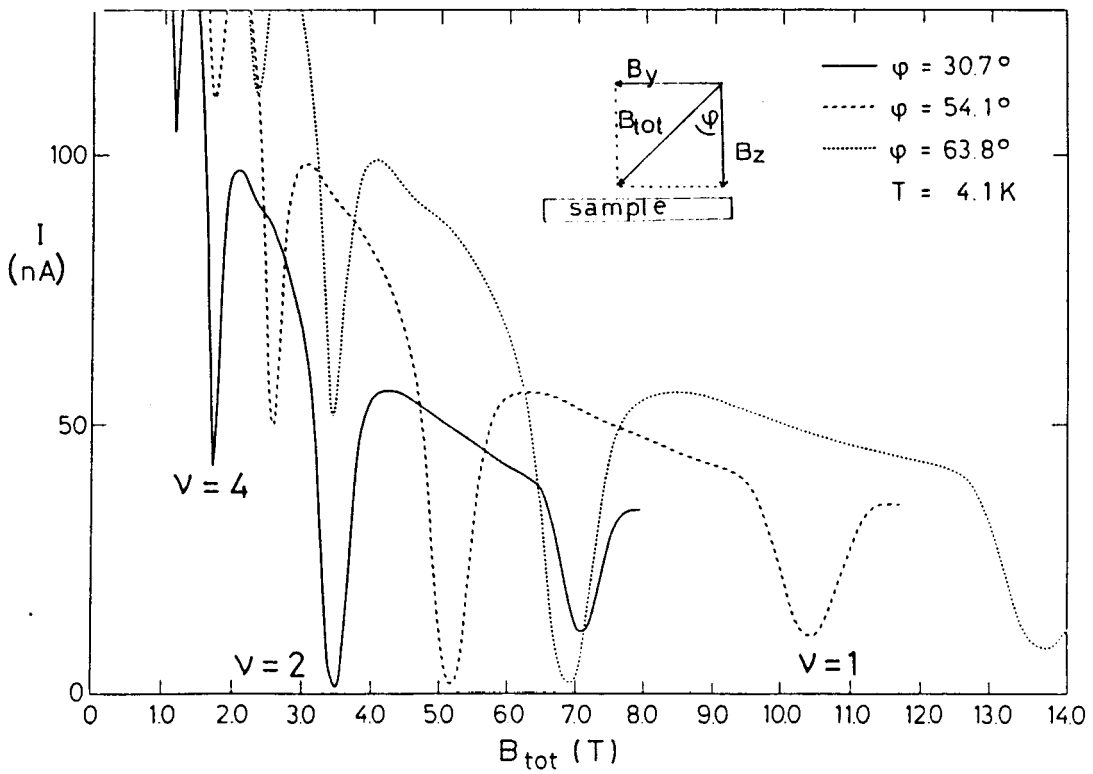

Fig.4.1 Measured SdH effect with different parallel fields (W1527b).

An example of the SdH effect at different temperatures is shown in fig.4.2a and fig.4.2b. To determine the values of σ_{xx} one magnetic field is chosen corresponding to the minimum at the lowest temperature. The conductivity is plotted logarithmically versus 1/T (W1527b: fig.4.3a-f). For sample W1561b the measurements are not carried out as systematically as on W1527b, but only as a check to see if the observed behaviour is not unique (fig.4.4a-f).

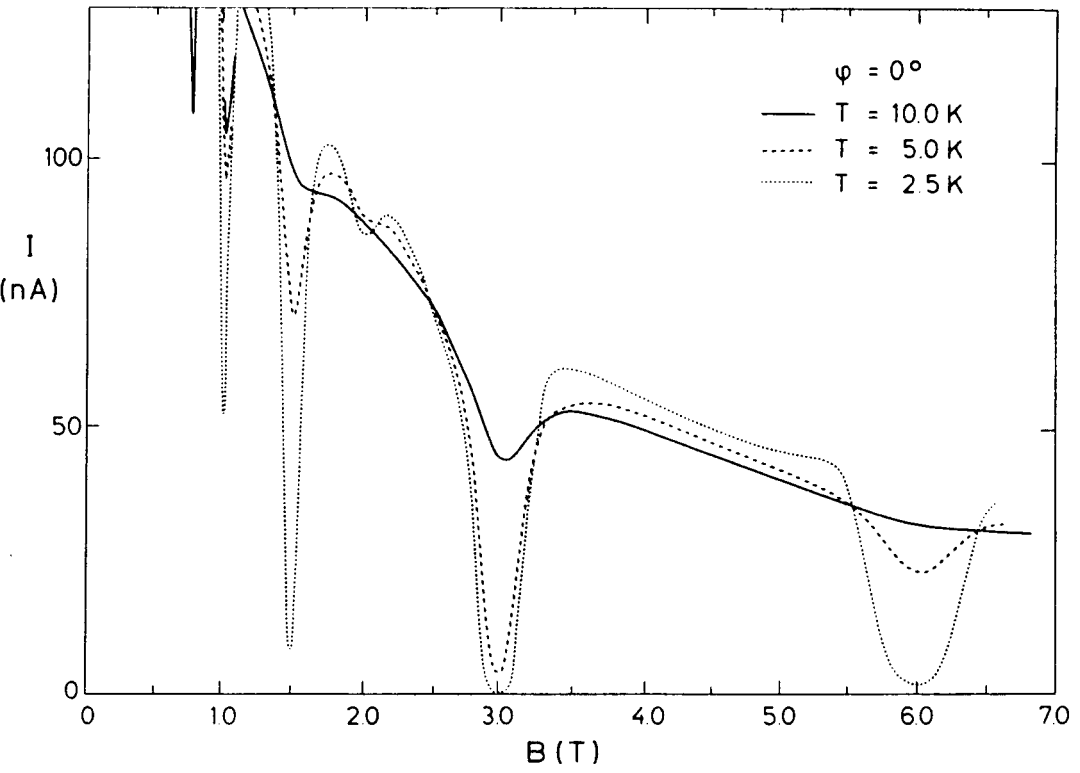

Fig.4.2a. SdH effect at different temperatures (W1527b).

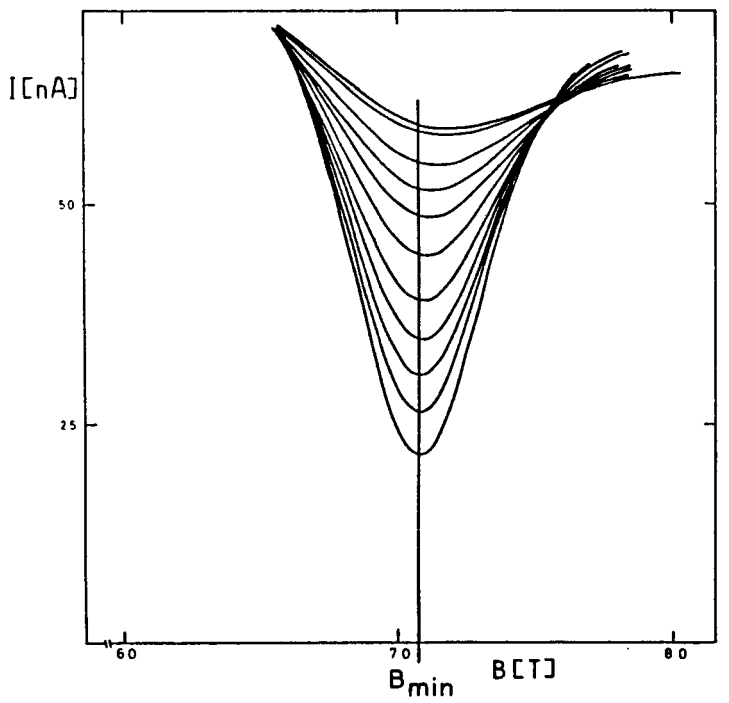

Fig.4.2b. Temperature dependence in more detail (υ = 6, φ = 82.0°, W1527b).

Fig.4.3a W1527b υ = 1

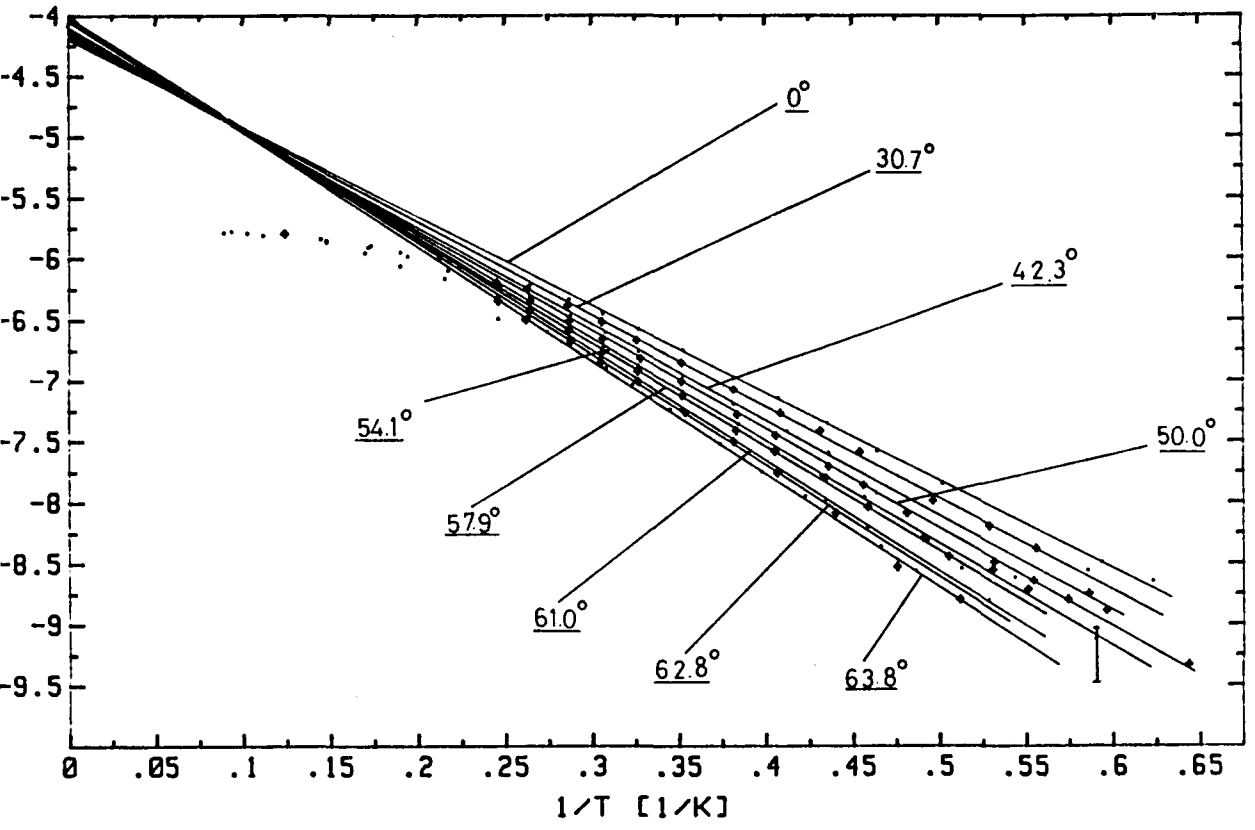

Fig.4.3b W1527b v = 2

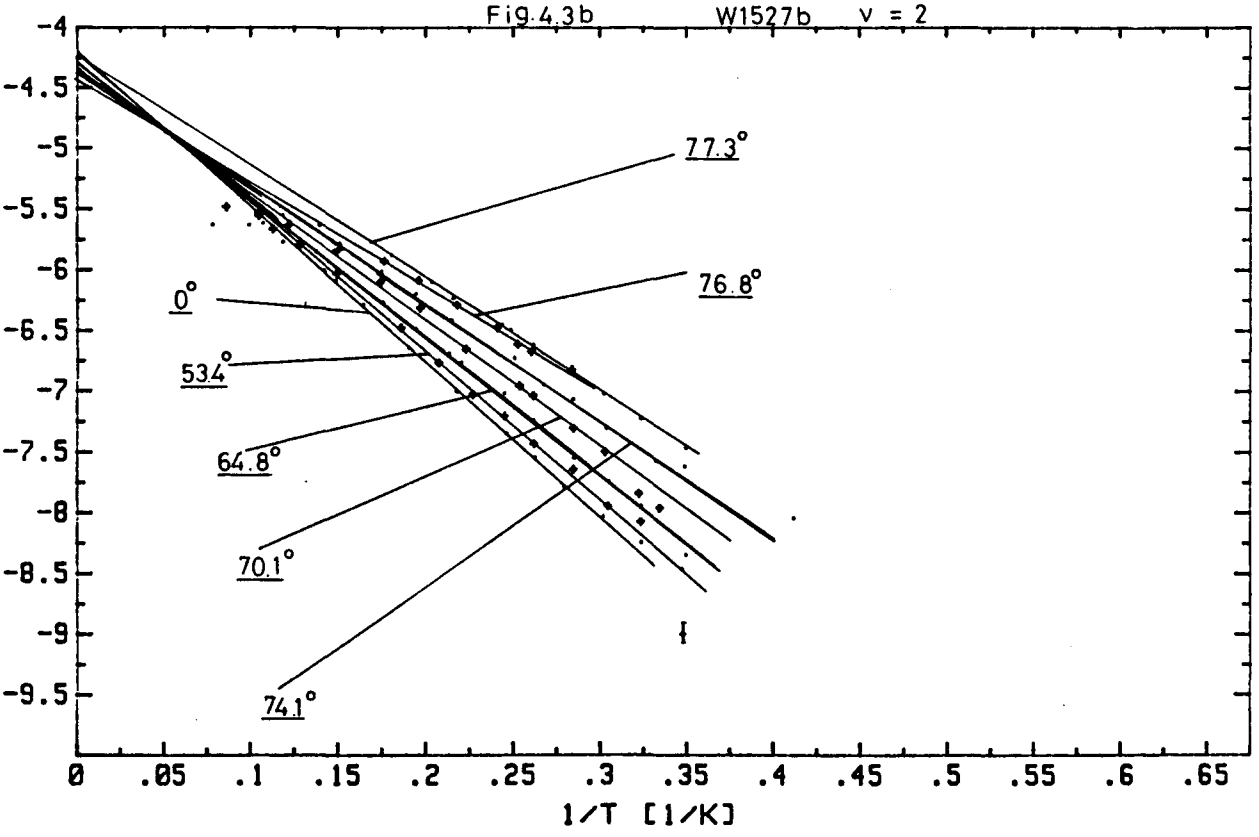

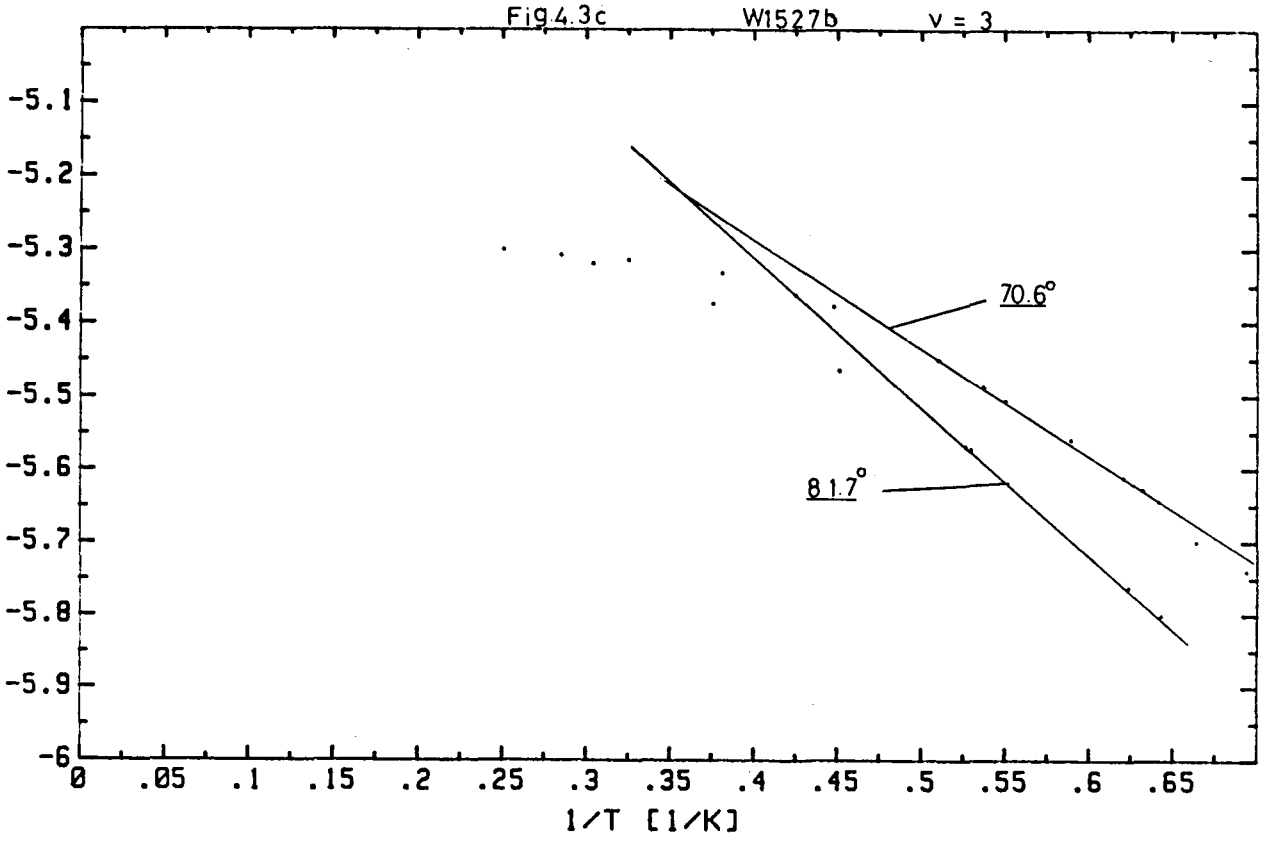
Fig.4.3c
W1527b
v = 3
-5.1
-5.2
-5.3
-5.4
-5.5
-5.6
-5.7
-5.8
-5.9
-6
70.6°
81.7°
0
.05
.1
.15
.2
.25
.3
.35
.4
.45
.5
.55
.6
.65
1/T [1/K]

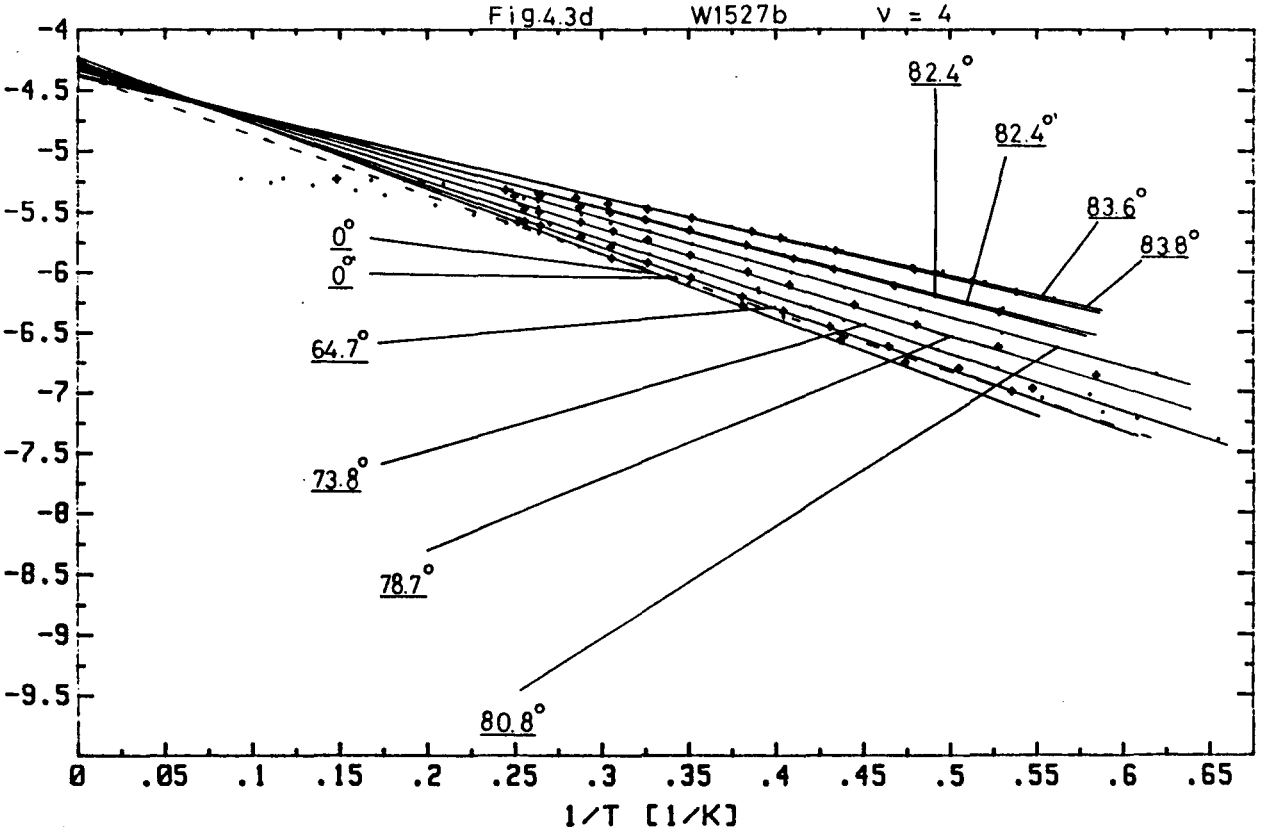
Fig.4.3d
W1527b
v = 4
-4
-4.5
-5
-5.5
-6
-6.5
-7
-7.5
-8
-8.5
-9
-9.5
82.4°
82.4°
83.6°
83.8°
0°
0°
64.7°
73.8°
78.7°
80.8°
0
.05
.1
.15
.2
.25
.3
.35
.4
.45
.5
.55
.6
.65
1/T [1/K]

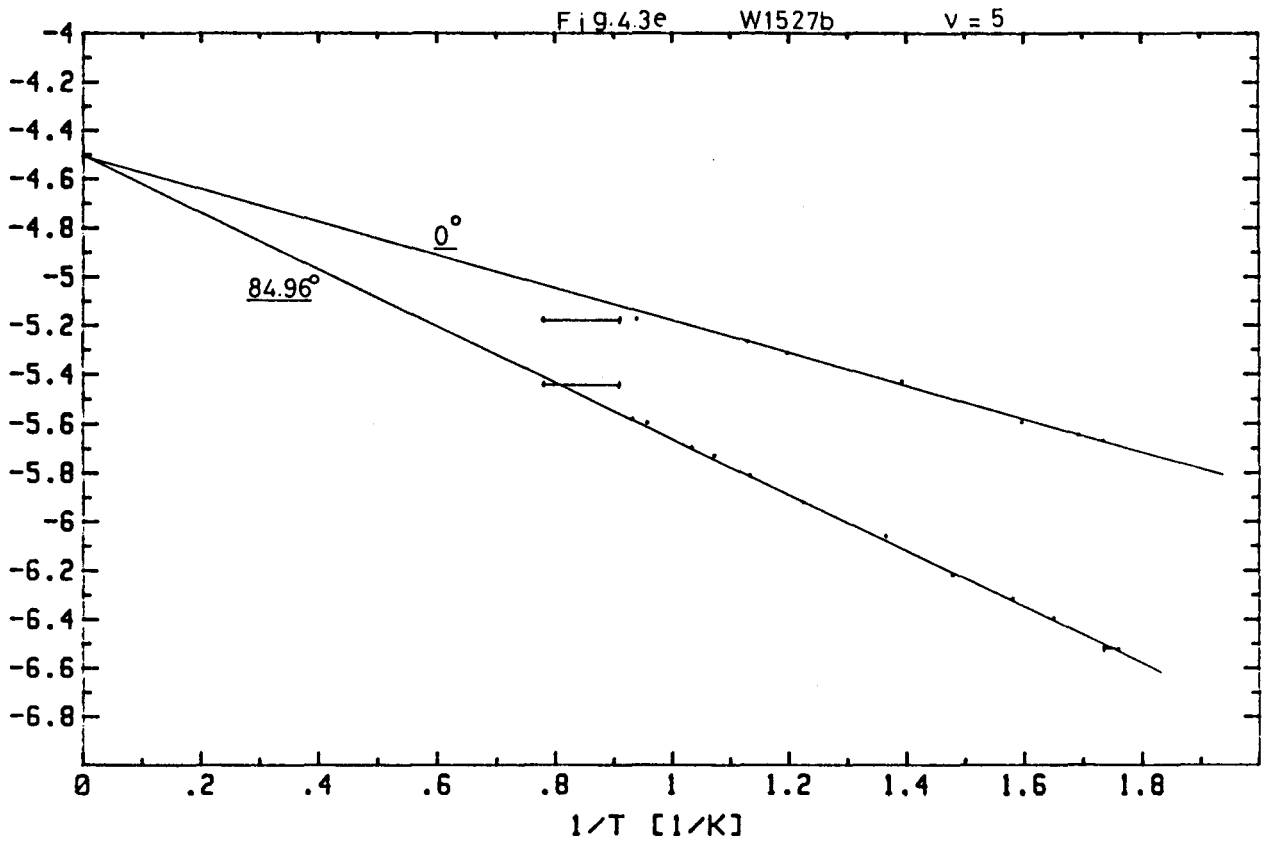
Fig.4.3e W1527b ν = 5
-4
-4.2
-4.4
-4.6
-4.8
-5
-5.2
-5.4
-5.6
-5.8
-6
-6.2
-6.4
-6.6
-6.8
0°
84.96°
0
.2
.4
.6
.8
1
1.2
1.4
1.6
1.8
1/T [1/K]

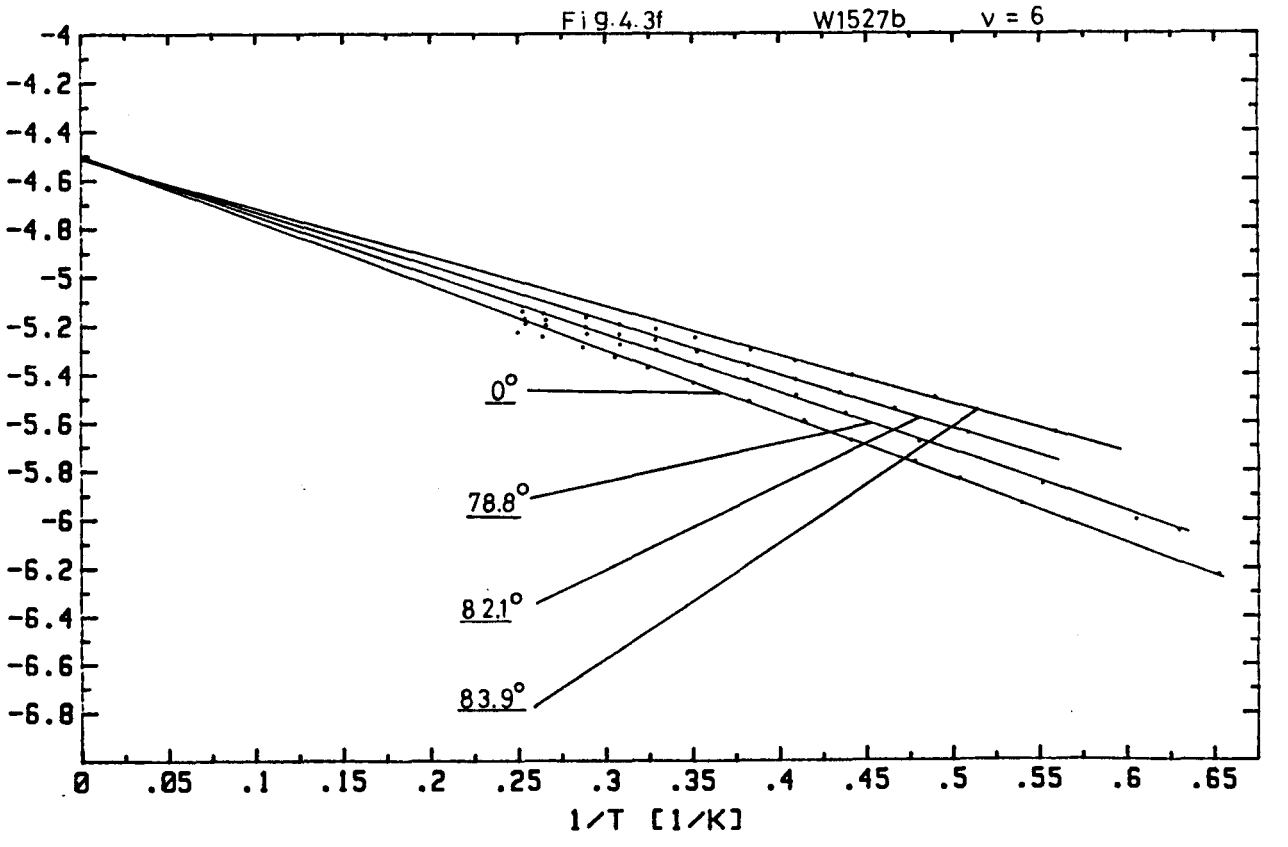
Fig.4.3f W1527b ν = 6
-4
-4.2
-4.4
-4.6
-4.8
-5
-5.2
-5.4
-5.6
-5.8
-6
-6.2
-6.4
-6.6
-6.8
0°
78.8°
82.1°
83.9°
0
.05
.1
.15
.2
.25
.3
.35
.4
.45
.5
.55
.6
.65
1/T [1/K]

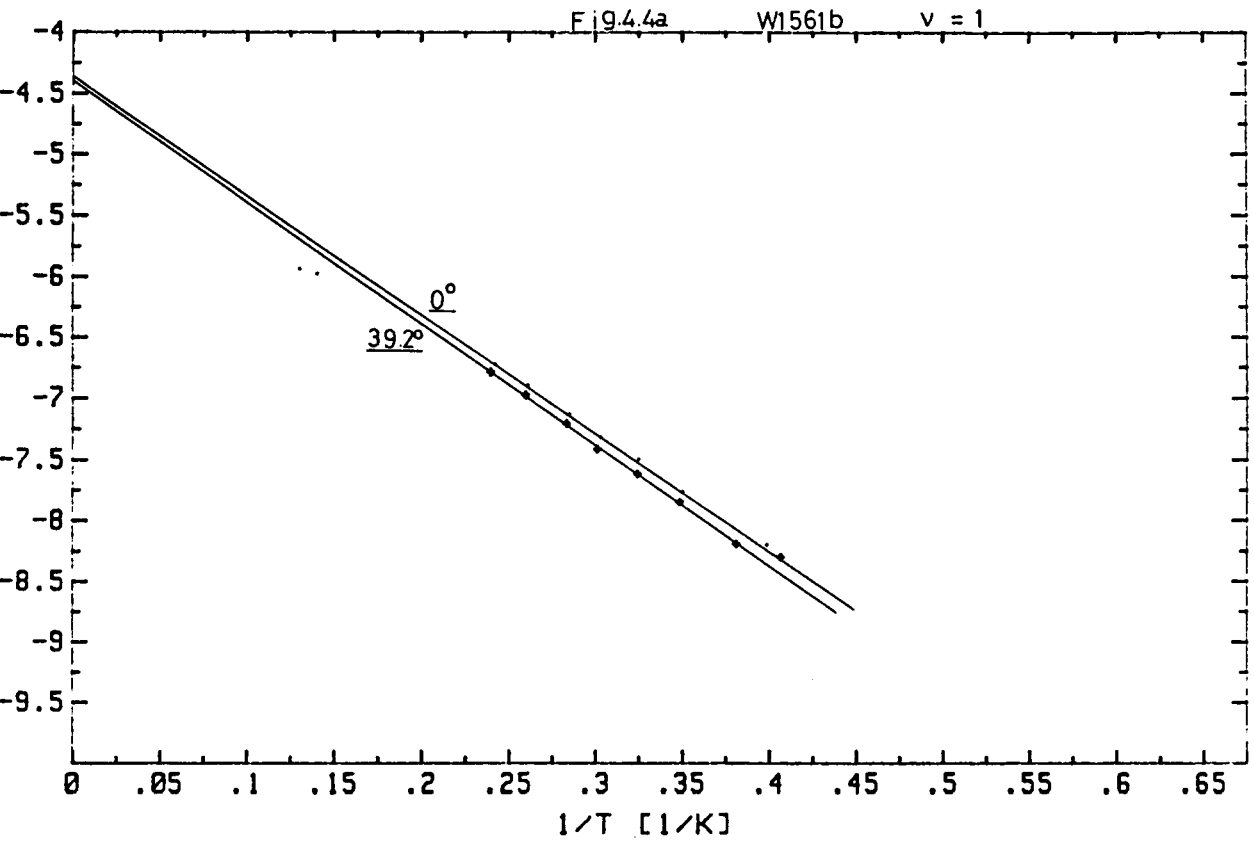
Fig.4.4a W1561b v = 1
-4
-4.5
-5
-5.5
-6
-6.5
-7
-7.5
-8
-8.5
-9
-9.5
0°
39.2°
0 .05 .1 .15 .2 .25 .3 .35 .4 .45 .5 .55 .6 .65
1/T [1/K]

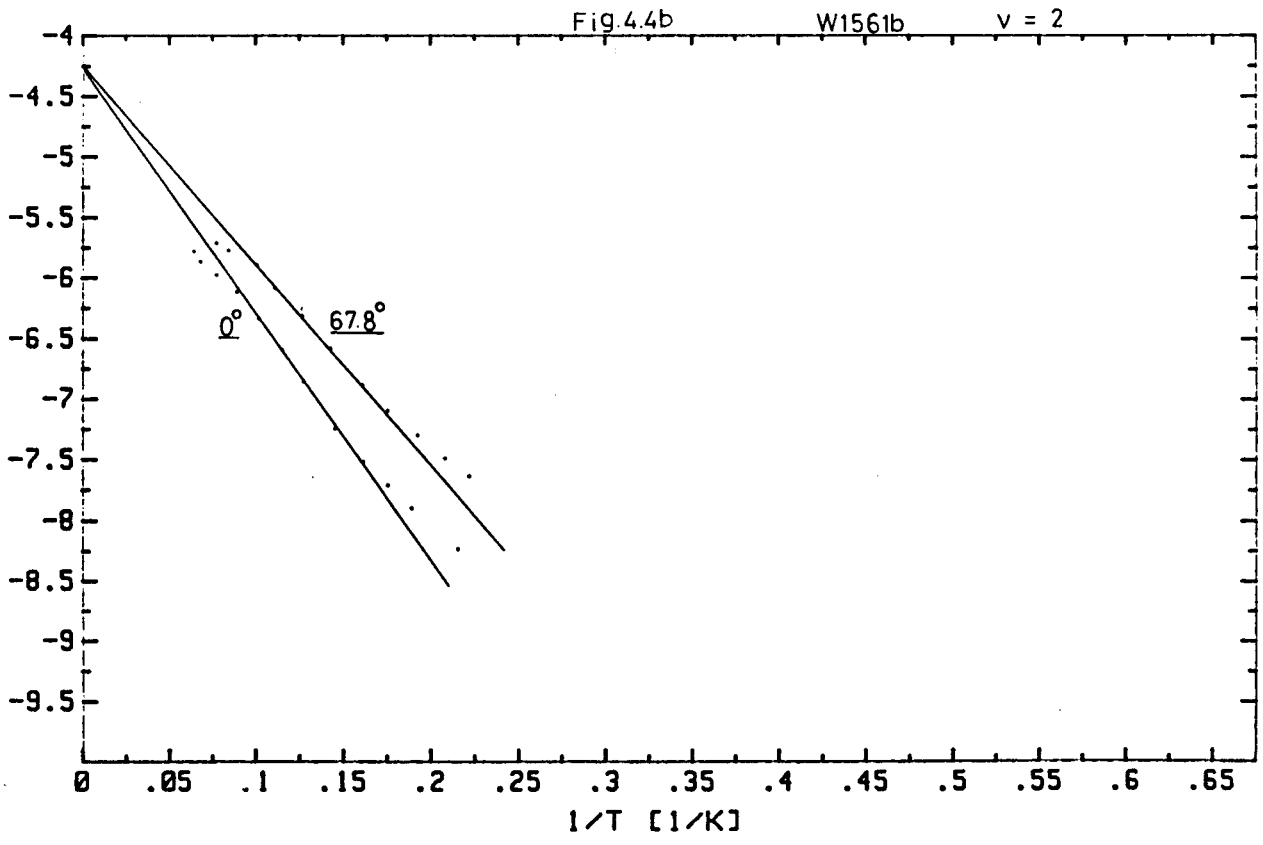
Fig.4.4b W1561b v = 2
-4
-4.5
-5
-5.5
-6
-6.5
-7
-7.5
-8
-8.5
-9
-9.5
0°
67.8°
0 .05 .1 .15 .2 .25 .3 .35 .4 .45 .5 .55 .6 .65
1/T [1/K]

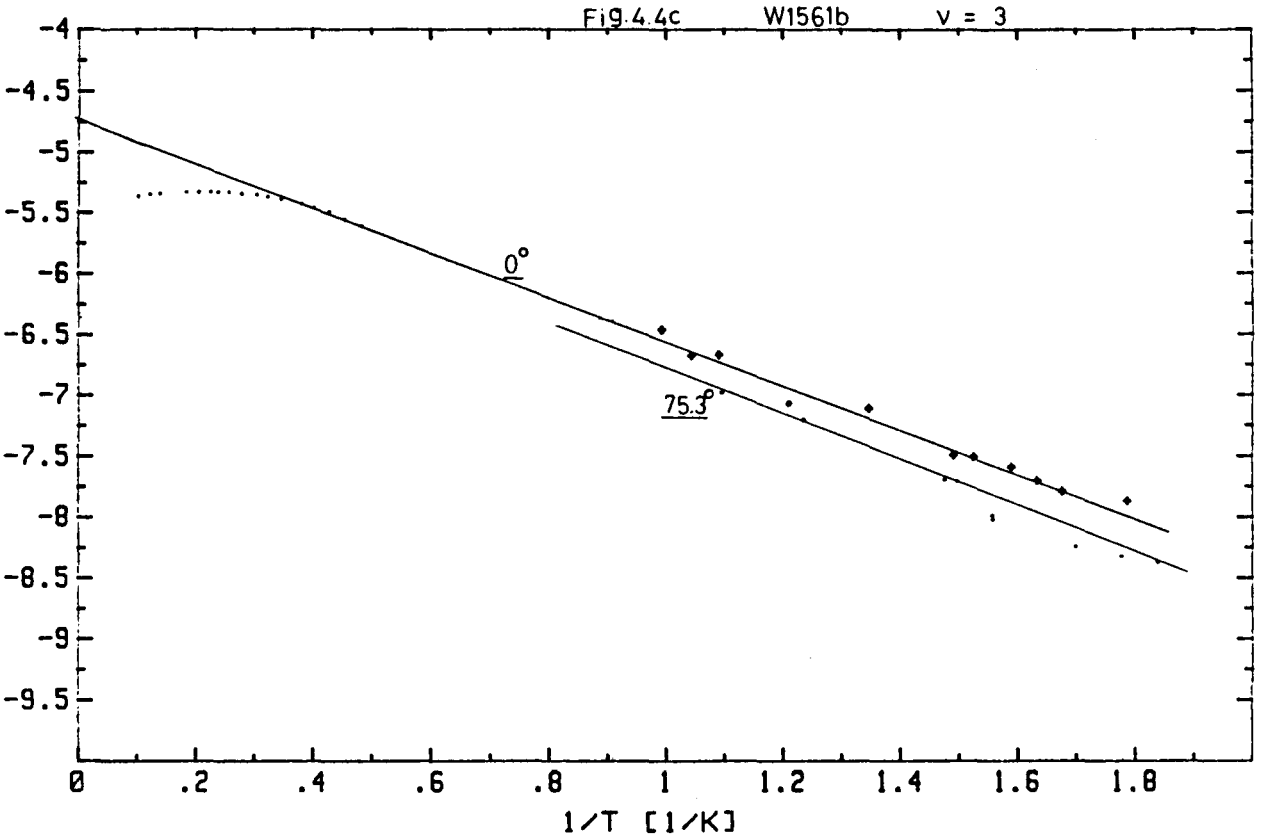
Fig.4.4c W1561b v = 3
-4
-4.5
-5
-5.5
-6
-6.5
-7
-7.5
-8
-8.5
-9
-9.5
0°
75.3°
0
.2
.4
.6
.8
1
1.2
1.4
1.6
1.8
1/T [1/K]

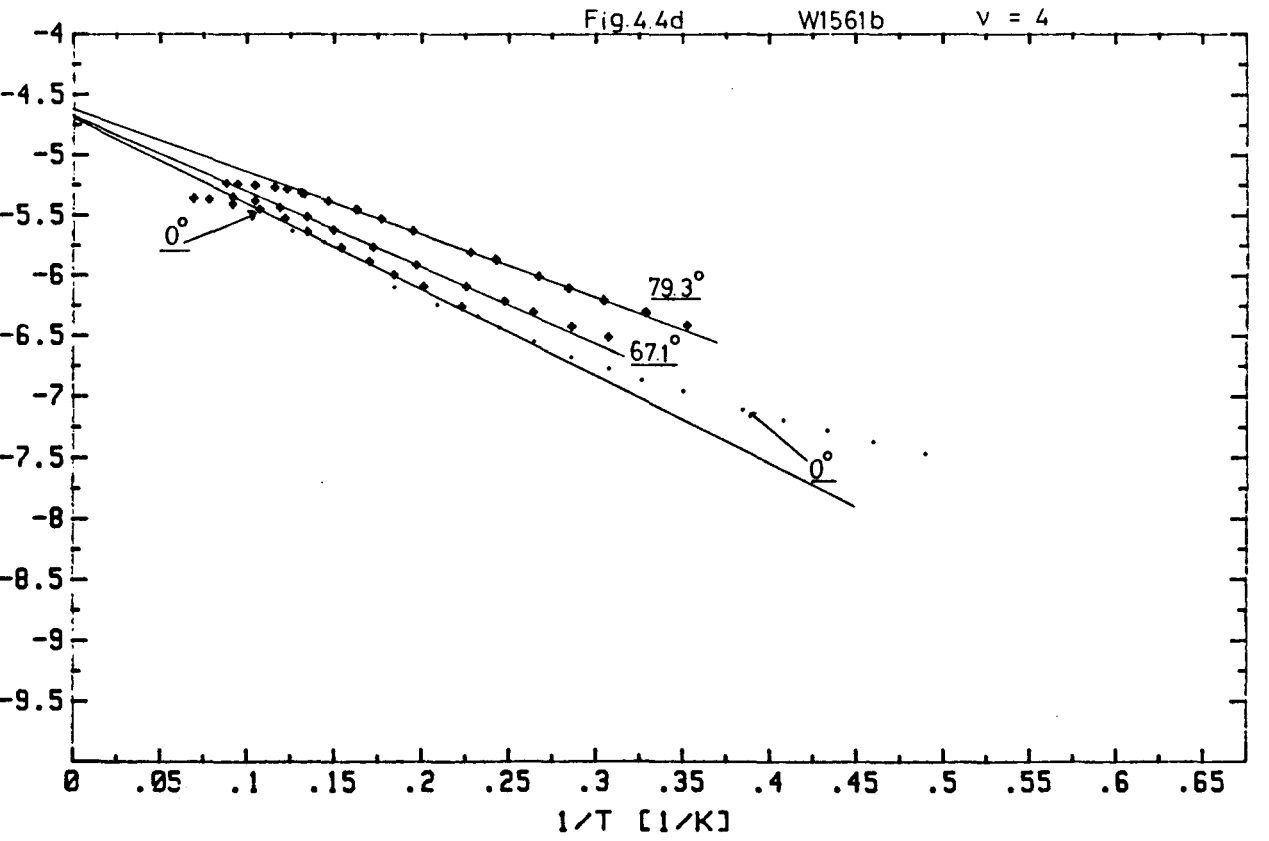
Fig.4.4d W1561b v = 4
-4
-4.5
-5
-5.5
-6
-6.5
-7
-7.5
-8
-8.5
-9
-9.5
0°
79.3°
67.1°
0°
0
.05
.1
.15
.2
.25
.3
.35
.4
.45
.5
.55
.6
.65
1/T [1/K]

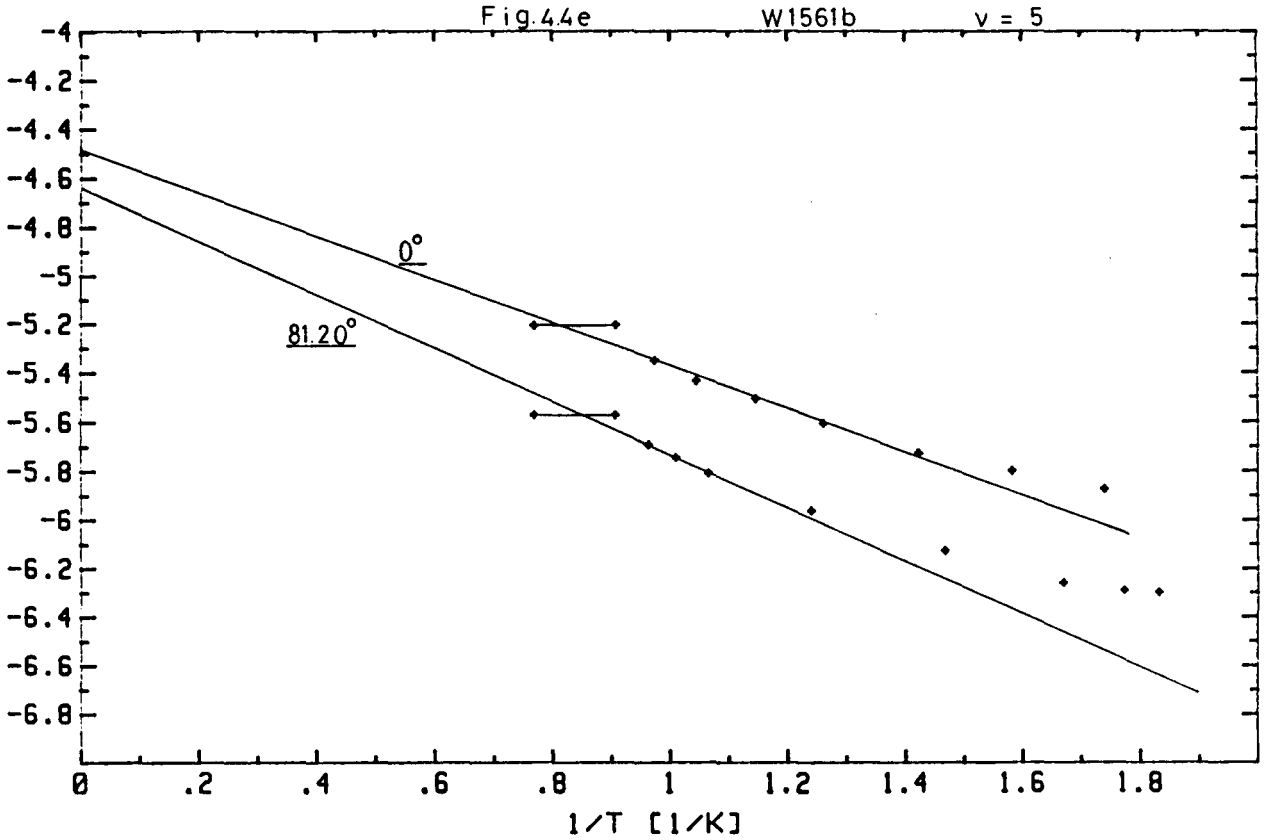
Fig.4.4e
W1561b
ν = 5
0°
81.20°
-4
-4.2
-4.4
-4.6
-4.8
-5
-5.2
-5.4
-5.6
-5.8
-6
-6.2
-6.4
-6.6
-6.8
0
.2
.4
.6
.8
1
1.2
1.4
1.6
1.8
1/T [1/K]

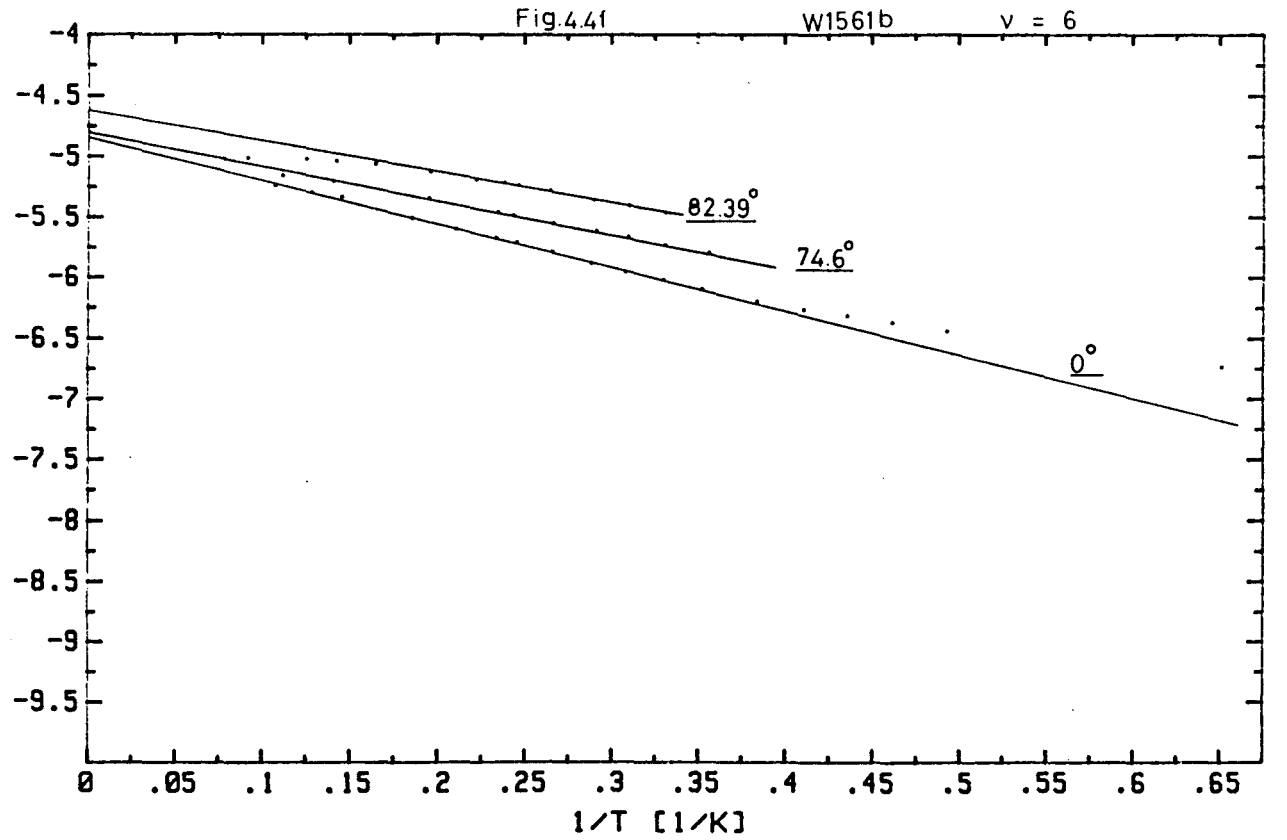
Fig.4.4f
W1561b
ν = 6
82.39°
74.6°
0°
-4
-4.5
-5
-5.5
-6
-6.5
-7
-7.5
-8
-8.5
-9
-9.5
0
.05
.1
.15
.2
.25
.3
.35
.4
.45
.5
.55
.6
.65
1/T [1/K]

The error in the determination of the temperature itself (<0.02 K) is unimportant. The accuracy of the measurements is mainly limited by the stability of the temperature during the sweeps of the magnetic field. In the helium-4 system the errors in the range below 1.6 Kelvin are predominantly determined by the pressure stabilization (fig.4.3a). The helium-3 system is equiped for accurate pressure measurements below 1.5 Kelvin (fig.4.3e). For the voltage measurements the accuracy is better than 1%, except at the lowest temperatures for $\nu = 1$ and $\nu = 2$ in W1527b, which are a very low minima. The lower limit for these DC-measurements is about 1 μV (fig.4.3a,b).

In appendix B the crossings of the curves in fig.4.3 and the extrapolations to $1/T = 0$ are analysed. We do not use the two measurements for the largest tilt angles in fig.4.3b, because the sample is warmed up at night, and the electron density n_s changed ($\simeq$1%). The dashed zero-angle line in fig.4.3d is the first measurement of this series. The other zero-angle line is recorded at the end, after which the measurement at 82.4^{o}' is repeated to check the reproducibility.

The exponential behaviour in figures 4.3 and 4.4 is shown over sometimes even more than two decades. The justification for the interpretation as an activation energy comes from the large range over which this exponential dependence is found. In chapter 6 we will also see that the activation energy for $\nu = 2$ is of the same order as expected from the cyclotron energy. The tails that end up higher than the exponential straight lines can be understood in terms of phonon-assisted tunneling over localized states as mentioned in the end of chapter 2.

Current dependent measurements done by Dominguez indicated that the activation energies are independent of the current in the range below 10 μA [45].

As can be seen from fig.4.2b the SdH minimum slightly shifts to the left. This shift does not happen for every filling factor, but when it happens it appears to be reproducible. In only one case (fig.4.5a) a

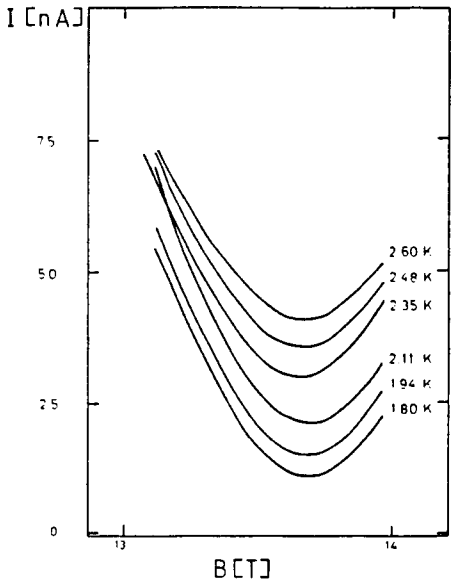

Fig.4.5a. SdH minima shifting to the right.

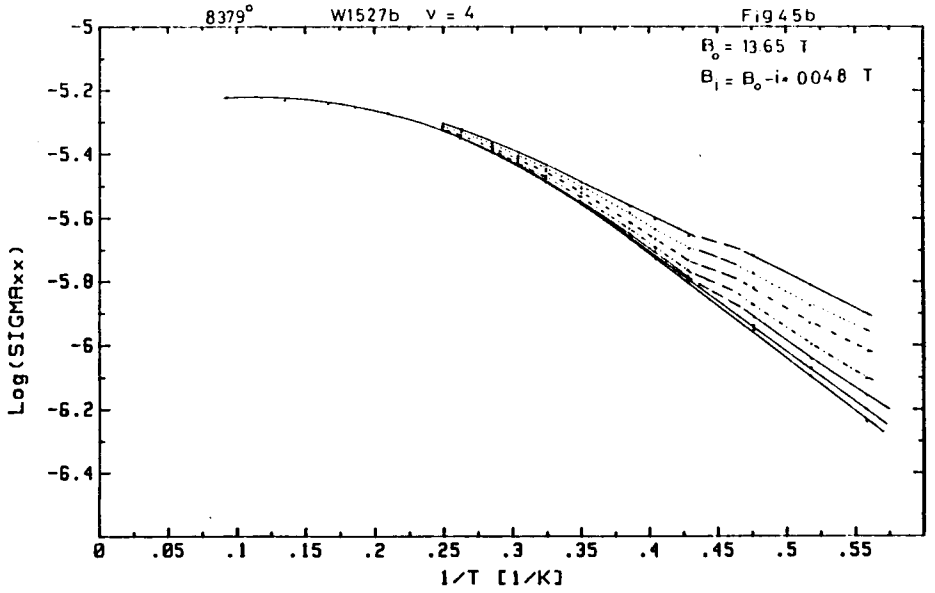

Fig.4.5b The temperature dependence of the shifting curves.

shift in the opposite direction is shown. This shift is reproducible too. To make it clear that this shift does not affect the activation energy in the minimum a plot of $\ln\sigma_{xx}$ versus 1/T for several magnetic fields near the minimum is shown (fig.4.5b). In this case the deviation in the temperature dependence becomes visible at fields more than 0.1 Tesla away from beside the minimum. The shift of the SdH minimum is possibly indicating a transition from the thermal activation to another electrical transport process like hopping. Another possiblity to understand this shift is that inhomogeneities in the electron density would result in another 1/B periodic component, or that Coulomb scattering by impurities would be important. This is not very clear at the moment. The magnetic field with the highest activation energy is the one chosen in the lowest non-shifting minimum.

Similar plots like fig.4.5b are made for $\upsilon = 1$ and $\upsilon = 2$ (W1527b) in an attempt to find the thermodynamical density of states (DOS) as a function of tilt angle. It is not the DOS that is resulting for $\upsilon = 1$ (fig.4.6a) because the background density would then exceed the total density. Perhaps the spin states are overlapping each other too much to fulfil the conditions needed for this method (section 2.7). We did not study this in full detail. For $\upsilon = 2$ (fig.4.6b) we see that it is difficult to determine the DOS in high-mobility samples, just like Stahl reported earlier [36]. The DOS is calculated using (2.50) and not (2.51). But around $\Delta B_z = 0$ the holes and the electrons are both contributing to ΔE_F via ΔE_a, thus a value that is two times the DOS, will appear. The errors in the DOS can be very large, because a certain ΔB_z has to be divided by a very small ΔE_F and a small error in E_a will result in a large deviation of the DOS. Our values for the DOS for $\upsilon = 2$ (10^{-9} to 10^{-10} $cm^{-2}meV^{-1}$) are the same as has been reported

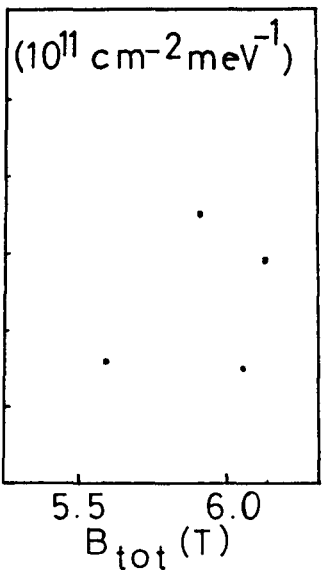

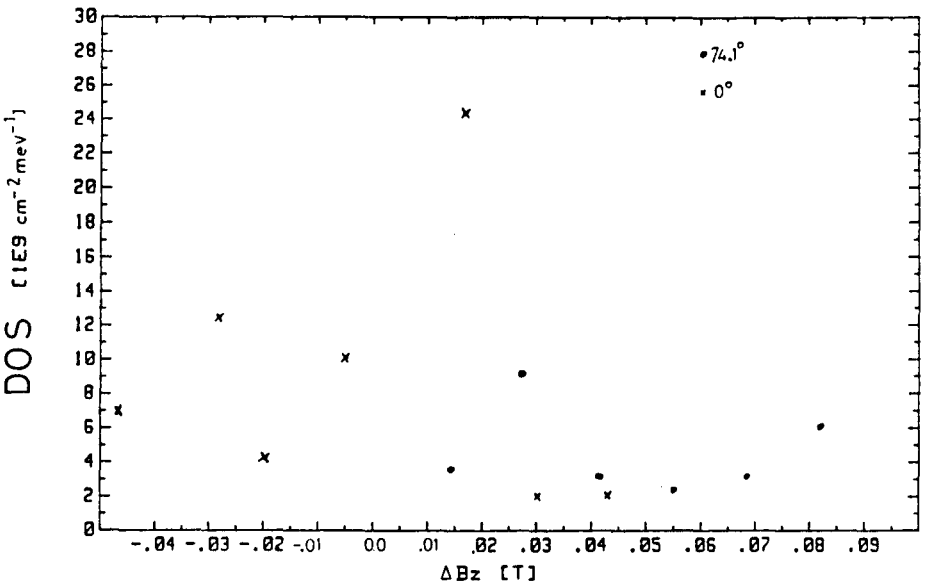

Fig.4.6a. dn/dE_F for $\upsilon = 1$ (W1527b); $B_z = 5.94$ T; $\varphi = 0^o$.

Fig.4.6b. dn/dE_F for $\upsilon = 2$ for two tilt angles (W1527b).

earlier [35,36]. No large changes of the DOS by tilting the sample are seen.

In this chapter it has been shown that an activation energy can be determined in these samples. In the next two chapters the interpretation in relation to the energy gaps around the Fermi-energy is pointed out. The absolute errors in the activation energy are determined by hand, making extra logarithmic plots of σ_{xx}.

Chapter 5: Activation energies between two spin levels

5.1: Filling factor one

In order to get insight in the relation between the spin splittings and the Landau splittings the activation method of the preceeding chapter is used to analyse both in combination on one sample (W1527b). First, the experiment between two spin levels is worked out in this chapter. Then the Landau levels are reviewed in chapter 6. The measured activation energies for $\upsilon = 1$ are shown in fig.5.1. In this situation the Fermi-energy is lying in a SdH minimum in the middle between two spin levels (fig.2.12).

The activation energy shows a linear increase with total field. Assuming that the ranges in which the extended states appear, are neglegibly small in tilted magnetic fields we can directly deduce the spin splitting, which is twice as large as the activation energy. In

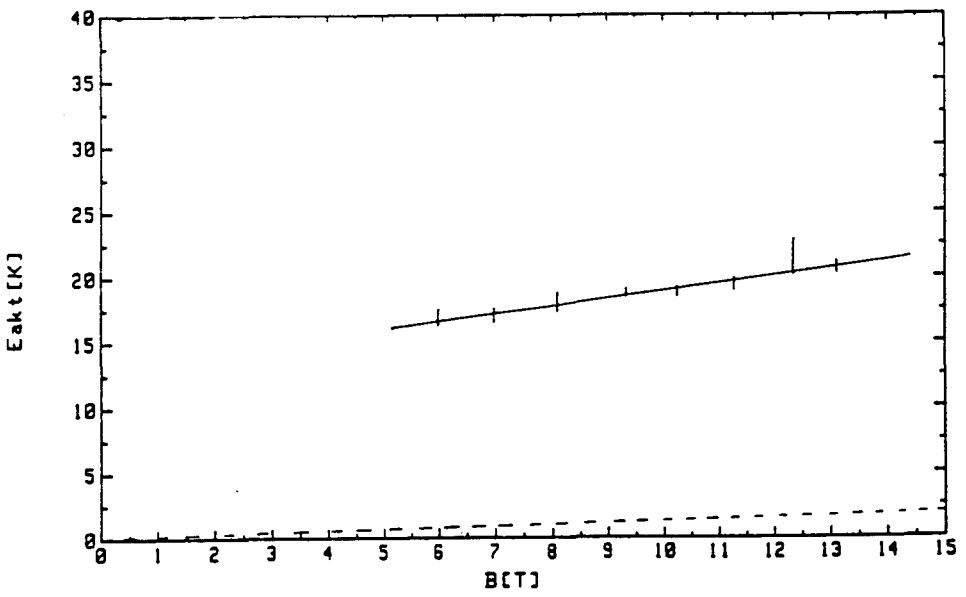

Fig.5.1. Measured activation energies for $\upsilon = 1$ (W1527b), $B_z = 6.00$ T. The dashed line indicates $1/2 g_o \mu_B B_{tot}$ with $g_o = 0.44$.

an attempt to understand this behaviour of the spin splitting we plotted g^* (fig.5.2) that is

$$g^* = \frac{2E_a}{\mu_B B_{tot}} \quad . \tag{5.1}$$

From fig.5.1 it is clear that the spin splitting increases with increasing total magnetic field. We plotted g^* against $1/B_{tot}$ in fig.5.3. The points show a more or less linear behaviour. Extrapolation of the straight line in fig.5.3 gives an intersection at the vertical axis between 1.5 and 2.0. When we take a closer look at the theory of Janak we see in fig.5.3 that in the case of $g_o = 0.4$ the exchange energy e.g. the occupation difference in (2.22b) which would belong to g^*, would increase with increasing B_{tot}. This exchange energy is calculated using (2.22a) with the bulk GaAs g-factor of 0.44 for g_o. In fig.5.4 the magnitude of this exchange energy is shown. In order to compare these results with another sample with lower electron density the results of Haug and Nicholas [44,50,54] are shown in fig.5.5. The points are also activation measurements, the solid line

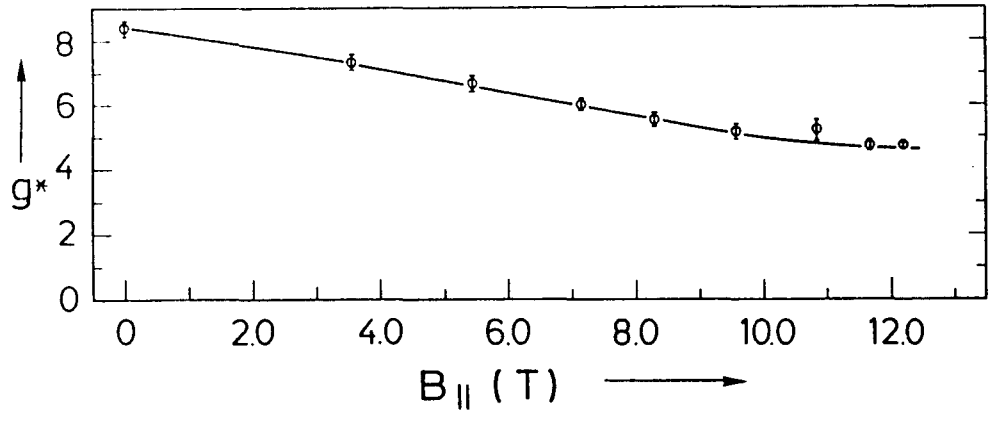

Fig.5.2 The relative decrease of g^* against B_y ($\upsilon = 1$, W1527b).

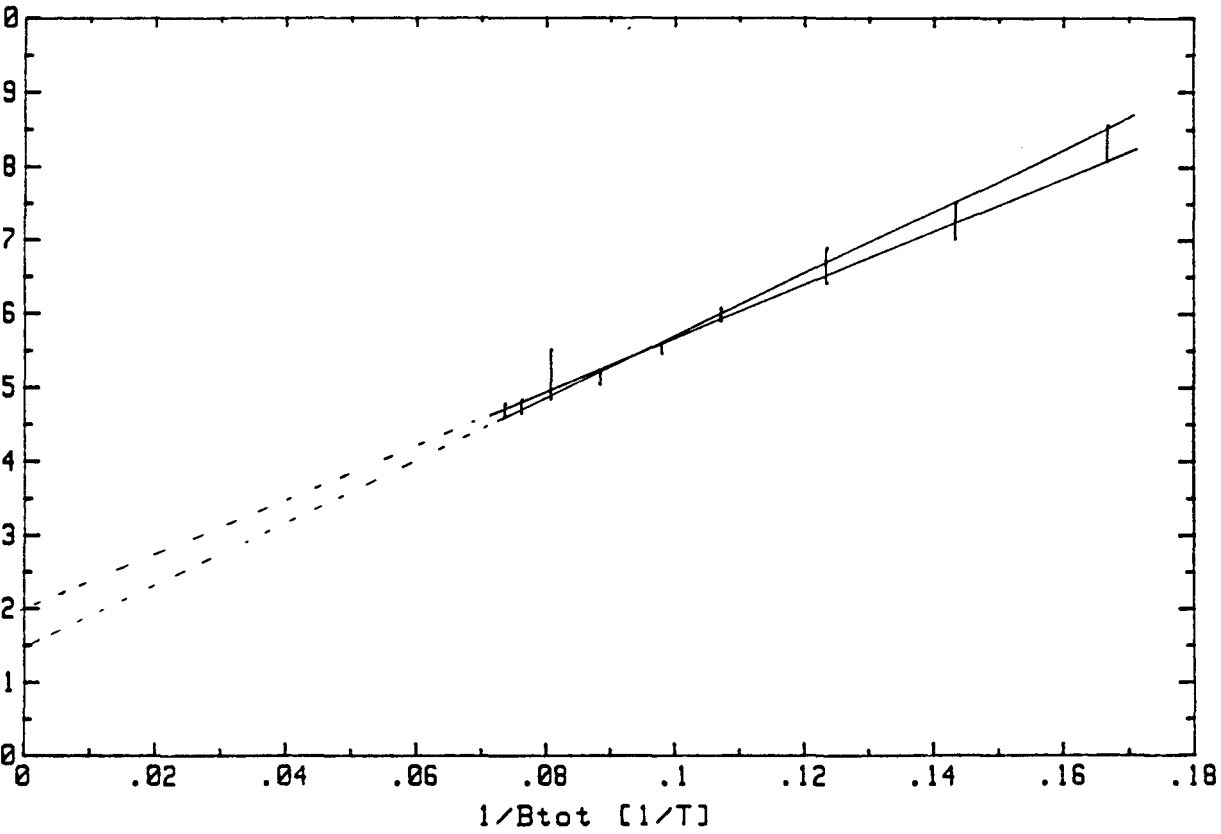

Fig.5.3 The slope is 40.4 ± 2 T; $B_{tot} = B_z$ when $1/B_{tot} = 0.1667\ T^{-1}$.

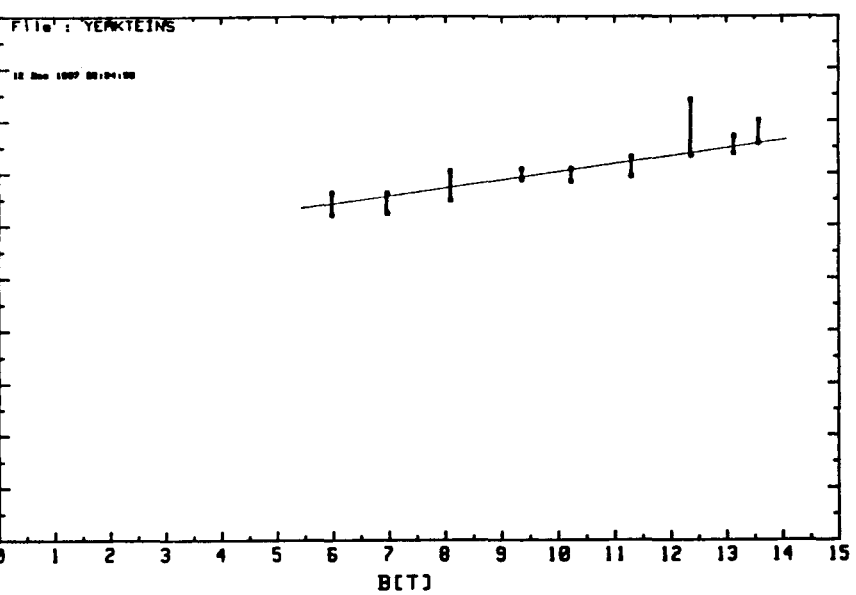

Fig.5.4 The exchange part of the enhanced spin splitting (υ = 1, W1527b).

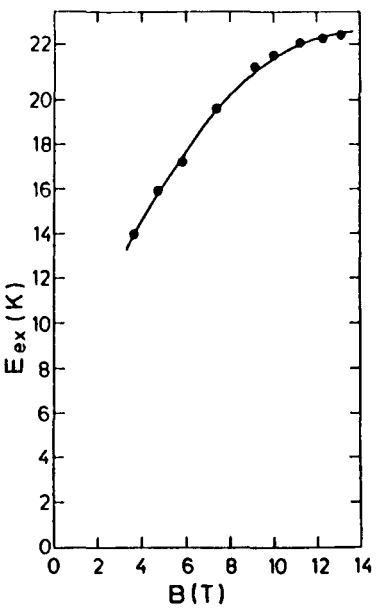

Fig.5.5 Similar measurements with $n_s = 8.1\ .10^{10} cm^{-2}$, $\mu = 4.5\ .10^5 cm^2/Vs$ [44,50,54].

is a calculated fit with a level broadening of 22 K (1.9 meV). Haug and Nicholas explained the sublinear behaviour with (2.22b). The separation of the spin polarized levels increases as a function of parallel magnetic field. Due to the overlap in energy of the two spin polarized level the difference in occupation increases, but it will saturate when the levels are completely separated. Up to now no theory of many-particle exchange interaction has been developed for tilted magnetic fields. This possibility to understand our measurements is discussed in chapter 8.

In an attempt to analyze the measurements as a function of tilt angle, we use (2.31). The measurement without parallel field ($\varphi = 0^o$) gives the perpendicular g-factor $g_z = g^*(0^o) = 8.4 \pm 0.3$. Using (2.30) we calculated for every angle the parallel element g_y of the g-matrix (table 5.1).

Table 5.1. Indicated are deviating values for g_y, based on the absolute errors in E_a.

W1527b, $\nu = 1$, $B_z = 6.00$ T

B_{tot} (T)	B_y (T)	E_a	$\pm$ (10^{-22}J)	g^*	$\pm$	g_y	high / low
6.00	0.00	2.34	0.07	8.4	0.3	-	
6.98	3.56	2.37	0.08	7.3	0.2	2.1	5 / 0
8.11	5.46	2.50	0.09	6.7	0.2	3.5	4.9 / 0
9.34	7.15	2.61	0.04	6.0	0.2	3.5	4.1 / 2.7
10.23	8.29	2.62	0.04	5.5	0.1	3.0	3.6 / 2.4
11.30	9.57	2.69	0.07	5.1	0.1	3.0	3.5 / 2.3
12.38	10.83	2.98	0.19	5.2	0.3	3.7	4.4 / 2.8
13.12	11.67	2.88	0.06	4.7	0.1	3.1	3.4 / 2.7
13.58	12.18	2.97	0.08	4.7	0.1	3.2	3.5 / 2.8

The average is $g_y = 3.3$ (standard deviation 0.3). Every point is in agreement with these values of g_y and g_z. We see that $g_z > g_y$.

The activation energy between the spin levels of the lowest Landau in a Si-MOSFET as measured by Kleinmichel, also leads to constant g-factors which are approximately the same as found here. The regressive increase in the activation energy as measured by Haug and Nicholas cannot be described with two constant g-factors; the two parameters g_y and g_z both decrease, but in their sample is also $g_z > g_y$. In their sample g^* starts at 6.23 and falls down to 3.0 at 74.1°. The possibility to explain our measurements in terms of a constant anisotropic g-factor is discussed in chapter 8.

5.2: Other odd filling factors

To get a more complete picture of the activation energies between the spin levels more values are given in table 5.2. First, we note that in the perpendicular case for filling factor $\upsilon = 3$ the activation took place in a range that was covered partially by the helium-4 system and partially by the helium-3 system. Due to this no activation

Table 5.2

W1527b

	B_y (T)	E_a (K)	g^*	$1/2\hbar\omega_c$ (K)	E_{ex} (K)	g_z	g_y
$\upsilon = 3$	5.61	3.4 ± 0.3	1.6	20	5.2 ± 0.7	4.2	
B_z = 1.98 T	13.61	4.6 ± 0.3	1.0	20	5.1 ± 0.7		0.80
$\upsilon = 5$	0.00	1.50 ± 0.06	3.9	11.5	2.66 ± 0.2	3.9	
B_z = 1.143 T	12.97	2.65 ± 0.06	0.61	11.5	1.45 ± 0.2		0.51

Table 5.3

W1561b

	B_y (T)	E_a (K)	g^*	$1/2\hbar\omega_c$	E_{ex}	g_z	g_y
$\upsilon = 1$	0.00	22.2 ± 0.9	6.2 ± 0.2	107	41.2 ± 1.8	6.2	
B_z=10.69 T	8.73	22.5 ± 0.4	4.9 ± 0.1	107	40.9 ± 0.8		1.5
$\upsilon = 3$	0.00	4.65 ± 0.2	4.12 ± 0.16	33.7	8.30 ± 0.04	4.12	
B_z=3.365 T	12.79	4.65 ± 0.4	1.02 ± 0.07	33.7	5.39 ± 0.08		-
$\upsilon = 5$	0.00	2.02 ± 0.08	2.95 ± 0.2	20.4	3.43 ± 0.2	2.95	
B_z=2.035 T	13.14	2.63 ± 0.4	0.59 ± 0.04	20.4	1.33 ± 0.4		0.4

energy was determined at zero angle for $\upsilon = 3$. The measurements on W1561b are given in table 5.3.

For $\upsilon = 1$ of W1561b the sample was tilted less than 40^o degrees, so it is not surprising not to see any effect in the activation energy. The decrease of the exchange energy as a function of angle (table 5.2 and table 5.3) seems to be quite surprising and in disagreement with the theory of Janak and Ando et al (see (2.22)) and with the measurements discussed previously, which are all carried out in higher magnetic fields and result in larger activation energies. The activation energies in table 5.2 and table 5.3 result in a fast decreasing g-factor g^*. For W1561b, v = 3, formula (2.20) gives a negative value for g_y^2, thus it is not possible to describe these measurements by means of constant g-factors g_y and g_z. Several possibilities to explain the activation energies in table 5.2 and table 5.3 are discussed in section 8.1.

In fig.5.6 the g-factors of three samples are shown as is measured in the absence of parallel fields. The sample with the highest mobility is W1561b. Its g-factor is smaller than for W1527b. This is also discussed in section 8.1, together with the measurements of the next chapter.

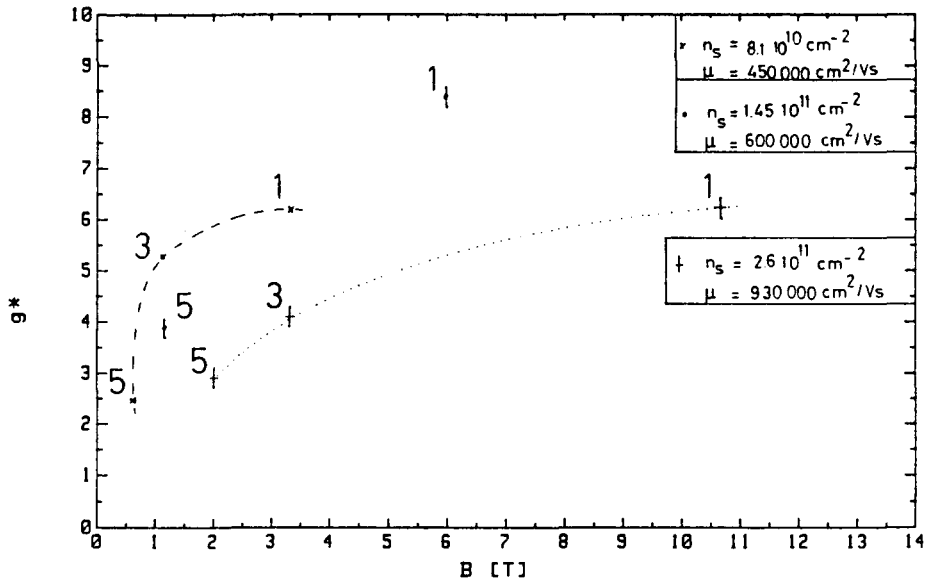

Fig.5.6 Measured g-factors for three high mobility samples in perpendicular fields. The filling factor is indicated. The samples are in order of electron density: W1532 (fig.5.5), W1527b, W1561b.

Chapter 6: Comparing the activation energy and the cyclotron energy

6.1: The activation energy between two Landau levels

The measured activation energy between two Landau levels clearly decreases as a function of parallel field (fig.6.1 and table 6.1). This decrease is smaller for larger filling factors. The activation energy in the perpendicular field for $\nu = 2$ is in agreement with the expected cyclotron energy ($E_a = 1/2\ \hbar\omega_{cz}$). For larger filling factors the activation energy without parallel field is smaller than expected. This is the case for every measured filling factor of sample W1561b (table 6.1). This point is left for discussion in the first section of chapter 8.

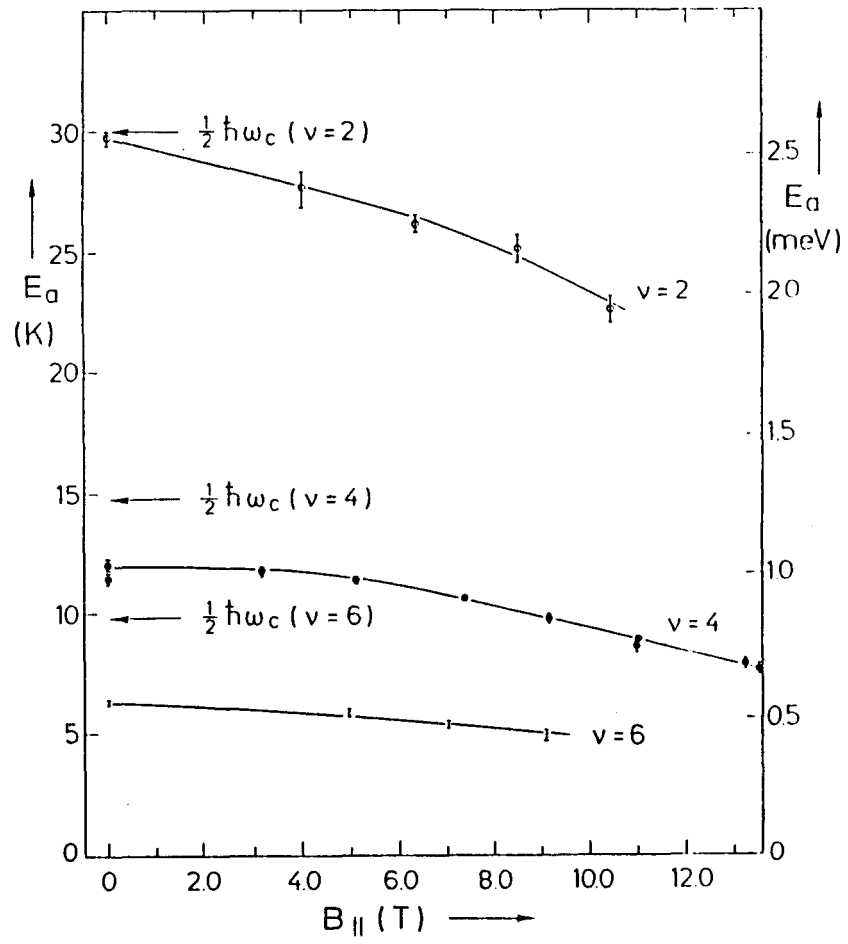

Fig.6.1 Measured activation energies with even fi]ling factors (W1527b).

Table 6.1

W1561b

	B_y	E_a	$1/2\ \hbar\omega_{cz}$
$\upsilon = 2$	0.00	45.7 ± 0.3	51.4
	12.56	36.2 ± 0.3	51.4
$\upsilon = 4$	0.00*	18.0 ± 0.5	26.6
	0.00	16.6 ± 0.4	25.7
	6.58	14.4 ± 0.4	25.7
	13.56	12.0 ± 0.3	25.7
$\upsilon = 6$	0.00*	8.4 ± 0.2	17.7
	6.41	6.36±0.15	18
	13.20	6.34±0.19	18

* not belonging to the same series

In the $\ln\sigma_{xx}$ versus 1/T plots (fig.4.3) it is shown that when the activation energy is larger, due to the larger slope of the straight line in the logarithmic plots the uncertainty in temperature causes a larger deviation in E_a. The errors for $\upsilon = 2$ are thus significantly larger than for $\upsilon = 4$ and $\upsilon = 6$ (fig.6.1). The footnote in table 6.1 (W1561b) indicates measurements that do not belong to the same series, because the sample has been warmed up in between.

The activation energy in perpendicular fields often deviates from $1/2\hbar\omega_c$ (fig.6.2). In fig.6.2 we also show measurements of Ebert [57]. We discuss the behaviour in perpendicular fields in section 8.1. The interpretation of the activation energy at $\upsilon = 2$ in W1527b seems to be less complicated than for the other filling factors, because of the good agreement with the expected value from the cyclotron energy as

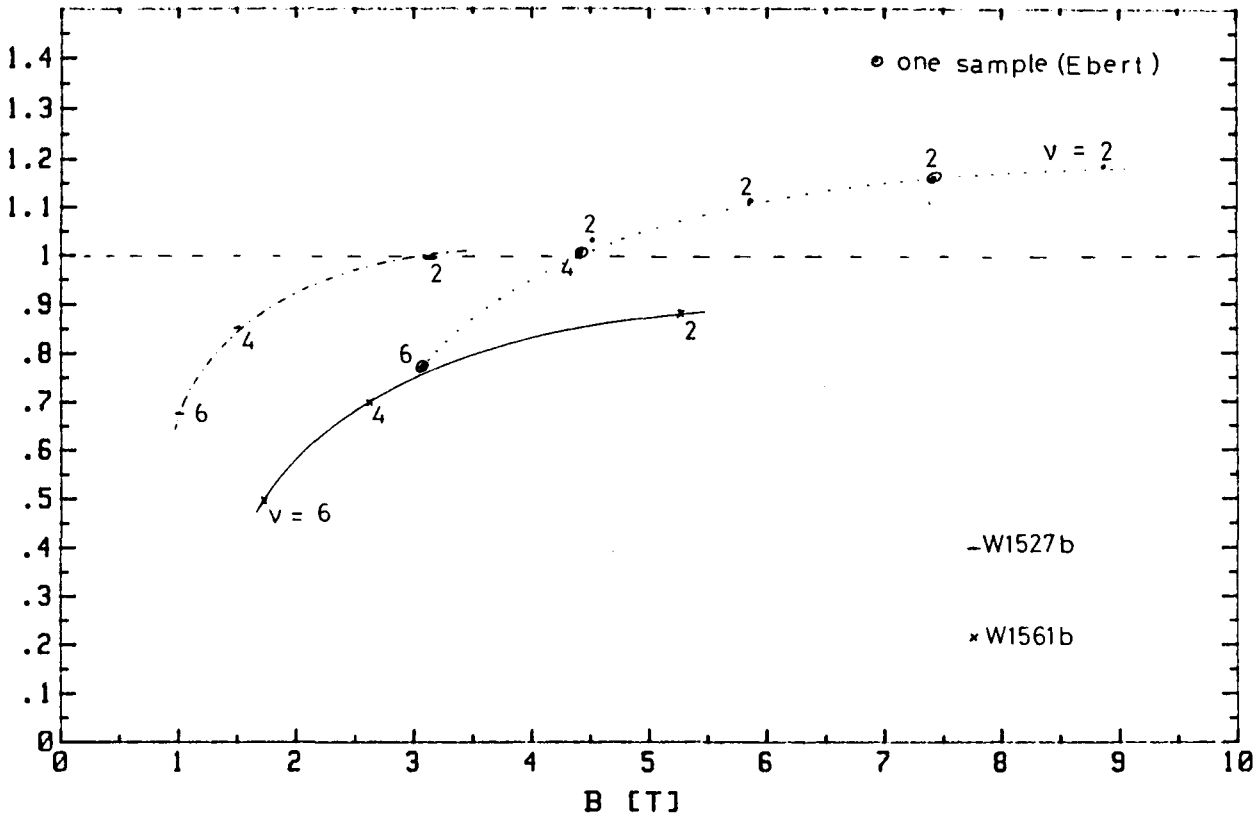

Fig.6.2 Activation energy in a perpendicular magnetic field ($B_y = 0$). The filling factor is indicated. The circular dots are taken from Ebert [57].

Table 6.2: $1/2\hbar\omega_{cz}$ minus E_a in Kelvin ($B_y = 0$)

ν	W1527b	W1561b
2	0.2 ± 0.4	6.3 ± 0.3
4	3.3 ± 0.1	8.9 ± 0.2
6	3.5 ± 0.1	9.3 ± 0.2

mentioned before. Therefore, we start our analysis with this particular series of measurements.

An interpretation of the decreasing activation energy in tilted magnetic fields in terms of an increasing spin splitting leads to a g-factor g^* starting at almost zero and rising to more than 2. The occupation of the spin levels on either side of the Fermi-energy with

electrons and holes respectively, is fairly low, while the Fermi-energy lies between two Landau levels with $3 < T < 10$ K and $1/2\hbar\omega_c$ being 30 K. Kukushkin did not see such an enhancement of g^* with the Fermi-energy between two Landau levels (fig.2.4).

A second possibility we consider is an enlarged but constant g-factor, which would cause the decrease of E_a with $\nu = 2$. This has been suggested for Si-MOSFETs [34] in which the bulk g-factor is about 5 times larger than in GaAs. It would imply $g^* = 3.4 \pm 0.3$ for $\nu = 2$ and g^* between 1.2 and 1.5 for $\nu = 4$, which seems to be quite large compared to ESR ($g = 0.4$) [7]. We note that in chapter 5 g_y is found to have a value for $\nu = 1$ ($g_y = 3.3 \pm 0.3$) which is consistent with this interpretation for $\nu = 2$.

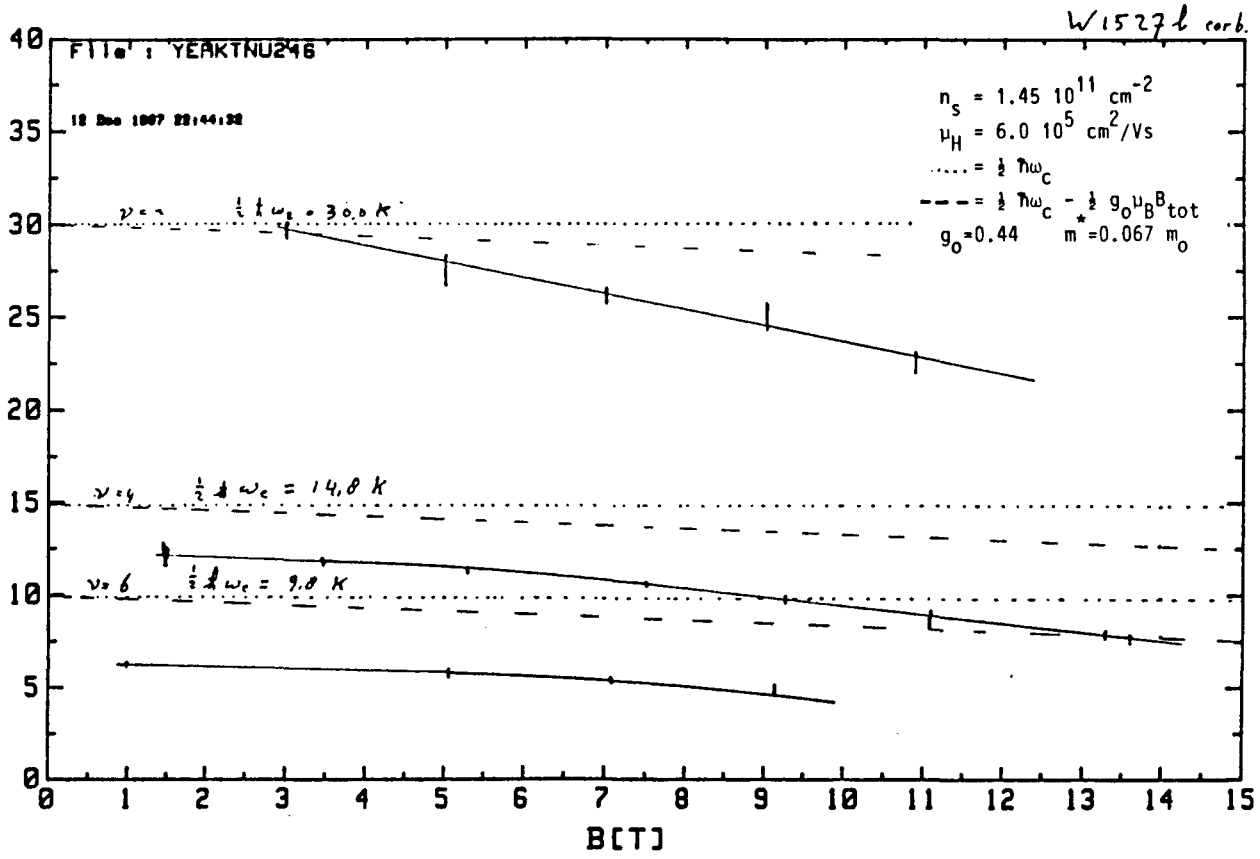

Fig.6.3 The measured activation energies compared with $1/2\hbar\omega_{cz} - 1/2g_o\mu_B B_{tot}$. The dashed line represents the bare spin splitting.

Now we take a look at these measurements assuming that the spin splitting can be described by a 'bare' g-factor g_o. For fig.6.3 g_o is set to be the bulk value of GaAs (0.44). The problem to be discussed is the difference between the dashed line and the measured points with $\nu = 2$ (fig.6.3).

6.2: Comparison with theory

The Hamiltonian (2.8) gives equidistant Landau levels if only a perpendicular magnetic field is present. In general, it is impossible to separate the Hamiltonian into coordinates due to the term

$$H_2 = \frac{e B_y}{m^*} z p_x \,. \qquad (2.9c)$$

Ando [13] showed that this term does not disturb the Landau levels inside one subband by interaction with each other. Only Landau levels from different subbands and with different Landau quantum numbers ($\Delta N = \pm 1$) have interaction. We have carried out perturbation theory to estimate the influence of B_y on the cyclotron energy. Odd order perturbations lead to odd powers of B_y in the energy. The energy may not be changed by a change of sign in B_y. Thus only even order perturbation terms contribute to the energy. We treat the influence of the first subband ($i = 1$) on the ground subband ($i = 0$) by means of second order perturbation theory. This is described in appendix A. The assumptions for this calculation are:

- the effective mass m^* is isotropic in the plane of the 2-DEG
- the subband energies E_{0i} are constant
- the influence of the higher subbands on the ground level is

neglectible compared to the coupling between the two lowest subbands ($E_{0i} \gg E_{01}$ for $i > 1$)

- the change of the energy distance between the Nth Landau level in the ground subband and the $(N \pm 1)$th Landau level in the first subband is much smaller than the unperturbed energy distance between these two levels. In other words, the change of the energy is a relative small perturbation.

The resulting formula for the cyclotron energy as a function of parallel magnetic field, relative to the cyclotron energy in the untilted case is

$$\frac{\hbar\omega_c(B_y)}{\hbar\omega_{cz}} = 1 - z_{01}^2 \frac{m^*}{\hbar^2} \tan^2\varphi \; \frac{\{\hbar\omega_{cz}\}^2}{E_{01}} \frac{1}{1-\{\hbar\omega_{cz}/E_{01}\}^2} \qquad (6.1)$$

with $\tan\varphi = B_y/B_z$ and z_{01} being the intersubband matrix element. The index z indicates the value belonging to the perpendicular component of the magnetic field. This formula appears to be independent of the Landau level quantum number for $N = 0$, 1 and 2. The same formula has already been given in [46]. For measurements of the activation energy it is convenient to write (6.1) as

$$\frac{\hbar\omega_c(B_y)}{\hbar\omega_{cz}} = 1 - a.\tan^2\varphi \; . \qquad (6.2a)$$

The quantity a is fixed when $\hbar\omega_{cz}$ is constant. Another way to write this formula is

$$\frac{\hbar\omega_c(B_y)}{\hbar\omega_{cz}} = 1 - b.\{\hbar\omega_{cz}\}^2\tan^2\varphi \; . \qquad (6.2b)$$

B_z appears both in the numerator of $\hbar\omega_{cz}$ and in the denominator of $\tan\varphi$, so there is left only a small dependence on B_z in the denominator of b, (see (6.1)). In fig.6.4a we have drawn a line for the case of a triangular well z_{01}= 44 Å and for z_{01}= 35 Å as is given

by a fit of Oelting et al [46]. For this sample we use E_{01}= 20 meV [52]. Fig.6.4a and fig.6.4b are corrected for the bare spin splitting, (see also fig.6.3). Fig.6.4b gives the interpretation in terms of a changing effective mass as is done in [46]. Actually, the cyclotron energy is a function of the tilt angle, and not m^*. We conclude that the qualitative decrease of the activation energy for υ = 2 is mainly due to the change of the cyclotron energy.

For υ = 4 and υ = 6 the same calculation does not give quantitative agreement, even not when the deviation of $2E_a$ from the cyclotron energy in the perpendicular case is treated as an offset. The downward

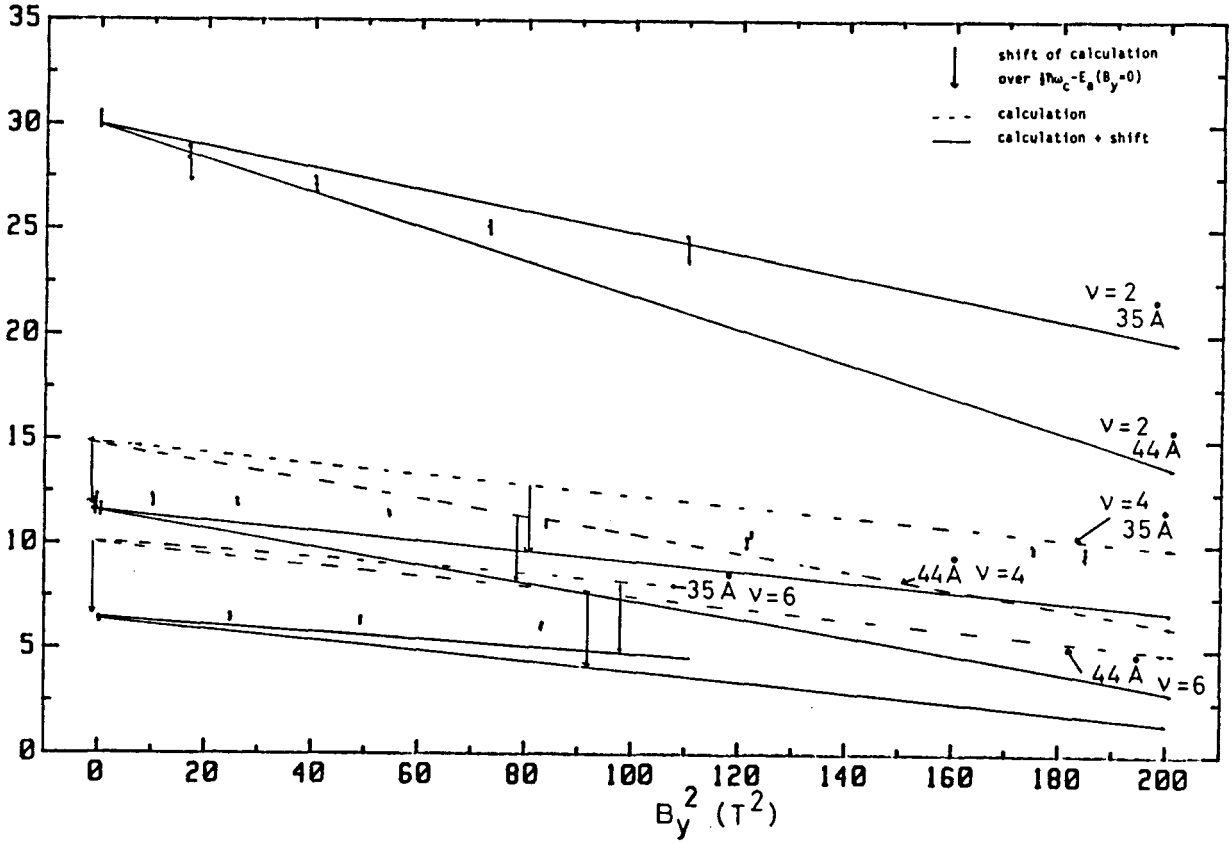

Fig.6.4a. The points are the activation energies plus $1/2g_o\mu_B B_{tot}$ (g_o= 0.4). The dotted lines are calculated with the indicated values for z_{01}. The solid lines are the calculations shifted over $1/2\hbar\omega_c - E_a(B_y=0)$, as indicated by the arrows.

shifted theoretical curves show a smaller slope than for $\upsilon = 2$, as is also shown by the measurements, but their slopes are too large. We also see that the points for $\upsilon = 2$ are getting too large values for higher tilt angles.

To finish this comparison with theory we note that the analytical solution of a parabolic quantum well in a tilted field also shows a decreasing cyclotron energy [14,15].

Fig.6.4b. Relative decrease of the cyclotron energy $\hbar\omega_c$ as a function of B_y (see(6.2a)).

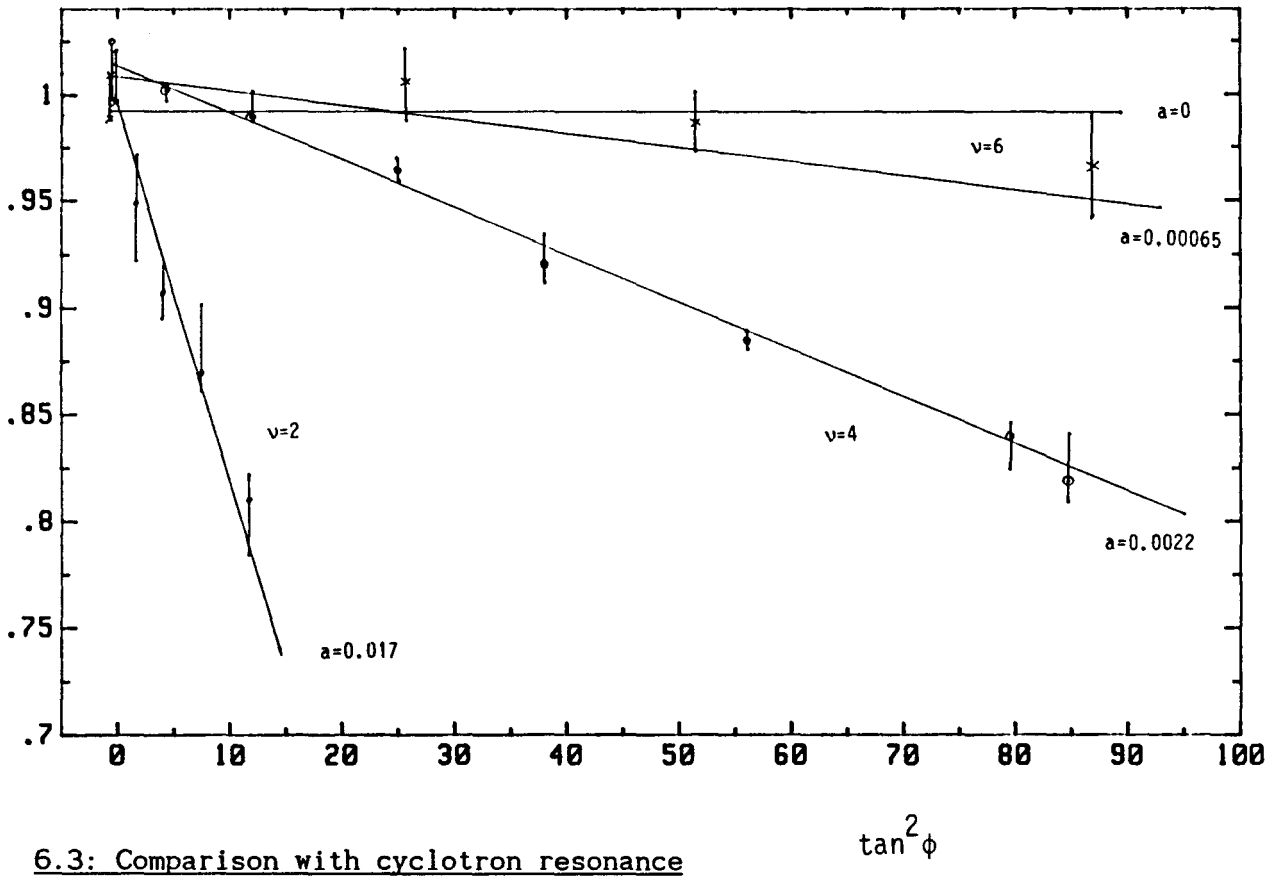

6.3: Comparison with cyclotron resonance

Cyclotron resonance is carried out on a piece of wafer W1527 as a second experiment. The resonance energy is fixed and the magnetic field is swept up and down. In fig.6.5 a shift of the resonance to

higher magnetic fields is observed. The parameters are:

$T = 1.9$ K; $\lambda = 513.0$ μm; $B_z(\upsilon=4) = 1.296$ T; $B_{CR}(0^o) = 1.428$ T;

$B_{CR_{tot}} = 10.403$ T.

A photocurrent effect between $\upsilon = 3$ and $\upsilon = 4$ appears at the resonance position (curves b,d,f). The spin minimum $\upsilon = 3$ (curves i,k) becomes more pronounced for large parallel fields.

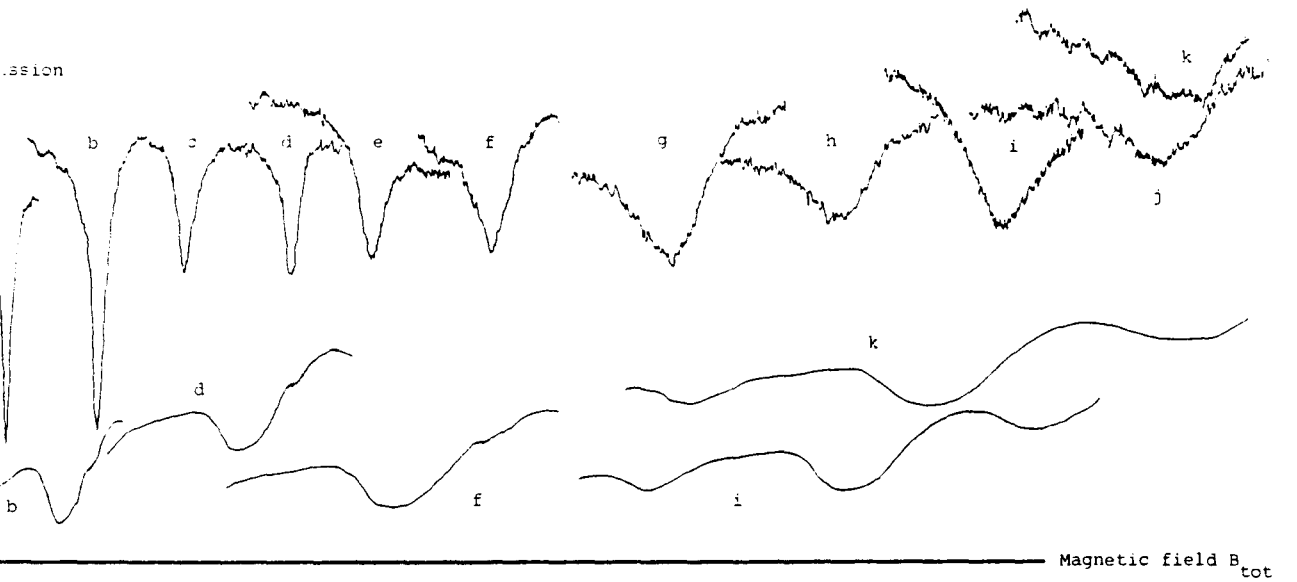

Fig.6.5 The transmission against total magnetic field, both in arbitrary units. a: 0^o; b: 37.4^o; c: 51.2^o; d: 57.9^o; e: 64.8^o; f: 68.2^o; g: 71.7^o; h: 74.9^o; i: 78.7^o; j: 80.1^o; k: 80.6^o. Some Shubnikov-de Haas minima are shown (curves b: $\upsilon=4$, $\upsilon=6$; d,f: $\upsilon=4$; i,k: $\upsilon=3$, $\upsilon=4$, $\upsilon=6$).

In fig.6.6 we show a series of resonance positions. In the untilted case the resonance takes place at B_{CR} = 2.416 T and for large tilt angles (82^o) it shifts to B_{CR_z} = 2.829 T. Other parameters are:

T = 1.9 K; λ = 302.28 μm; $B_z(\upsilon=2)$ = 2.618 T; $\hbar\omega_{cz}(0^o)$ = 4.18 meV .

$B_z(\upsilon=2)$ is determined with the help of SdH oscillations. The resonance position starts at $\upsilon > 2$ and ends at $\upsilon < 2$.

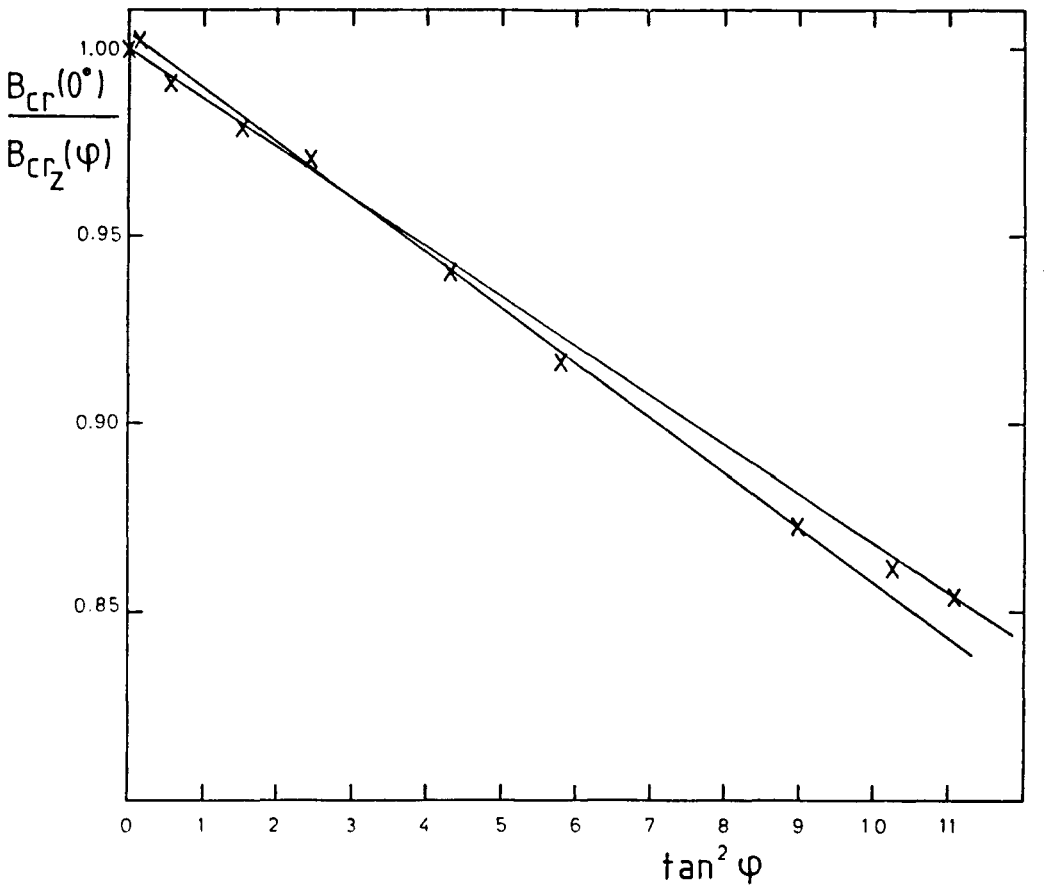

Fig.6.6 Cyclotron resonance in tilted magnetic fields.

The straight lines in fig.6.6 indicate that

$7.5\ 10^{-4} < b < 8.4\ 10^{-4}$ meV^{-2}. Earlier we have carried out two series of measurements with slightly different electron densities and a less stable laser. The results are similar (fig.6.7a,b). According to the

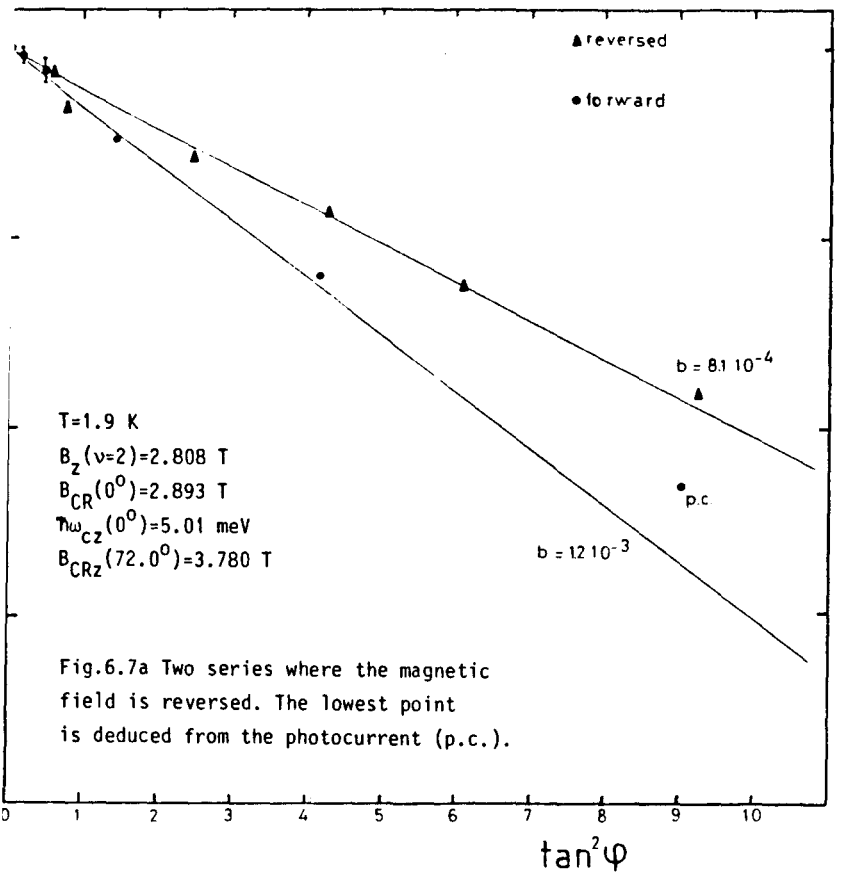

Fig.6.7a Two series where the magnetic field is reversed. The lowest point is deduced from the photocurrent (p.c.).

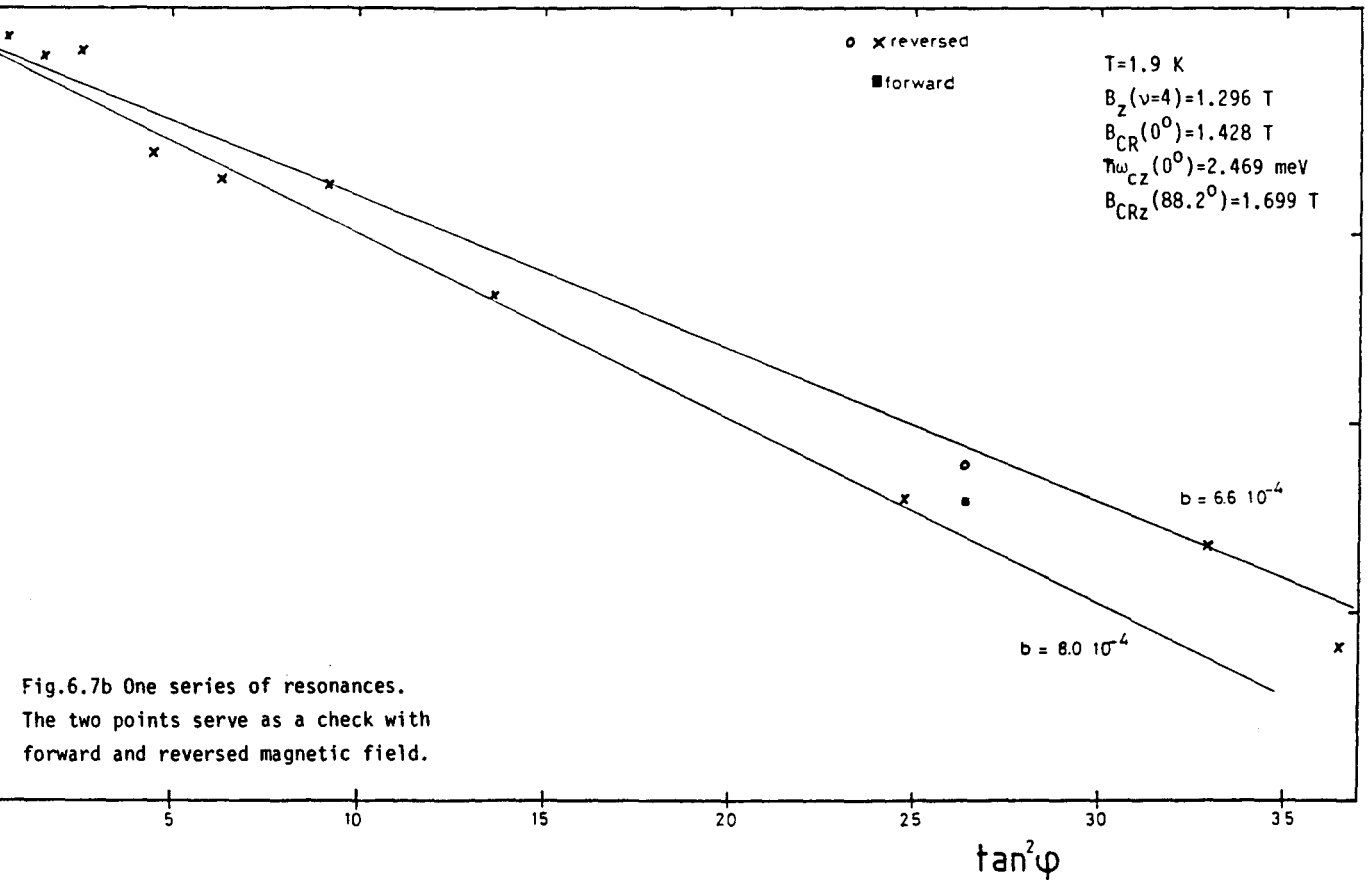

Fig.6.7b One series of resonances. The two points serve as a check with forward and reversed magnetic field.

first series the measurements seem to be dependent on the sign of the magnetic field (fig.6.7a), but a later check (fig.6.7b) shows it to be due to external circumstances like the instability of the laser or the sample.

It seems to be a fairly good choice to plot the effective mass as a function of $\tan^2\varphi$ or B_y^2 as predicted by the second order perturbation theory (6.1). The coefficient b should be almost independent of the filling factor. From (6.1) and (6.2b) it is deduced that b has a somewhat larger value when $\hbar\omega_{cz}$ is larger and υ is smaller. This trend is recognizable in the resulting values for b.

Other effects, which are thought to play a marginal role and perhaps deviate from the global linear behaviour, are not investigated here. One can think of the diamagnetic shift and intersubband coupling [48], filling factor dependent effects [56], a decreasing expectation value for the z coordinate influencing the level broadening [58], and perhaps non-parabolicity [5,6].

To compare these measurements with the activation energy we have calculated the quantity a in (6.2a) using $b = 8\ 10^{-4}$ for $\upsilon = 2$, 4 and 6 (fig.6.8). The indicated point in fig.6.8 is the cyclotron energy when the cyclotron resonance of fig.6.6 passes through $\upsilon = 2$. Using

$$z_{01}^2 = \frac{\hbar^2}{m^*} E_{01} \{1 - (\hbar\omega_{cz}/E_{01})^2\} b \cdot 1.602\ 10^{-22} \qquad (6.3)$$

with the energies in meV, it follows that this b leads to a z_{01} of 42 Å. The agreement with the triangular well and with the thermally activated conductivity is quite satisfying (fig.6.8) (see also [52]).

We have to note here that during the cyclotron resonance experiments the electron density has been slightly smaller than in the sample used for the conductivity measurements. In the latter case $B_z(\upsilon = 2)$ has been equal to 2.99 T.

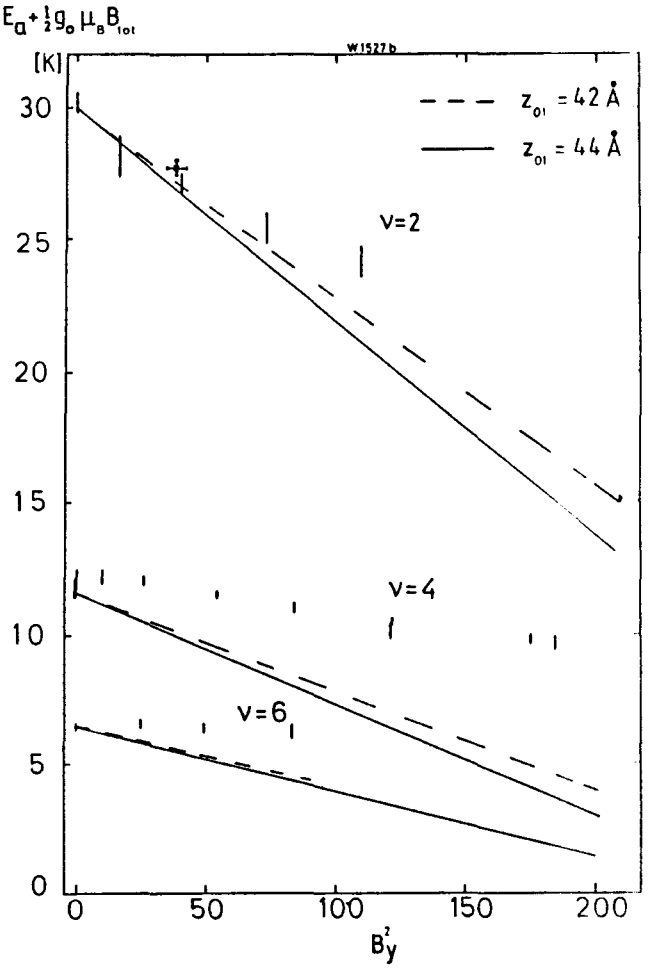

Fig.6.8 The same picture like in fig.6.4a, compared with the cyclotron resonance using (6.2a) and (6.2b). The dashed lines for υ=4 and υ=6 are shifted.

Chapter 7: Large tilt angles;
Landau and spin splitting in one sample

In this chapter we report on an experiment in which we compare the Zeeman splitting with the Landau splitting. We have tried in the same situation to find the activation energy by doing temperature dependent measurements of the conductivity σ_{xx}.

In 1968 Fang and Stiles [19] made the remark that the spin splitting can be enlarged by a parallel magnetic field. With an odd value of the filling factor, then the Fermi-energy lies between two spin levels. Each spin level is thought to have a region with extended states (fig.2.11). An increasing spin splitting increases the energy distance from the Fermi-energy to the extended states, thus the occupation of the higher (lower) extended states with electrons (holes) decreases. By tilting the sample under the condition of a constant perpendicular magnetic field component, the spin splitting increases and the SdH minimum becomes deeper. Fang and Stiles showed that for a certain tilt angle a spin minimum will be as deep as one of the adjacent Landau minima (fig.7.1). Assuming that the cyclotron energy is constant they deduced values for the g-factor g^*.

By tilting to a larger angle the situation can be obtained in which two spin polarized levels of different Landau quantum numbers coincide. At this tilt angle the Landau minimum has disappeared completely (fig.7.2). This situation has led to the name 'coincidence method' for these experiments.

In AlGaAs/GaAs heterojunctions both the effective mass ($m^* = 0.067\ m_o$) and the g-factor ($g_o = 0.4$) are smaller than in Si-MOSFETs ($m^* = 0.19\ m_o$; $g_o = 2$). Therefore, the ratio of the cyclotron

energy to the spin splitting $\hbar\omega_c/\Delta E_s = (eB_z/m^*)/(g^*\mu_B B_{tot})$ is much larger in AlGaAs/GaAs heterojunctions than in Si-MOSFETs. This implies that it is more difficult to achieve a coincidence of spin levels in AlGaAs/GaAs. Recently Haug and Nicholas [44,50] succeeded in reaching a coincidence in AlGaAs/GaAs.

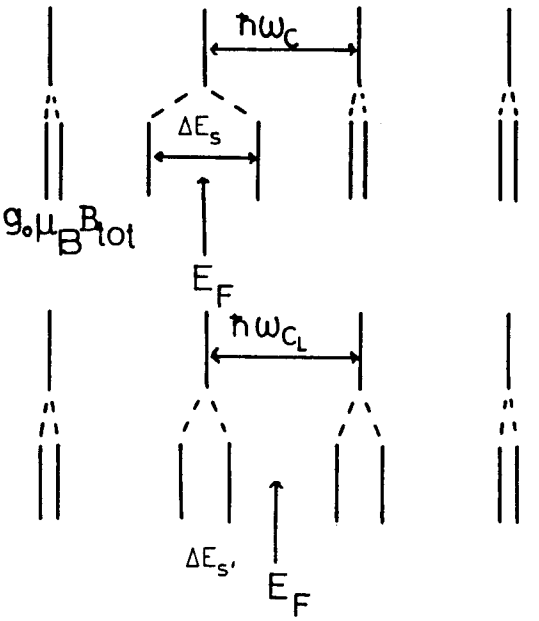

Fig.7.1 Comparison of spin and Landau minima. The spin minimum corresponds to the upper part. The Landau minimum is represented in the lower part of this figure.

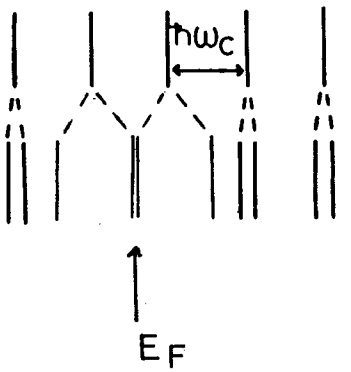

Fig.7.2 Situation of coincidence: the Landau minimum disappears and instead a maximum is seen.

Fig.7.3 SdH oscillations of W1527b at high tilt angles.

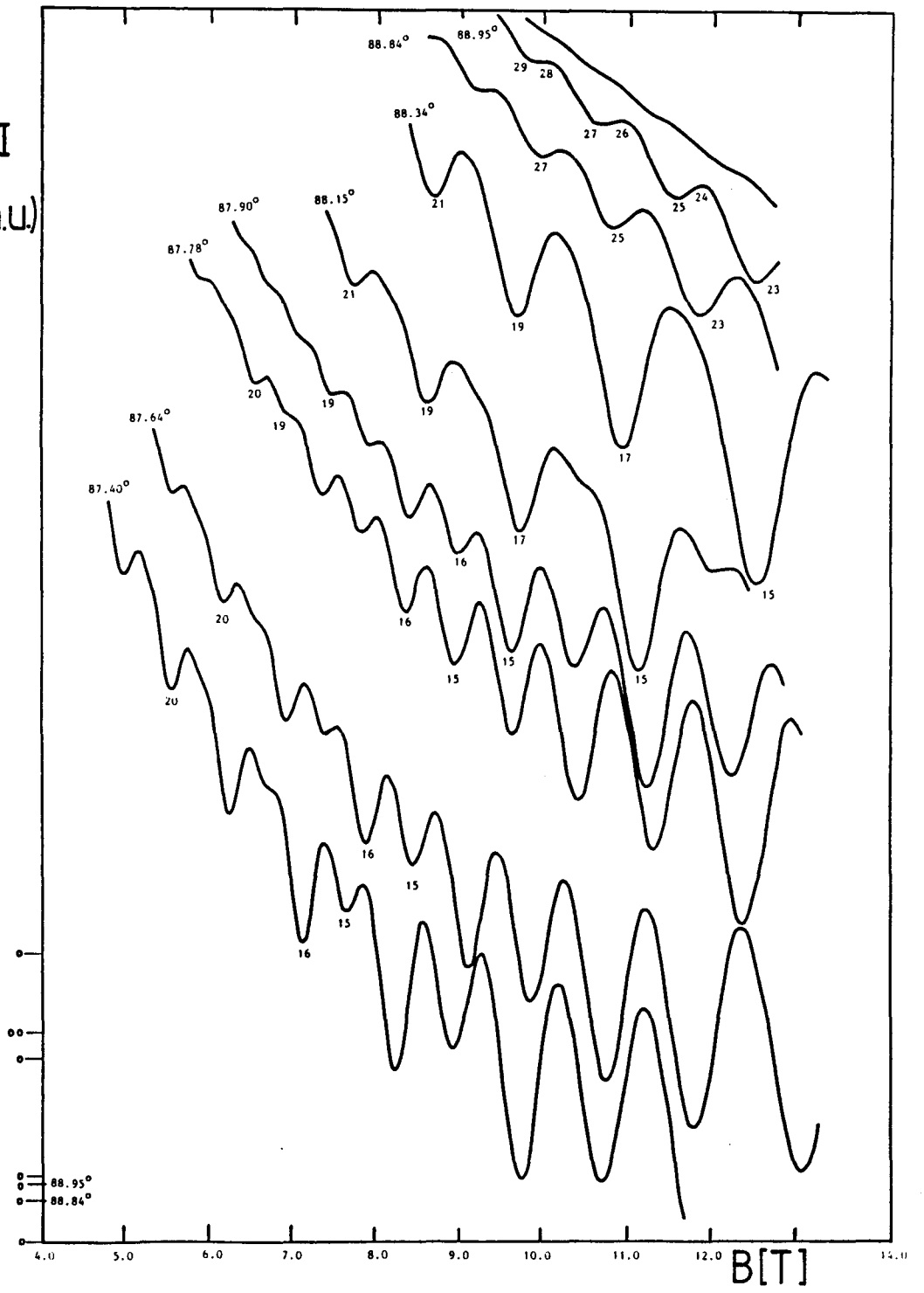

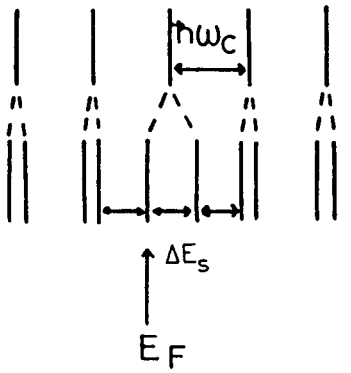

Fig.7.4 The SdH maximum has its lowest value when the adjacent levels are both far away from E_F.

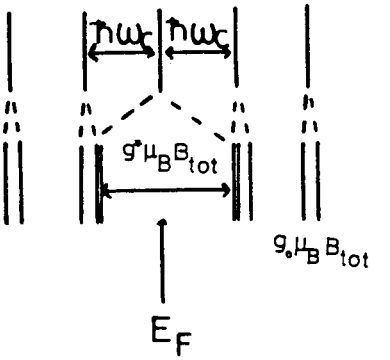

Fig.7.5 The situation in which the spin minimum has its lowest value.

Typical SdH oscillations of sample W1527b at various large tilt angles are given in fig.7.3. The spin minimum $\upsilon = 15$ becomes deeper while the adjacent Landau minimum $\upsilon = 16$ disappears. The curve obtained at a tilt angle of 87.78^{o} corresponds to the situation illustrated in fig.7.1. In this situation we have

$$\Delta E_s = \hbar\omega_{cL} - \Delta E_{s'} . \qquad (7.1)$$

Further, a low value of a maximum corresponds to a low maximum in the density of states. In the situation of fig.7.4, in which the neighbouring levels have a maximum distance to the Fermi-energy, the overlap of the spin levels is very small. The situation in fig.7.4 corresponds to the value of the magnetic field at which the SdH maximum has its lowest value. If the filling factor has an even value

and the Fermi-energy lies between two different Landau levels, then we adopt a g-factor g_o equal to 0.4. From $3\Delta E_s + g_o \mu_B B_{tot} = 2\hbar\omega_c$ it follows that

$$\Delta E_s = \frac{2}{3}\hbar\omega_c - \frac{1}{3} g_o \mu_B B_{tot} \cdot \qquad (7.2)$$

We also see that the lowest minimum for an odd filling factor corresponds to figure 7.5:

$$\Delta E_s = 2\hbar\omega_c - g_o \mu_B B_{tot} \cdot \qquad (7.3)$$

In fig.7.3 it is shown that the total curve shifts upwards if the sample is turned to a larger angle. To avoid any influence of this shift it is necessary to determine the minima relative to the adjacent maxima, instead of using the absolute values of the minima. Thus, in order to find the situation of fig.7.5 the deepest odd minimum relative to the neighbouring maxima is chosen.

The results are given in table 7.1. In this analysis we assume that the cyclotron energy is not influenced by the parallel component of the magnetic field. Therefore, the obtained g-factors are the largest possible values. The angles in table 7.1 are determined with the help of fig.7.6a-d, where the conductivity minima and maxima are plotted as a function of $1/\cos\varphi$. The tilt angles follow from the 1/B periodicity of the conductivity. As an example the situation at 87.78^o (fig.7.3), in which the minima for υ = 14, 15 and 16 are comparable, is recognizable in table 7.1. The quantity g^*_{av} is the average of the g-factors which are determined under the conditions $\sigma_{xx}(\upsilon=14) = \sigma_{xx}(\upsilon=15)$ and $\sigma_{xx}(\upsilon=15) = \sigma_{xx}(\upsilon=16)$. These two situations are shown as intersection points in fig.7.6b. Equation (7.1) holds somewhere between these two points, as is also shown in fig.7.3 (87.78^o: $1/\cos\varphi$=25.8).

Typical curves for the temperature dependence of the current are

shown in fig.7.7a; a logarithmic plot of σ_{xx} versus 1/T is given in fig.7.7b. The SdH-curves (fig.7.7a) have no intersections with each other. Instead, the complete curve moves downwards with decreasing temperature. The activation energy is found with the aid of fig.7.7b and is about kT (table 7.1). We remind here that the activation energies in small perpendicular fields are difficult to interpret. These values for the activation energies are only 10 % or even less than the values expected from $\hbar eB_z/m^*(0^o)$. As long as no cyclotron resonance measurements at these extremely large angles have been carried out it is questionable whether these activation energies are representative for the energy spectrum of Landau and spin levels or not.

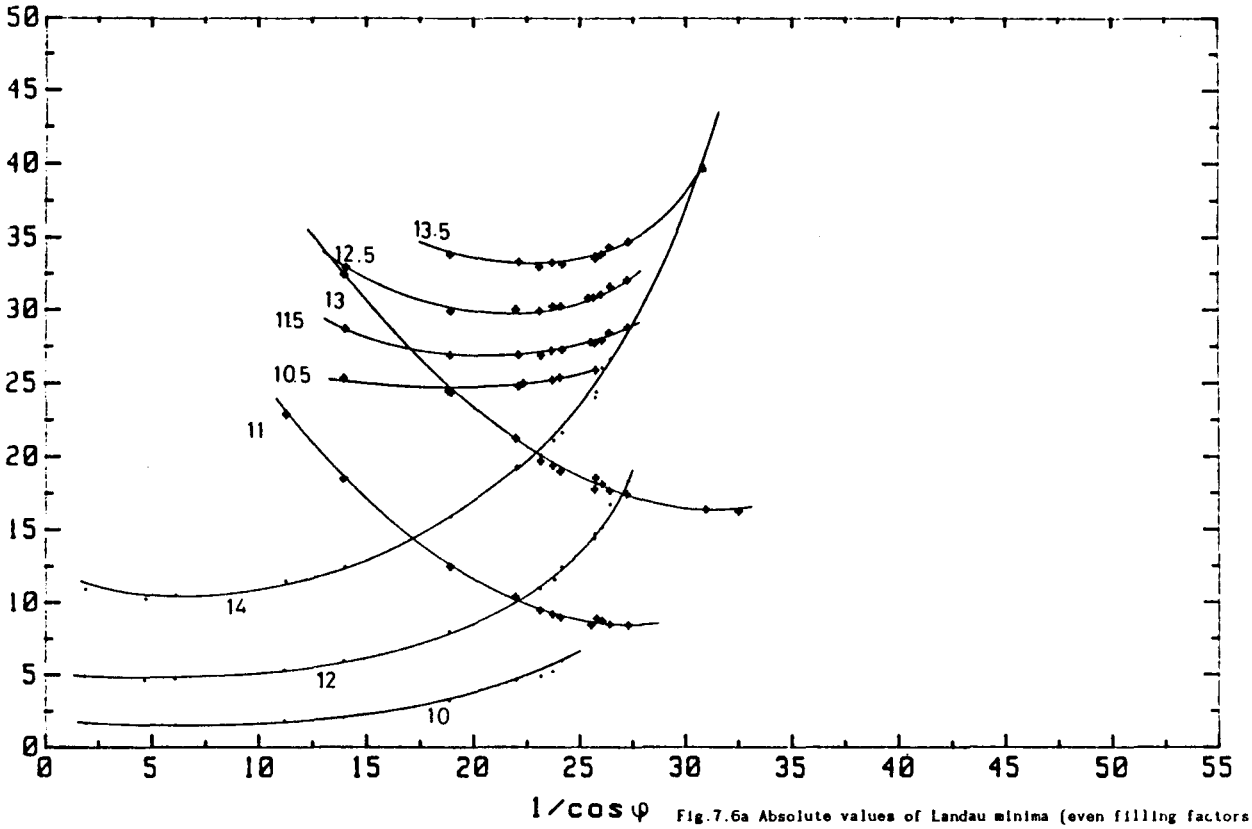

Fig.7.6a Absolute values of Landau minima (even filling factors) and spin minima (odd filling factors). The two splittings are comparable in the region where the odd minimum is between the two neighbouring minima.

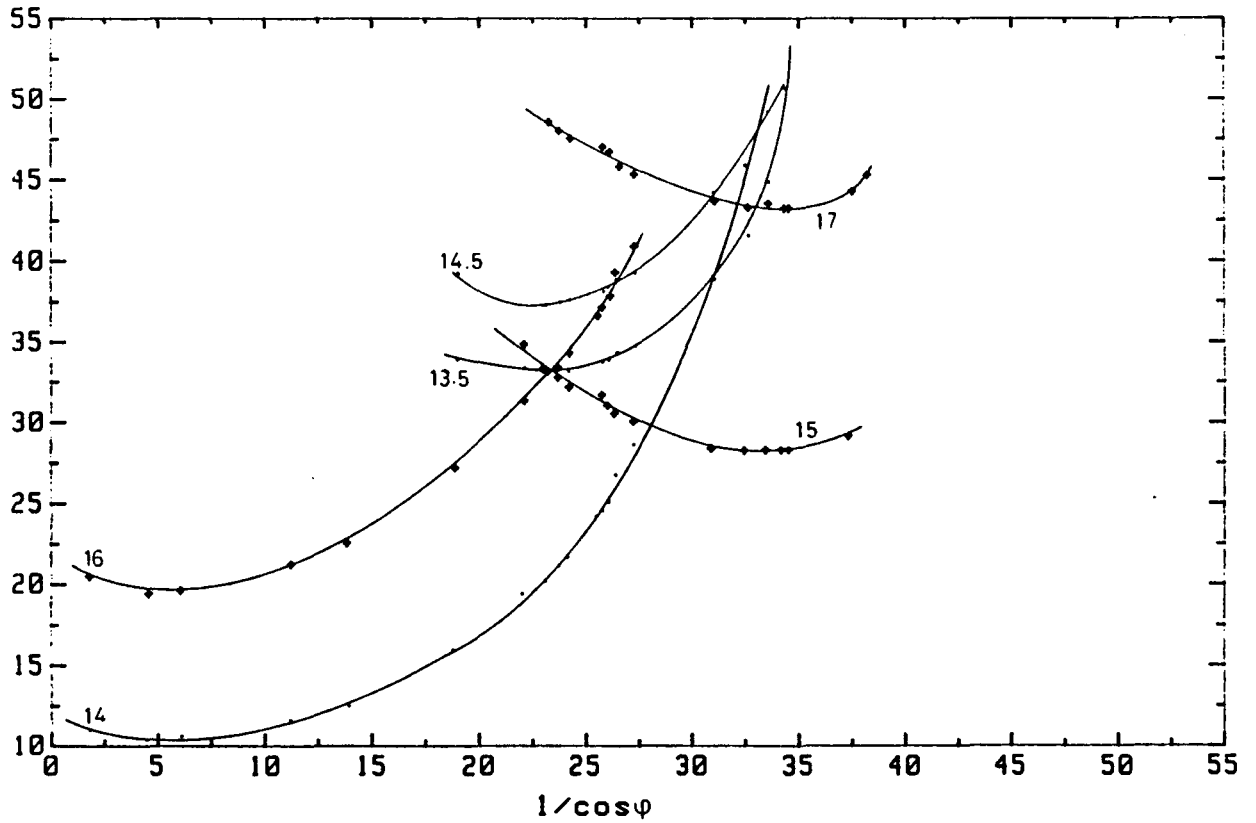

Fig.7.6b The lowest values for the spin minima 15 and 17 can be recognized.

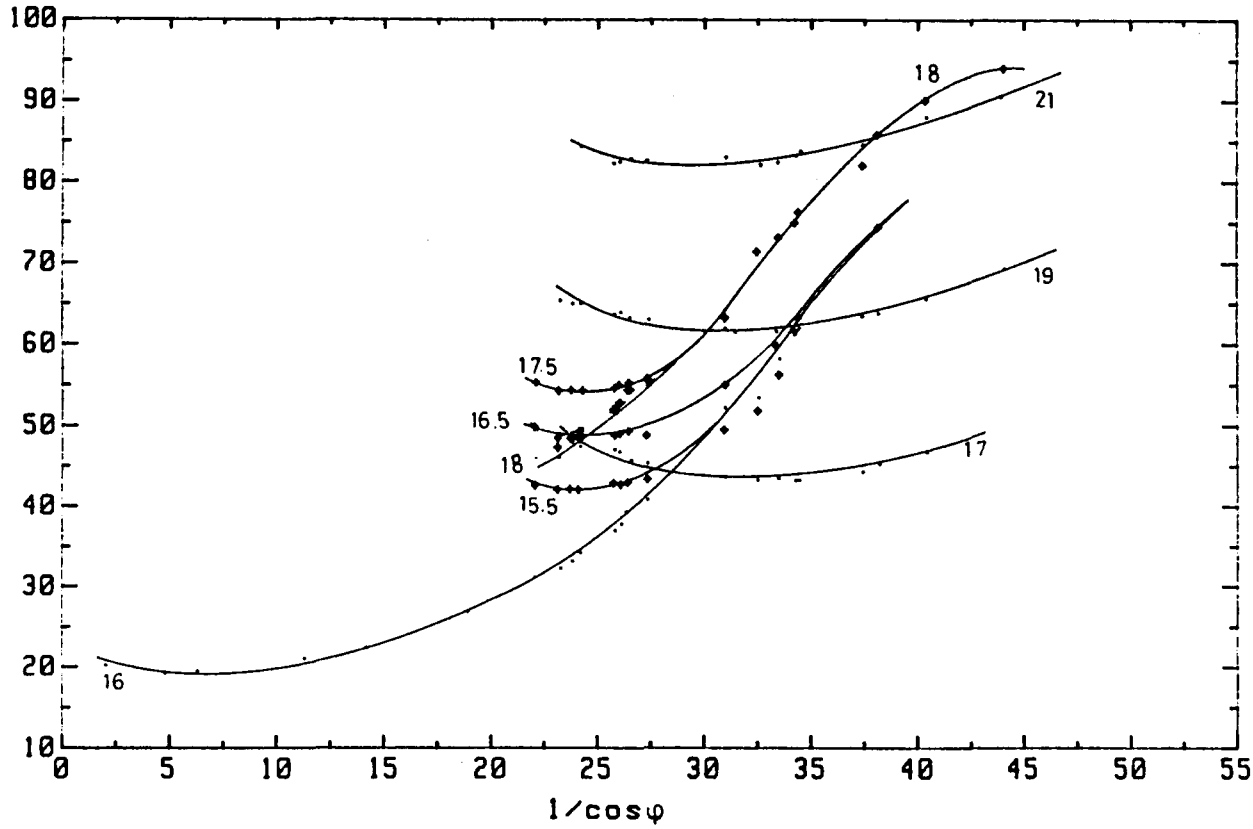

Fig.7.6c The Landau minima 16 and 18 disappear and form a new maximum with the neighbouring maxima.

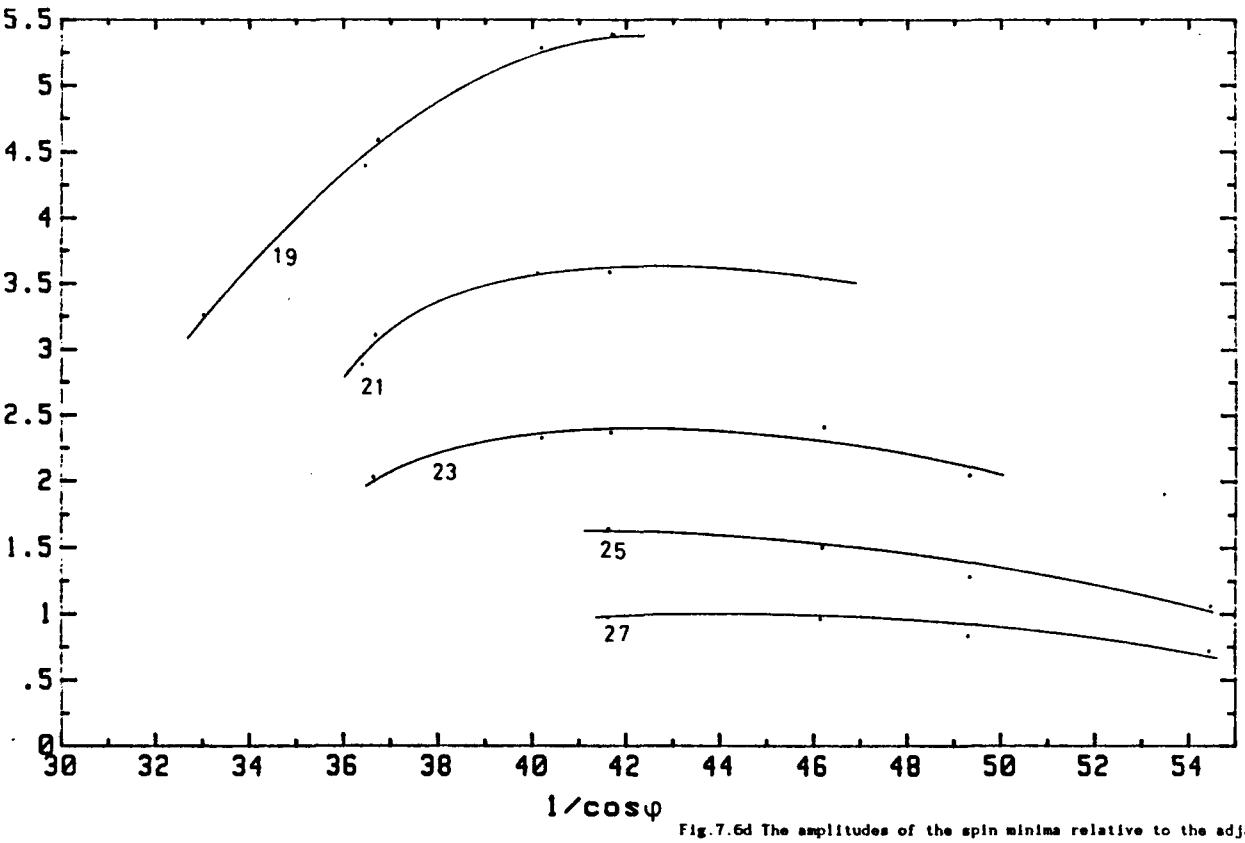

Fig.7.6d The amplitudes of the spin minima relative to the adjacent maxima.

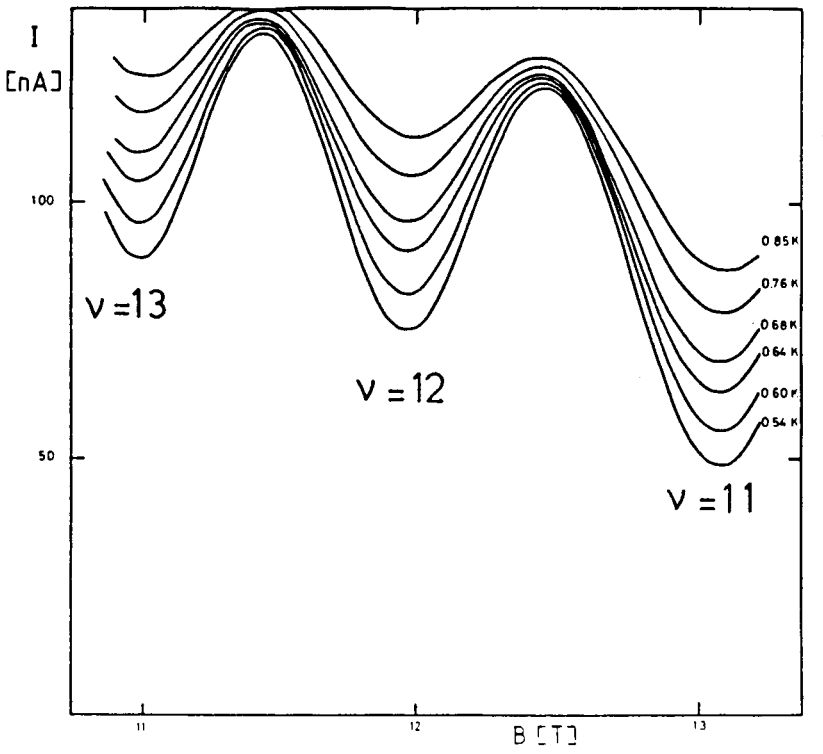

Fig.7.7a The temperature dependence of SdH curves at very large tilt angles.

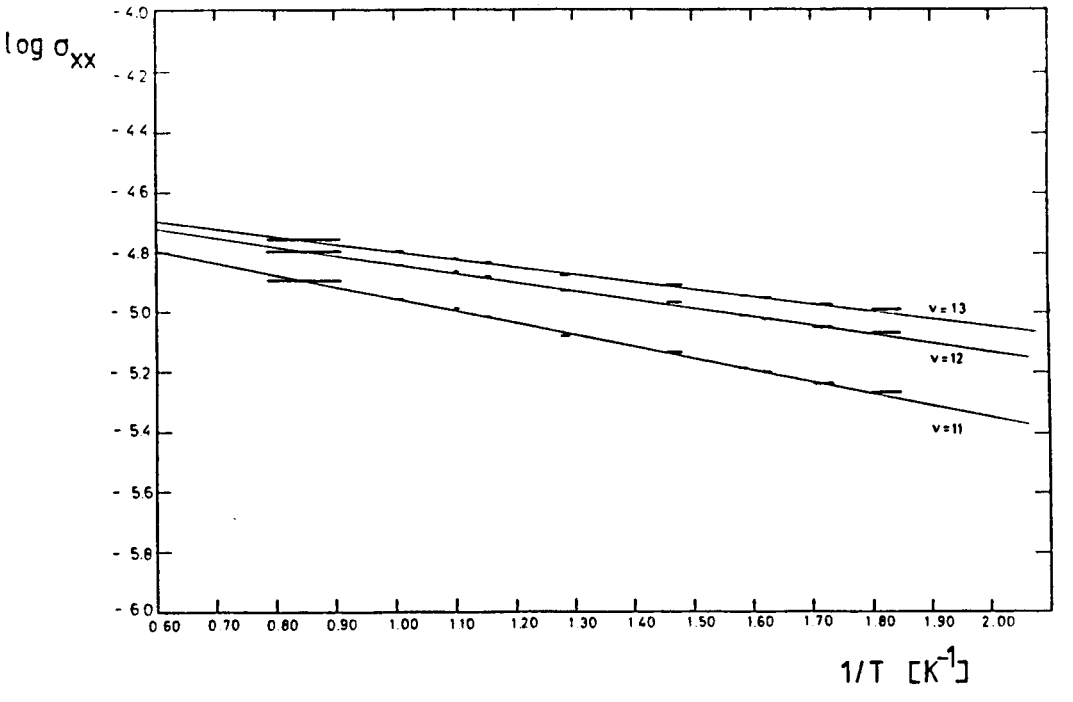

Fig.7.7b Logarithmic plot of the conductivity σ_{xx} (fig.7.7a) versus 1/T. An exponential behaviour is shown.

Table 7.1

Typical error: $0.5 < \Delta(1/\cos\varphi) < 1.$

Comparable even and odd minima:

$\sigma_{xx}(\upsilon_1) = \sigma_{xx}(\upsilon_2)$ at angle φ

υ_1	υ_2	$1/\cos\varphi$	g_s^*	$\hbar\omega_c$(K)	av.g^*
11	12	22.3	0.86	9.27	0.81
12	13	27.1	0.76	"	0.80
13	14	23.0	0.83	7.97	0.78
14	15	27.8	0.73	"	0.77
15	16	23.6	0.81	6.95	0.74
16	17	28.9	0.68	"	0.74
17	18	23.8	0.81	6.23	0.74
18	19	30.4	0.62	"	0.72

Activation energy:

$1/\cos\varphi$ = 25.58			$1/\cos\varphi$ = 26.05		
υ	E_a(K)	g^*	υ	E_a(K)	g^*
11	0.96	0.22	11	0.76	0.21
12	0.75	0.19	12	0.67	0.17
13	0.61	0.17	13	0.48	0.15

Maxima as low as possible:

υ	$1/\cos\varphi$	g^*	$\hbar\omega_c$(K)
10.5	18.8	0.93	10.64
11.5	20.8	0.82	9.70
12.5	21.0	0.82	8.91
13.5	22.8	0.74	8.25
14.5	22.0	0.77	7.68
15.5	24.0	0.70	7.20
16.5	24.2	0.69	6.76
17.5	24.2	0.69	6.38

Maximum amplitude of the spin minimum relative to the "Landau maximum":

υ	$1/\cos\varphi$	$\hbar\omega_c$(K)	g^*	B_{tot}
21	42.0-43.8	5.39	1.02-0.96	11.3-11.8
23	42.6-45.2	4.93	1.00-0.92	10.5-11.1

Chapter 8: Discussion

8.1: The activation energy in perpendicular and tilted magnetic fields

It has been shown in section 6.1 that the activation energies determined by means of the temperature dependence of σ_{xx} for $\upsilon = 4$ and $\upsilon = 6$ in W1527b (fig.4.3d,f) and for $\upsilon = 2$, $\upsilon = 4$ and $\upsilon = 6$ in W1561b (fig.4.4d,f) are significantly smaller than $1/2\hbar\omega_c$ (fig.6.2).

Furthermore, it has been demonstrated in section 5.2 that the interpretation of the activation energies between spin levels leads to an exchange energy which decreases as a function of tilt angle (table 5.2 and table 5.3). This is not expected from the theory of Janak [17] and Ando et al [20].

The question why at even filling factors the deviation of the activation energy relative to $1/2\hbar\omega_c$ is larger in smaller perpendicular fields, cannot be answered here. One suggestion is that the broadening of the extended range is more important for small splittings.

It is remarkable that the activation energy shows the largest deviations from $1/2\hbar\omega_c$ in the sample with the highest mobility (W1561b); one would expect less scattering and thus a small level broadening in samples with higher mobilities. Ebert [57], Stahl [36] and Nicholas [51] reported activation energies for a filling factor equal to 2 which increase relative to $1/2\hbar\omega_c$ as a function of electron density (fig.6.2). They observed a definite trend that the activation energy is larger than $1/2\hbar\omega_c$ for samples with the same electron density as W1561b. We mention here that sample W1561b is less stable than W1527b. In order to get useful symmetric minima and a reproducible value for the electron density sample W1561b has to be

cooled down more carefully than sample W1527b. Not only the activation energy for $\upsilon = 2$ is too small in W1561b, also the g-factor determined from the activation energy at $\upsilon = 1$ ($g^* = 6.2$) is smaller than for $\upsilon = 1$ in W1527b ($g^* = 8.4$). The measurements of Kleinmichel on a Si-MOSFET [34] ($g^* = 8$ or 9) and the measurements of Nicholas on a number of AlGaAs/GaAs heterostructures [51] ($g^* = 7.5$) indicate that for $\upsilon = 1$ a g-factor g^* of 6 is perhaps a bit small for a 2-DEG.

The mobility μ is determined under circumstances (B = 0 T) in which possibly other scattering processes are dominant. Without a magnetic field the mobility in the sample is relatively high and screening of the long-range scattering potentials is probable. But the thermally activated conductivity in a strong magnetic field is very low compared to the conductivity without magnetic field. Level broadening caused by both long- and short-range potentials is likely when the filling factor is integer [18]. Thus the mobility is not necessarily a true representation for the level broadening in magnetic fields, and a broadening of the range with extended states can be responsible for the very small values of the activation energy in W1561b.

A broadening of the range with extended states is not the only possibility to understand the deviations for the activation energy in perpendicular magnetic fields. If the current is carried by electrons in a range of extended states which is wide relative to kT, then for small cyclotron energies the Boltzmann exponent has a T dependent pre-factor. This leads to different values for the activation energy [36]. Furthermore, it is not sure that the mobility edges are sharp [25]. And also the better confinement of the 2-DEG lowers the expectation value $\langle z \rangle$ of the z coordinate [58]. Finally, we note that an exciton effect [64], or an impurity effect [65] can be important.

In conclusion, for small energy gaps ($\hbar\omega_c \leq 30$ Kelvin) the activation energy is shown here to deviate from $1/2\hbar\omega_c$. Up to now no interpretation can be accepted as being unequivocal for these deviations.

Before one determines a spin splitting by means of an activation energy it seems to be necessary to measure the activation energy at an even filling factor in the same sample. This has to be compared with the cyclotron energy before an interpretation in terms of a spin splitting can be trusted.

8.2: Cyclotron energy and spin splitting in tilted magnetic fields

The conductivity σ_{xx} is shown to be an exponential function of temperature between 1 and 4 Kelvin (fig.4.3). This behaviour is observed over a range of two decades or more for $\upsilon = 1$ and for $\upsilon = 2$ in the investigated sample (W1527b, Corbino). The activation energy for $\upsilon = 2$ is in quite good agreement with $1/2\hbar\omega_c$. We interprete this exponential energy as being half of the Landau level splitting for $\upsilon = 2$, and for $\upsilon = 1$ we interpret the activation energy as being half of the spin splitting. In the density of states the spin splitted Landau levels are assumed to have a range in which states exist that can carry current and this range is thought to have a neglegible width. If the filling factor is equal to 2 and the Fermi-energy lies between two different Landau levels we adopt a spin splitting which is described by the ESR g-factor ($g_o = 0.4$).

In sample W1527b the activation energy for $\upsilon = 2$ decreases 20 % if a parallel magnetic field B_y of 10.89 T is added to the perpendicular magnetic field B_z of 2.99 T. The same behaviour is seen in sample W1561b.

To calculate the influence of the first subband on the ground state subband a formula is derived by means of second order perturbation theory. Changes of the intersubband energy E_{01} are not included. These calculations give a decrease of $\hbar\omega_c$ proportional to B_y^2, if B_z is kept constant. Calculations with this formula show that the measured points, corrected for the spin splitting (g_o= 0.4), lie near the line with intersubband matrix element for a triangular well (z_{01}= 44 Å) with this intersubband energy (E_{01}= 20 meV, fig.6.4a).

To test whether the cyclotron energy really decreases in tilted magnetic fields or not, a cyclotron resonance experiment is carried out on a sample of the same wafer (W1527). A series of resonance experiments is carried out with tilt angles up to 82^o. The perpendicular magnetic field at which the resonance occurs, shifts and a linear increase of 15 % of this perpendicular field is shown (fig.6.6). The intersubband matrix element z_{01} is determined with the aid of the second order perturbation formula. The result is z_{01} = 42 Å. Thus the cyclotron resonance appears to be in excellent agreement with the theoretical formula and the thermally activated conductivity measurements (fig.6.8).

In conclusion, it is shown by simple perturbation theory and cyclotron resonance experiments that the decrease of the activation energy as a function of parallel magnetic field can indeed be interpreted in terms of Landau levels approaching each other. This decrease of the cyclotron energy has its origin in a mixing of the parallel and the perpendicular wave functions.

The activation energy between spin polarized levels (υ = 1, W1527b) increases 23% as a function of parallel field B_y with B_z= 6.00 T and

$0 \leq B_y \leq 12.2$ T. These activation energies are interpreted as being half of the spin splitting. A straight line can be drawn through the points as is shown in figure 5.1. This extrapolation does not go

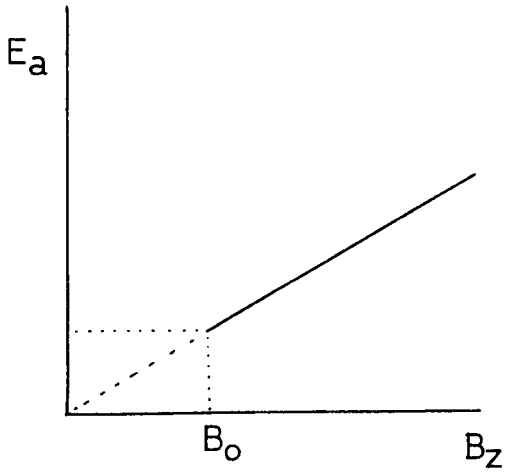

Fig.8.1 Spin splitting in a perpendicular magnetic field.

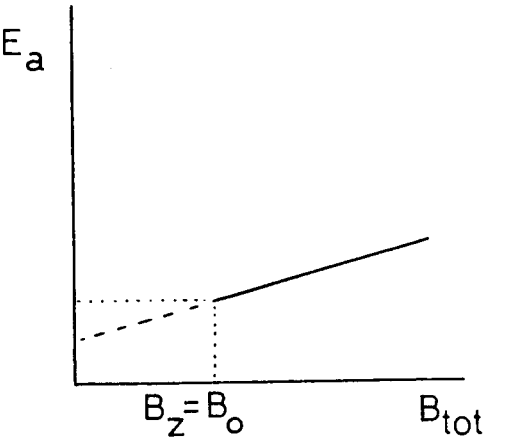

Fig.8.2 Spin splitting changed by a parallel magnetic field.

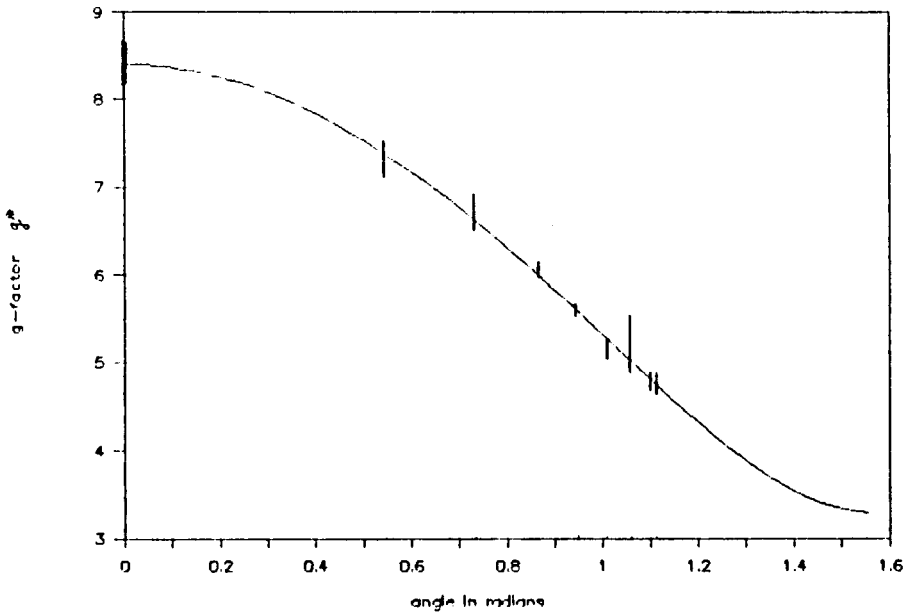

Fig.8.3 The solid line is calculated using $g_z = 8.4$ and $g_y = 3.3$ and equation (2.31).

through zero, while in perpendicular fields Kleinmichel [34] found in an Si-MOSFET an extrapolation which goes through zero and Nicholas [51] observed the same in GaAs/AlGaAs heterojunctions. This difference (fig.8.1 and fig.8.2) is understood as an anisotropy of the 2-DEC.

In an attempt to explain this anomaly we have treated the 2-DEC as an anisotropic spin system. The spin splitting of the Landau levels is described using a parallel g-factor g_y and a perpendicular g-factor g_z. They represent the coupling of the magnetic field components B_y and B_z with the electron spin. From the Hamiltonian we get

$$g^{*2} = g_z^2 \cos^2\varphi + g_y^2 \sin^2\varphi \qquad (2.31)$$

for a 2-DEC in the xy-plane with $\underline{B} = (0, B_y, B_z)$ and $\tan\varphi = B_y/B_z$. The quantity g^* is still defined as the dimensionless spin splitting.

The perpendicular component g_z is found to be equal to 8.4 ± 0.3. Assuming g_z to be constant, the parallel component g_y appears to be much smaller: $g_y = 3.3 \pm 0.3$. In fig.8.3 the quantity g^* is plotted as a function of tilt angle, together with the measurements. Similar values for g_y and g_z can be deduced from measurements on a 2-DEC in a Si-MOSFET [34]. Surprisingly, under the assumption of a constant cyclotron energy $\hbar\omega_c$ the activation energies at $\nu = 2$ also suggest a g-factor $g_y = 3.4 \pm 0.3$. In contrast with this interpretation the cyclotron resonance experiments give unequivocal evidence for a decrease of the cyclotron energy $\hbar\omega_c$ as a function of tilt angle. Comparison of the activation energy and the cyclotron resonance experiment by means of the second order perturbation formula (fig.6.8) shows that a significant enhancement of the g-factor is not probable. Thus, for even filling factors the spin splitting is shown to be smaller than for odd filling factors.

As a consequence of the decreasing cyclotron energy in parallel

fields the coincidence method (chapter 7) as it has been suggested by Fang and Stiles [19], is not valid for a determination of the spin splitting. It results in a maximum value for the g-factor g^*. Measurements of the activation energies cannot solve this problem, due to the difficulties which exist for the interpretation of the activation energy, when the levels around the Fermi-energy have a small energy difference. A combination of the coincidence method with f.i. cyclotron resonance experiments at very high tilt angles is needed to perform a true estimation of the g-factor.

To investigate the complete behaviour of the spin splitting, measurements with a constant B_y but changing B_z and for different Landau quantum numbers should be done. To investigate whether the exchange energy is responsible for the spin splitting or not, the theory of Ando and Uemura [20] has to be worked out for tilted magnetic fields.

Summary

The temperature dependence of the conductivity σ_{xx} in a two-dimensional electron gas (2-DEG) is determined in tilted magnetic fields ($\lesssim$ 14 Tesla). The measurements are carried out on a high mobility AlGaAs/GaAs heterostructure (sample W1527b; μ=6.1 $10^5 cm^2/Vs$; n_s=1.45 $10^{11} cm^{-2}$) and they are duplicated on a second sample (sample W1561b; μ=9.3 $10^5 cm^2/Vs$; n_s=2.59 $10^{11} cm^{-2}$). The thermally activated conductivity is used as a tool to investigate the Landau and spin splitting in tilted magnetic fields. For further investigations of the Landau levels cyclotron resonance experiments are carried out on a sample of the same wafer (W1527).

To interpret the measurements a model of broadened spin splitted Landau levels with current carrying states in the centre of each spin level is adopted. In order to determine the conductivity the current through the sample ($\gtrsim$1nA) is measured with the aid of a shunt (1kΩ) while a DC voltage source (1mV) is used. The measurements are carried out in helium-4 (1.5K<T<20K) and in helium-3 (0.5K<T).

The temperature dependence of the conductivity in several minima of the Shubnikov-de Haas effect (filling factor ν=1 to 6) shows a linear relation between $\ln\sigma_{xx}$ and 1/T. This is interpreted as an activation energy, which should represent half the energy gap of the two levels around the Fermi-energy.

The activation energy for ν=2 (W1527b) in a perpendicular magnetic field is approximately equal to half of the cyclotron energy ($1/2\hbar\omega_c$). The activation energy for the other even filling factors in both samples appears to deviate from $1/2\hbar\omega_c$. Several mechanisms exist which can be responsible for this.

As a function of parallel magnetic field ($B_y \leq 12T$) the activation energy for $\nu=2$ ($B_z=2.99T$) decreases by 20% and for $\nu=1$ ($B_z=6.00T$) it increases by 23%.

The increasing activation energy for $\nu=1$ is interpreted in terms of an increasing spin splitting. An explanation by means of an anisotropic g-factor is apparently inconsistent with the measurements for $\nu=2$. Our measurements give evidence that the enhanced g-factor is significantly smaller in the case of $\nu=2$ than for $\nu=1$. An interpretation of the spin splitting in tilted magnetic fields in terms of a many-particle exchange enhancement leads to an exchange energy which increases linearly with the total magnetic field.

We have shown by means of cyclotron resonance experiments with a fixed laser frequency, that the cyclotron energy $\hbar\omega_c$ decreases proportional to the parallel magnetic field squared. Second order perturbation theory shows this to be due to a mixing of the parallel and perpendicular parts of the wave function. The resulting intersubband matrix element z_{01} is nearly equal to the value for a triangular well. This decrease of $\hbar\omega_c$ as a function of parallel magnetic field is thought to be the main source for the decreasing activation energy at $\nu=2$.

As a consequence the coincidence method of Fang and Stiles cannot be used to determine the spin splitting in tilted magnetic fields. It only results in a maximum possible value for the enhanced g-factor. The activation energy in the situation of equal spacings between Landau levels and spin levels (angle$\simeq 87.8^o$) does not offer a good opportunity to estimate the spin splitting.

In short, some questions that remain, are:

- What causes the activation energy at even filling factors to deviate

from $1/2\hbar\omega_c$?

- Why do the activation energies at even filling factors seem to result in too large values compared to the cyclotron resonance experiments and the second order perturbation formula, if an additional parallel magnetic field is applied?
- What is the source for the enlarged spin splitting of the Landau levels?
- And if this is due to a many-particle enhancement as suggested by Janak: why show the activation energies between two spin levels the opposite trend than the activation energies between Landau levels in tilted magnetic fields?

Literature

1. K.v.Klitzing, G.Dorda, M.Pepper, Phys.Rev.Lett. 45, 494 (1980) 'New method for High-Accuracy Determination of the Fine-Structure Constant Based on Quantized Hall Resistance'.
2. M.Chmielowski, M.Glinski, W.H.Zhuang, G.B.Liang, D.Z.Sun, M.Y.Kong, W.Plesiewicz, T.Dietl, T.Skoskiewicz, Surface Science 196, 299 (1988), 'Fundamental high-field transport properties of a GaAs/AlGaAs modulation doped heterostructure'.
3. T.Ando, J.Phys.Soc.Jpn. 51, 3893 (1982), 'Self-Consistent Results for a GaAs/$Al_xGa_{1-x}As$ Heterojunction. I. Subband Structure and Light-Scattering Spectra'.
4. G.A.Hurkx and W.van Haeringen, J.Phys.C. 18, 5617 (1985), 'Self-consistent calculations on GaAs-$Al_xGa_{1-x}As$ heterojunctions'.
5. G.L.J.A.Rikken, H.Sigg, C.J.G.M.Langerak, H.W.Myron, J.A.A.J.Perenboom, G.Weimann, Phys.Rev.B, 34, 5590 (1986), 'Subband-Landau-level spectroscopy in GaAs-$Al_xGa_{1-x}As$ heterojunctions'.
6. M.A.Hopkins, R.J.Nicholas, M.A.Brummell, J.J.Harris, C.T.Foxon, to be published,'A Cyclotron Resonance Study of Non-parabolicity and Screening in GaAs-GaAlAs Heterojunctions'.
7. M.Dobers, dissertation Universität/MPI Stuttgart 1987. 'Elektronen-Spin-Resonanz im zweidimensionalen Elektronengas von GaAs-AlGaAs-Heterostrukturen'.
8. T.Ando, A.B.Fowler, F.Stern, Rev.Mod.Phys. 54, 552 (1982), 'Electronic properties of two-dimensional systems'.
9. T.Ando and Y.Murayama, J.Phys.Soc.Jpn. 54, 1519 (1985), 'Landau-Level Broadening in GaAs/AlGaAs Heterojunctions'.

10. H.Sigg, J.A.A.J.Perenboom, Solid State Commun. 61, 685 (1987), 'Non-parabolicity and anisotropy in the conduction band of GaAs'.

11. M.A.Hopkins, R.J.Nicholas, P.Pfeffer, W.Zawadzki, D.Gauthier, J.C.Portal, M.A.DiForte-Poisson, Semicond.Sci.Technol. 2, 586 (1987).

12. L.D.Landau and E.M.Lifshitz, Vol.3, 2nd ed. 'Quantum Mechanics non-relativistic theory', Pergamon Press Oxford.

13. T.Ando, Phys.Rev.B. 19, 2106 (1979), 'Theory of intersubband cyclotron combined resonances in the silicon space-charge layer'.

14. J.C.Maan, in 'Two Dimensional Systems, Heterostructures, and Superlattices', Springer series in Solid-state sciences 53, 183 (1984), 'Combined Electric and Magnetic Field Effects in Semiconductor Heterostructures'.

15. R.Merlin, Solid State Commun. 64, 99 (1987), 'Subband-Landau-level coupling in tilted magnetic fields: exact results for parabolic wells'.

16. G.Lommer, F.Malcher, U.Rössler, Phys.Rev.B 32, 6965 (1985), 'Reduced g factor of subband Landau levels in AlGaAs/GaAs heterostructures'.

17. J.F.Janak, Phys.Rev. 178, 1416 (1969), 'g Factor of the Two-Dimensional Interacting Electron Gas'.

18. I.Kukushkin, V.Timoteev, K.v.Klitzing, K.Ploog, to be published in Phys.Rev.B, 'Magnetooptics of Two-Dimensional Electrons under the conditions of Integral and Fractional Quantum Hall effect in Si-MOSFETs and GaAs-AlGaAs Single Heterojunctions'.

19. F.F.Fang, P.J.Stiles, Phys.Rev. 174, 823 (1968), 'Effects of a Tilted Magnetic Field on a Two-Dimensional Electron Gas'.

20. T.Ando, Y.Uemura, J.Phys.Soc.Jpn. 37, 1044 (1974), 'Theory of

Oscillatory g Factor in an MOS Inversion Layer under Strong Magnetic Fields'.

21. C.Kittel, 'Introduction to Solid State Physics', 6th ed. (1974) John Wiley & Sons, New York, p.142.
22. R.B.Laughlin, in 'Two Dimensional Systems, Heterostructures, and Superlattices', Springer series in Solid-state sciences 53, 272 (1984), 'The Gauge Argument for Accurate Quantization of the Hall Conductance'.
23. T.Ando, Y.Matsumoto, Y.Uemura, M.Kobayashi, K.I.Komatsubara, J.Phys.Soc.Jpn. 32, 859 (1972), 'Transverse Magneto-Conductivity of a Two-Dimensional Electron Gas'.
24. T.Ando, J.Phys.Soc.Jpn. 37, 622 (1974), 'Theory of Quantum Transport in a Two-Dimensional Electron System under Magnetic Fields. III. Many-Site Approximation'.
25. H.Aoki, Rep.Prog.Phys. 50, 655 (1987), 'Quantised Hall effect'.
26. R.J.Haug, R.R.Gerhardts, K.v.Klitzing, K.Ploog, Phys.Rev.Lett. 59, 1349 (1987), 'The Effect of Repulsive and Attractive Scattering Centers on the Magnetotransport Properties of a Two-Dimensional Electron Gas'.
27. A.Raymond, K.Karrai, to be published, 'Transfer of electrons and localization in the Quantum Hall Effect'.
28. M.Pepper, S.Pollit, C.J.Adkins, R.A.Stradling, CRC Critical Rev. in Solid State Sciences, 375 (1975), 'Anderson localization in silicon inversion layers'.
29. S.Kawaji, J.Wakabayashi, Solid State Commun. 22, 87 (1977), 'Temperature dependence of the magnetoconductivity in the ground Landau level in silicon inversion layers'.
30. Th.Englert, K.von Klitzing, Surf. Sci. 73, 70 (1978),

'Analysis of ρ_{xx} minima in surface quantum oscillations on (100) n-type silicon inversion layers'.

31. R.J.Nicholas, R.A.Stradling, S.Askenazy, P.Perrier, J.C.Portal, Surf. Sci. 73, 106 (1978), 'The analysis of thermal activation of two-dimensional Shubnikov-de Haas conductivity minima and maxima'.
32. B.Tausendfreund and K.von Klitzing, Surf. Sci. 142, 220 (1984), 'Analysis of quantized Hall resistance at finite temperatures'.
33. K.v.Klitzing, G.Ebert, N.Kleinmichel, H.Obloh, G.Dorda, G.Weimann, Proc. 17th Int. Conf. Physics of Semiconductors, San Francisco, 6-10 Aug. 1984, ed. by J.D.Chadi, W.A.Harrison, 'Energy dissipation processes in the Quantum Hall regime'.
34. N.Kleinmichel, Diplomarbeit Technische Universität München, 1984, 'Untersuchungen zum Magnetowiderstand an (100)-Silizium-n-Kanal MOS-Feldeffekt-Transistoren'.
35. E.Stahl, D.Weiss, G.Weimann, K.von Klitzing, K.Ploog, J.Phys.C. 18, L783 (1985), 'Density of states of a two-dimensional electron gas in a strong magnetic field'.
36. E.Stahl, Diplomarbeit Technische Universität München, 1985, 'Die Zustandsdichte in den Ausläufern der Landauniveaus eines zweidimensionalen Elektronengases'.
37. M.G.Gavrilov, I.V.Kukushkin, JETP Lett. 43, 103 (1986), 'State density in gaps in the energy spectrum of 2D electrons in a transverse magnetic field'.
38. V.Gudmundsson, R.R.Gerhardts, to be published, 'Interpretation of activated resistivity in the quantum Hall regime by a statistical model of inhomogeneities'.

39. A.A.Shakin, V.T.Dolgopolov, N.B.Zhitenev, Solid State Commun. 65, 323 (1988), 'Magnetic field dependence of the density of states minimum of a two-dimensional electron gas in silicon MOS-structures'.

40. N.F.Mott, E.A.Davis, 'Electronic Processes in Non-Crystalline Materials', 2nd ed. Clarendon Press, Oxford (1979).

41. G.Ebert, K.von Klitzing, C.Probst, E.Schuberth, K.Ploog, G.Weimann, Solid State Commun. 45, 625 (1983), 'Hopping conduction in the Landau level tails in GaAs-$Al_xCa_{1-x}As$ heterostructures at low temperatures'.

42. R.J.Nicholas, R.A.Stradling, R.J.Tidey, Solid State Commun. 23, 341 (1977), 'Evidence for Anderson localization in Landau level tails from the analysis of two-dimensional Shubnikov-de Haas conductivity minima.

43. D.C.Tsui, H.L.Störmer, A.C.Gossard, Phys.Rev.B 25, 1405 (1982), 'Zero-resistance state of two-dimensional electrons in a quantizing magnetic field'.

44. R.J.Haug, K.v.Klitzing, R.J.Nicholas, J.C.Maan, G.Weimann, 7th int.conf.on electr.prop.of two-dim. systems, Santa Fe, 1987, 'The Influence of a Tilted Magnetic Field on the Fractional Quantum Hall Effect and the Exchange Enhancement of the Spin Splitting'.

45. D.Dominguez, priv.comm.

46. S.Oelting, A.D.Wieck, E.Batke, U.Merkt, 7th int.conf.on electr. prop. of two-dim. systems, Santa Fe, 1987, 'Cyclotron masses of inversion electrons in tilted magnetic fields'.

47. K.Ensslin, priv.comm.

48. M.A.Brummell, M.A.Hopkins, R.J.Nicholas, J.C.Portal, K.Y.Chang,

A.Y.Cho, J.Phys.C. 19, L107 (1986), 'Subband-Landau level coupling in a two-dimensional electron gas in tilted magnetic fields'.

49. Th.Englert, D.C.Tsui, A.C.Gossard, Ch.Uihlein, Surf. Sci. 113, 295 (1982), 'g-Factor enhancement in the 2D electron gas in GaAs/AlGaAs heterojunctions'.

50. R.J.Nicholas, R.J.Haug, K.v.Klitzing, G.Weimann, Phys.Rev.B 37, 1294 (1988), 'Exchange enhancement of the spin splting in a GaAs-$Ga_xAl_{1-x}As$ heterojunction'.

51. R.J.Nicholas, priv.comm.

52. H.Sigg, priv.comm. In W1527b cyclotron resonance has shown E_{01} to be 20.73 meV. This is measured under the condition that $\hbar\omega_c(0^o)=E_{01}$. It also appeared that b=7.42 $10^{-4}meV^{-2}$. For this method we refer to [63].

53. Klaus von Klitzing, Rev.Mod.Phys. 58, 519 (1986), 'The quantized Hall effect'.

54. R.J.Haug, dissertation Universität/MPI Stuttgart 1988. 'Untersuchungen zum Magnetotransport in zweidimensionalen Elektronensystemen'.

55. F.Stern and W.E.Howard, Phys.Rev. 163, 816 (1967), 'Properties of Semiconductor Surface Inversion Layers in the Electric Quantum Limit'.

56. K.Ensslin, D.Heitmann, H.Sigg, K.Ploog, to be published, 'Cyclotron Resonance in $Al_xGa_{1-x}As$-GaAs Heterostructures with Tunable Charge Density via Front Gates'.

57. G.Ebert, dissertation Technische Universität München 1983, 'Magnetotransportuntersuchungen an GaAs-$Al_xGa_{1-x}As$-heterostukturen'.

58. D.A.Syphers, J.E.Furneaux, Solid State Commun. 65, 1513 (1988), 'The fractional quantum Hall effect in a tilted magnetic field'.

59. D.Wagner, 'Introduction to the theory of magnetism', 1st ed. (1972), Pergamon Press, Oxford (p.145).

60. A.M.C.Tinus, dissertation Eindhoven University of Technology 1986, 'Excitations in ferromagnetic quantum chains'.

61. M.E.Mohammed, dissertation Eindhoven University of Technology 1987, 'Relaxation studies on linear excitations in pure and impure Ising-type magnetic systems'.

62. J.C.Schouten, dissertation Eindhoven University of Technology 1981, 'Impurities in quasi one-dimensional systems'.

63. G.L.J.A.Rikken, H.Sigg, C.J.G.M.Langerak, H.W.Myron, J.A.A.J.Perenboom, G.Weimann, Phys.Rev.B 34, 5590 (1986), 'Subband-Landau-level spectrosopy in GaAs-$Al_xCa_{1-x}As$ heterojunctions'.

64. G.A.Baraff, D.C.Tsui, Phys.Rev.B 24, 2274 (1981), 'Explanation of quantized-Hall-resistance plateaus in heterojunction inversion layers'.

65. Yu.Bychkov, S.V.Iordanskii, G.M.Éliashberg, JETP Lett. 33, 143 (1981), 'Two-dimensional electrons in a strong magnetic field'.

66. M.A.Paalanen, D.C.Tsui, A.C.Gossard, Phys.Rev.B 25, 5566 (1982), 'Quantized Hall effect at low temperatures'.

67. Y.Ono, J.Phys.Soc.Jpn 51, 237 (1982), 'Localization of Electrons under Strong Magnetic Fields in a Two-Dimensional System'.

Appendix A

Second order perturbation theory

In this appendix we treat the mixing term in the Hamiltonian

$$H_2 = \frac{e}{m^*} B_y \, z p_x \, , \tag{A.1}$$

by means of second order perturbation theory. The wave function is separated in a z-sensitive part $\varphi_i(z)$, labelled by subband index i, and an x-sensitive part $\psi_n(x)$, of which the unperturbed eigenfunctions with eigenvalues $E_n^{(0)}$ are labelled by the Landau level index n. We only treat the influence of i=1 on i=0. The first order perturbation of the x-sensitive part

$$E_n^{(1)} = \langle i=0,n|H_2|i=1,n\rangle \tag{A.2}$$

is zero, because of $\langle n|p_x|n\rangle=0$. Remember that the operator p_x does not work on the subband functions, because they depend on z only; z also does not affect $\psi_n(x)$. The second order perturbation of the Landau level energies is

$$E_n^{(2)} = \sum_m{}' \frac{|\langle 1,m|H_2|0,n\rangle|^2}{(E_{i=0}+E_n^{(0)})-(E_m^{(0)}+E_{i=1})} \, . \tag{A.3}$$

The conditions that have to be fulfilled are mentioned in chapter 6. The perturbations of the Landau levels are:

$$E_{n=0}^{(2)} = -\frac{e^2}{m^{*2}} B_y^2 \, z_{01}^2 \, \frac{|\langle n=1|p_x|n=0\rangle|}{E_{01}+\hbar\omega_{cz}} \tag{A.4a}$$

$$E_{n=1}^{(2)} = -\frac{e^2}{m^{*2}} B_y^2 \, z_{01}^2 \, \{\frac{|\langle 0|p_x|1\rangle|^2}{E_{01}-\hbar\omega_{cz}} + \frac{|\langle 2|p_x|1\rangle|^2}{E_{01}+\hbar\omega_{cz}}\} \tag{A.4b}$$

$$E_{n=2}^{(2)} = -\frac{e^2}{m^{*2}} B_y^2 \, z_{01}^2 \, \{\frac{|\langle 1|p_x|2\rangle|^2}{E_{01}-\hbar\omega_{cz}} + \frac{|\langle 3|p_x|2\rangle|^2}{E_{01}+\hbar\omega_{cz}}\} \tag{A.4c}$$

$$E_{n=3}^{(2)} = -\frac{e^2}{m^{*2}} B_y^2 \, z_{01}^2 \, \{\frac{|\langle 2|p_x|3\rangle|^2}{E_{01}-\hbar\omega_{cz}} + \frac{|\langle 4|p_x|3\rangle|^2}{E_{01}+\hbar\omega_{cz}}\} \tag{A.4d}$$

in which

$$z_{01} = \langle i=0|z|i=1\rangle \tag{A.5}$$

is the intersubband matrix element. The matrix elements $\langle n|p_x|m\rangle$ can be calculated straightforward, because the unperturbed Landau level wave functions are the well-known one-dimensional harmonic oscillator functions. Thus, we get

$$\langle 0|p_x|1\rangle = \frac{1}{\sqrt{2}}\sqrt{(m^*\omega_{cz}\hbar)}\ ; \tag{A.6a}$$

$$\langle 1|p_x|2\rangle = \sqrt{(m^*\omega_{cz}\hbar)}\ ; \tag{A.6b}$$

$$\langle 2|p_x|3\rangle = \frac{1}{2}\sqrt{6}\ \sqrt{(m^*\omega_{cz}\hbar)}\ ; \tag{A.6c}$$

$$\langle 3|p_x|4\rangle = \sqrt{2}\ \sqrt{(m^*\omega_{cz}\hbar)} \tag{A.6d}$$

and for instance $\langle 0|p_x|3\rangle = 0$, $\langle 1|p_x|4\rangle = 0$. Note that $\hbar\omega_{cz}$ belongs to the perpendicular magnetic field in this, perturbed, situation. In a cyclotron resonance experiment in tilted fields, the resonance is shifting to another filling factor and another $\hbar\omega_{cz}$, so $\hbar\omega_{cz}$ is not equal to $\hbar\omega_c(0^o)$ in a cyclotron resonance experiment. Activation measurements always take place at a fixed filling factor. Then, $\hbar\omega_{cz}$ is fixed, and it can be replaced by $\hbar\omega_c(0^o)$.

After this correction the Landau levels energies become:

$$E(i=0,n=0) = E(i=0) + \frac{1}{2}\hbar\omega_{cz} - \frac{e^2}{m^{*2}}B_y^2 z_{01}^2 m^*\hbar\omega_{cz}\frac{1}{2}/(E_{01}+\hbar\omega_{cz})$$

$$E(i=0,n=1) = E(i=0) + \frac{3}{2}\hbar\omega_{cz} - \frac{e^2}{m^{*2}}B_y^2 z_{01}^2 m^*\hbar\omega_{cz}\left\{\frac{1/2}{E_{01}-\hbar\omega_{cz}}+\frac{1}{E_{01}+\hbar\omega_{cz}}\right\}$$

$$E(i=0,n=2) = E(i=0) + \frac{5}{2}\hbar\omega_{cz} - \frac{e^2}{m^{*2}}B_y^2 z_{01}^2 m^*\hbar\omega_{cz}\left\{\frac{1}{E_{01}-\hbar\omega_{cz}}+\frac{6/4}{E_{01}+\hbar\omega_{cz}}\right\}$$

$$E(i=0,n=3) = E(i=0) + \frac{7}{2}\hbar\omega_{cz} - \frac{e^2}{m^{*2}}B_y^2 z_{01}^2 m^*\hbar\omega_{cz}\left\{\frac{6/4}{E_{01}-\hbar\omega_{cz}}+\frac{2}{E_{01}+\hbar\omega_{cz}}\right\}$$

(A.7a-d)

The cyclotron energy is the difference between two adjacent Landau

levels:

$$E_c(\upsilon=2) = E(i=0,n=1) - E(i=0,n=0) \tag{A.8a}$$

$$E_c(\upsilon=4) = E(i=0,n=2) - E(i=0,n=1) \tag{A.8b}$$

$$E_c(\upsilon=6) = E(i=0,n=3) - E(i=0,n=2)\ . \tag{A.8c}$$

They appear to be the same after the perturbation:

$$E_c = \hbar\omega_{cz} - \frac{e^2}{m^*} B_y^2 z_{01}^2 \frac{\hbar\omega_{cz}}{E_{01}} \frac{1}{1-(\hbar\omega_{cz}/E_{01})^2}\ . \tag{A.9}$$

When we divide this by $\hbar\omega_{cz} = \hbar eB_z/m^*$ (A.9) formula can be written with the help of

$$\tan^2\varphi = B_y^2/B_z^2 \tag{A.10}$$

as

$$\frac{\hbar\omega_c(B_y)}{\hbar\omega_{cz}} = 1 - z_{01}^2 \frac{m^*}{\hbar^2} \tan^2\varphi \frac{(\hbar\omega_{cz})^2}{E_{01}} \frac{1}{1-(\hbar\omega_{cz}/E_{01})^2}\ . \tag{A.11}$$

Appendix B

Analysis of the pre-factor

Mott suggested that the mobility edge between the regions of extended states and localized states in the density of states D(E), are possibly sharp [40]. When the Fermi-energy passes this mobility threshold a phase change from a metallic to an insulating phase is taking place. For two-dimensional systems his theory predicts for disordered two-dimensional systems that the conductivity has a certain minimum value σ_{min} in the metallic phase, just before the change to the insulating phase takes place. This σ_{min} would be related to our experiments by [28,42]

$$\sigma_{xx} = \sigma_{min} \exp(-E_a/kT) \qquad (B.1)$$

where the width of the region with extended states is neglected.

The existence of one common pre-factor for every filling factor would offer the nice opportunity to estimate the level splitting for integer filling factors; only the pre-factor and the temperature are needed, together with σ_{xx} in the SdH minimum.

It is shown in fig.B.1, fig.B.2 and fig.B.3 that it is not possible to accept any value as pre-factor for this sample. The extra dots in these figures indicate the pre-factors which belong to the arbitrarily chosen common intersection points ($1/T \neq 0$) in fig.4.3. We see in fig.B.2 that we can even doubt the existence of such a crossing for $\nu = 2$. For $\nu = 4$ and $\nu = 6$ it is possible to draw a horizontal line through all the points. This means that a constant pre-factor is possible for each filling factor, and that it would be allowed to draw the lines in fig.4.3a,d and f through a common intersection point at the $1/T=0$ axis.

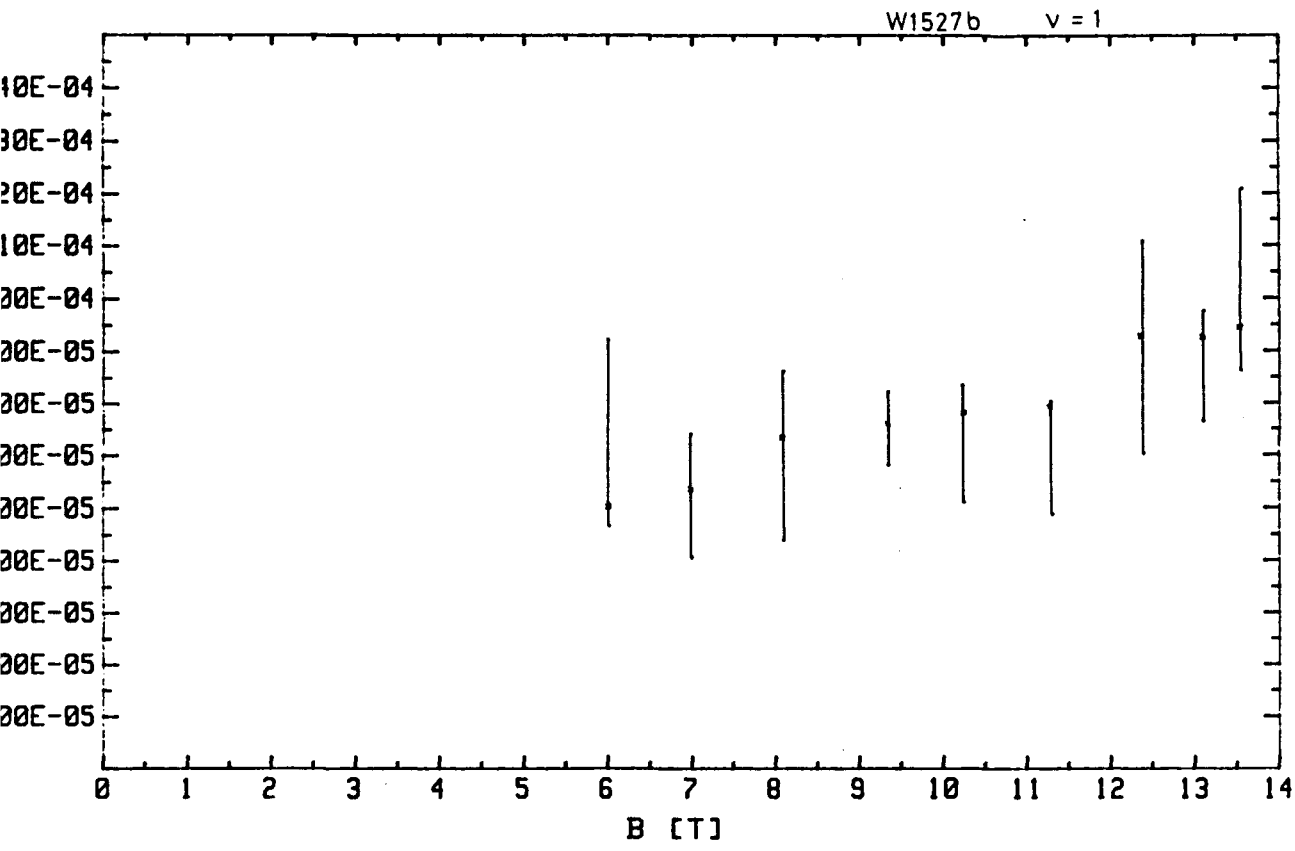
Prefactor (1/ohm)
W1527b ν = 1
10E-04
30E-04
20E-04
10E-04
00E-04
00E-05
00E-05
00E-05
00E-05
00E-05
00E-05
00E-05
00E-05
0 1 2 3 4 5 6 7 8 9 10 11 12 13 14
B [T]

Fig.B.1

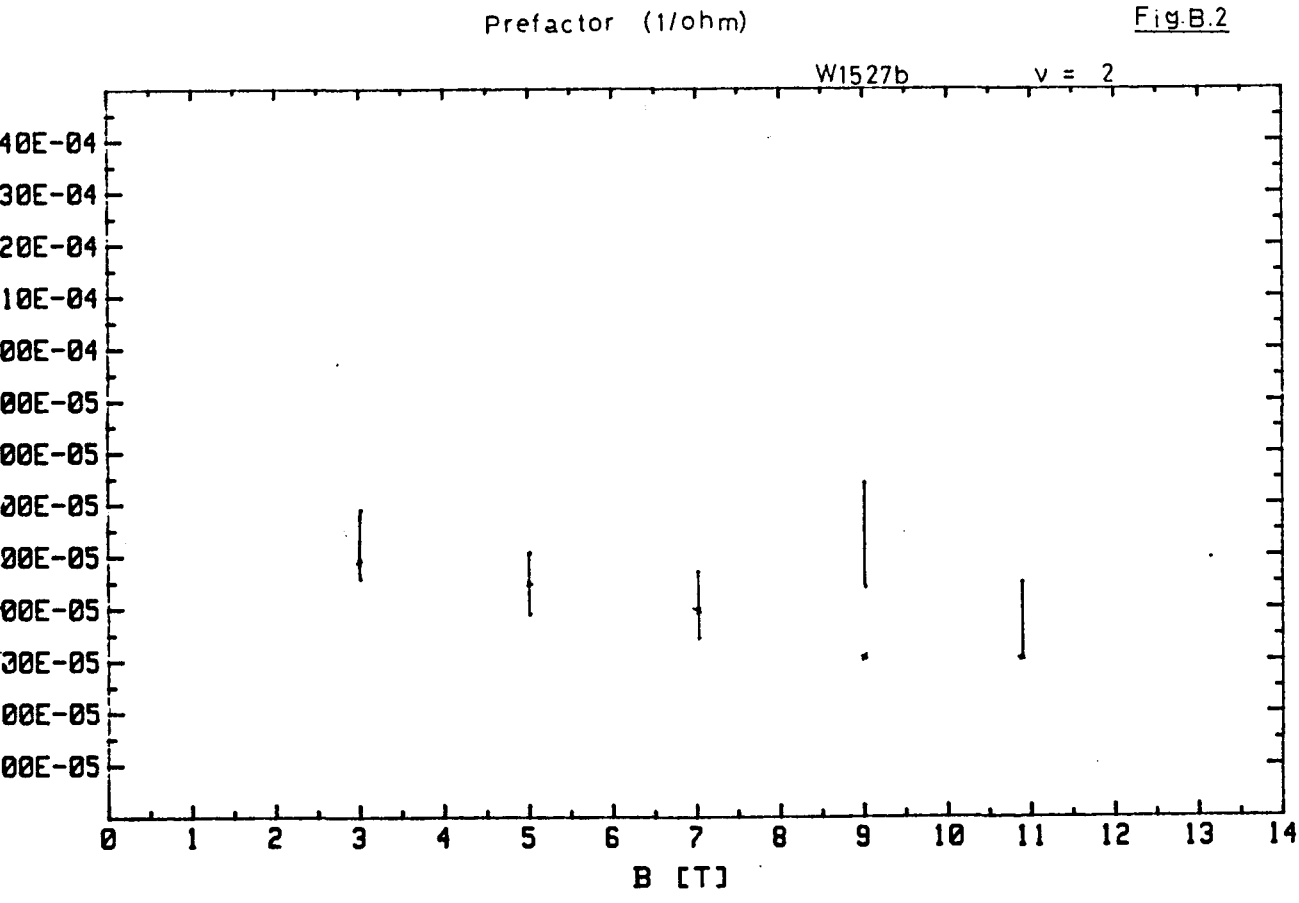
Prefactor (1/ohm)
W1527b ν = 2
40E-04
30E-04
20E-04
10E-04
00E-04
00E-05
00E-05
00E-05
00E-05
00E-05
30E-05
00E-05
00E-05
0 1 2 3 4 5 6 7 8 9 10 11 12 13 14
B [T]

Fig.B.2

Prefactor (1/ohm)

Fig.B.3